TRADEOFF BETWEEN INVESTMENTS IN INFRASTRUCTURE AND FORECASTING WHEN FACING NATURAL DISASTER RISK

A Dissertation

by

SEONG DAE KIM

Submitted to the Office of Graduate Studies of
Texas A&M University
in partial fulfillment of the requirements for the degree of

DOCTOR OF PHILOSOPHY

May 2009

Major Subject: Industrial Engineering

TRADEOFF BETWEEN INVESTMENTS IN INFRASTRUCTURE AND FORECASTING WHEN FACING NATURAL DISASTER RISK

A Dissertation

by

SEONG DAE KIM

Submitted to the Office of Graduate Studies of
Texas A&M University
in partial fulfillment of the requirements for the degree of

DOCTOR OF PHILOSOPHY

Approved by:

Chair of Committee,	J. Eric Bickel
Committee Members,	Guy L. Curry
	Donald R. Smith
	Michael K. Lindell
Head of Department,	Brett A. Peters

May 2009

Major Subject: Industrial Engineering

ABSTRACT

Tradeoff between Investments in Infrastructure and Forecasting when Facing Natural Disaster Risk. (May 2009)

Seong Dae Kim, B.S., Sungkyunkwan University;

M.S., Sungkyunkwan University

Chair of Advisory Committee: Dr. J. Eric Bickel

Hurricane Katrina of 2005 was responsible for at least 81 billion dollars of property damage. In planning for such emergencies, society must decide whether to invest in the ability to evacuate more speedily or in improved forecasting technology to better predict the timing and intensity of the critical event. To address this need, we use dynamic programming and Markov processes to model the interaction between the emergency response system and the emergency forecasting system. Simulating changes in the speed of evacuation and in the accuracy of forecasting allows the determination of an optimal mix of these two investments. The model shows that the evacuation improvement and the forecast improvement give different patterns of impact to their benefit. In addition, it shows that the optimal investment decision changes by the budget and the feasible range of improvement.

ACKNOWLEDGEMENTS

Though only my name appears on the cover of this dissertation, a great many people have contributed to its production. I owe my gratitude to all those people who have made this dissertation possible and because of whom my graduate experience has been one that I will cherish forever.

I would like to express my gratitude to all who helped me complete this dissertation. Above all, I am deeply indebted to my advisor Prof. J. Eric Bickel for motivating, inspiring, guiding, encouraging, and supporting me for all this work. I am also grateful for the consultations of Dr. Michael K. Lindell of the Hazard Reduction & Recovery Center at Texas A&M University and Dr. Fuqing Zhang of the Department of Meteorology at Pennsylvania State University. Without their help, I could not have done this difficult work.

Especially, none of this would have been possible without the love and patience of my family. I would like to give my special thanks to my wife JungBin whose patient love enabled me to complete this work.

TABLE OF CONTENTS

Page

LIST OF FIGURES

Page

Page

LIST OF TABLES

Page

Page

Page

1. INTRODUCTION

Every year, people around the world suffer from various hazards, which include human-made hazards and natural hazards. Human-made hazards include terrorism and accidents, and natural disasters include hurricanes, tornadoes, earthquakes, wildfires, volcanic eruptions, and tsunamis. Both types are hard to predict when, where, and how intensely they will strike. Unlike human-made disasters, however, natural disasters are virtually impossible to prevent. As recent events, including Hurricanes Katrina, Rita, and Ike, have made all too clear, many people face significant risks imposed by natural hazards.

In preparation for such risks, many governments, local and federal, have developed emergency forecasting systems (EFSs) and emergency response systems (ERSs). The EFS is a complex of sensors, computer models, and human experts that seek to forecast the occurrence, timing, and intensity of natural disasters. The ERS is the combination of infrastructures (e.g., evacuation routes) and supporting facilities (e.g., emergency shelters) that enables people to flee an oncoming disaster or to mitigate the damage if it occurs. One example of an ERS is an evacuation system, which includes evacuation routes. As shown in Figure 1, there is one-way information flow from natural hazard to human-made systems, and human-made systems cannot influence the natural hazard. However, EFSs and ERSs are interconnected to each other. Without EFSs and ERSs, the damage from natural hazards would be far more severe. Yet, due to lack of proper in-

---

This dissertation follows the style of *Decision Sciences*.

vestment, these systems fall well short of their potential to prevent damage from a natural disaster.

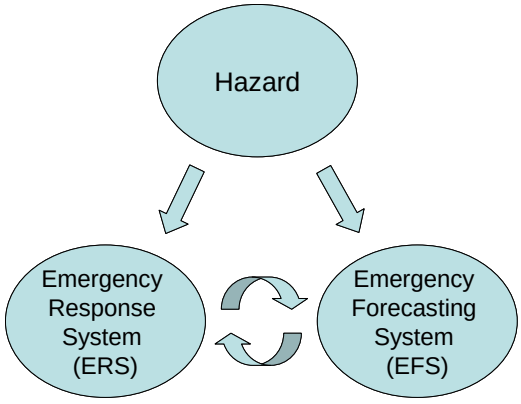

Figure 1. Roads/radar system.

Given limited funding, a natural question can arise: Is society better off improving its EFS or its ERS? That is, are we better off trying to predict the occurrence of a natural disaster (e.g., the track and intensity of a hurricane) or building infrastructure (e.g., shelters and roads) to respond to these disasters? This work uses dynamic programming (DP) and Markov processes (MPs) to model a multi-stage hurricane-evacuation decision problem. This formulation allows estimating the value of improved forecasting performance and improved evacuation speed. The use of this model is demonstrated using an example based on a community along the Texas Gulf Coast. Although the model is examined in the context of hurricane forecasting and evacuation, it is quite general and could apply to other natural or even human-made hazards.

Forecast accuracy and evacuation speed are modeled here based on the characteristics of hurricane forecasts and evacuation decisions, which were estimated from historical data and previous studies. By devising a parameter to model each improvement, a

sensitivity analysis helps determine how improvements in forecast accuracy or evacuation speed affect the model. The example illuminates the tradeoff between the two investments and shows how the optimal investment decision is made.

This dissertation is organized as follows. Section 2 reviews related literature. Section 3 develops the model. Section 4 illustrates the results of the model using real data. Section 5 discusses probability assessment and verification, which are crucial to making a good decision. Finally, Section 6 concludes this dissertation.

2. LITERATURE REVIEW

Much research has focused on assessing the value of hurricane forecasts. Considine et al. (2004) examined the value of hurricane forecasts to oil and gas producers in the Gulf of Mexico, who respond to the threat of hurricanes by evacuating offshore drilling rigs and suspending production. Through the use of a probabilistic cost-loss model, Considine et al. estimated that the incremental value of hurricane forecast information to oil and gas producers in that area over the past two decades exceeds the annual budget of the National Hurricane Center.

Regnier and Harr (2006) modeled the decision to prepare for an oncoming hurricane using a discrete Markov model of hurricane travel that is derived from historical tropical cyclone tracks. This was combined with the dynamic decision model to estimate the additional value that can be extracted from existing forecasts by anticipating updated forecasts. They used a variable hurricane preparation cost, which is defined as a fraction of the maximum loss, increasing linearly or exponentially after a critical lead-time. They used a discrete Markov model for multi-period decision making with respect to a sequence of more than two forecasts with improving accuracy for a single event. Simulation was used to compare the expense in different cases. Their model was shown to reduce the expected total cost associated with a hurricane strike by up to 8% relative to repeated static decisions.

Czajkowski (2007) developed a dynamic model of hurricane evacuation behavior in which a household's evacuation decision is framed as an optimal stopping problem

where every potential evacuation stage prior to actual hurricane landfall presents the choice either to evacuate or to wait one more period for a revised hurricane forecast. Czajkowski used a Markov chain to represent the revision of hurricane status and used a state variable named "risk index" for the transition matrix. He showed that his model explains plausibly actual evacuation timing outcomes by location as well as for various household types and that it provides a deeper understanding of evacuation-timing empirical outcomes.

Regnier (2008) viewed the hurricane evacuation problem from the perspective of public officials having the authority to order hurricane evacuation. To show the relationship between lead-time and track uncertainty for Atlantic hurricanes, she used a stochastic model of storm motion derived from historical tracks using a discrete Markov model. She showed that being able to tolerate no more than a 10% probability of failing to evacuate before a striking hurricane (a false negative) implies that at least 76% of evacuations will be false alarms. She also showed that reducing decision lead-times from 72 to 48 hours for major population centers could save an average of hundreds of millions of dollars in annual evacuation costs for the region surrounding each target, assuming 460 miles of coastline was subject to evacuation.

Lodree and Taskin (2009) sought to determine the optimal inventory of hurricane supplies and formulated this as an optimal stopping problem with Bayesian updates, where the updates are made on hurricane wind-speed prediction. The inherent tradeoff in this inventory control problem is between hurricane wind-speed forecast accuracy, which improves with time, and logistics cost efficiency, which worsens with time. Their

model revises in Bayesian fashion the predicted hurricane wind speed upon landfall, using the observation of hurricane wind speed every 6 hours. Their model defines two classes of hurricane, “regular” and “extreme,” which determine its cost functions. They suggested devising a decision model that specifies the optimal quantity and timing of this inventory decision, which would be the foundation for a practical disaster recovery plan.

Czajkowski (2007) is the most closely related work to this research, but the latter separated the uncertainty of track forecast from the uncertainty of intensity forecast and modeled the accuracy of each forecast. None of the above-cited studies modeled the two uncertainties separately or modeled the improvement of forecasting ability and response speed. In addition, none of them worked on the optimal investment decision using real data. This dissertation addresses these aspects and demonstrates how the improvement of forecast accuracy and evacuation speed can be modeled using Markov decision processes. This technique is illustrated with an example based on the Texas Gulf Coast community of San Patricio County.

3. MODEL FOR FORECAST ACCURACY AND EVACUATION SPEED

3.1. Decisions Involved in Minimizing the Cost of a Disaster

The task of minimizing the cost of a natural or human-made disaster depends on two key decisions: a high-level decision about investment and a low-level decision about hurricane-evacuation, as illustrated in Figure 2. Each is made by a "decision maker." Because the model assumes that the low-level decision is always optimal given the available information, the actual identity of the decision maker at this level is not considered here.

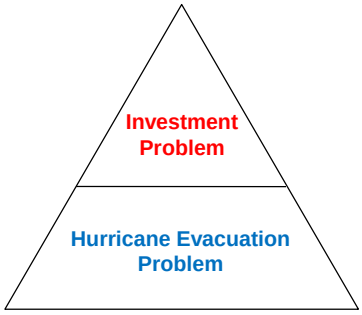

Figure 2. High-level decision problem and low-level decision problem.

3.2. Modeling the Evacuation-Decision Problem

The evacuation-decision problem can be viewed as a Markov Decision Process (MDP) with finite state space, finite action set, and finite (planning) horizon. This problem is solved typically using the value iteration method, dynamic programming, or successive iteration.

The natural hazard evacuation problem is naturally viewed as a multi-stage decision problem in which the decision maker (DM) can select one of three alternatives at

each stage: she can ignore the hazard (i.e., cease monitoring it), take preventive action (e.g., evacuate), or defer the decision for one stage. If evacuation takes a finite amount of time, then the advantage of waiting and learning more about the hazard must be weighed against the value of evacuating now and thereby reducing future risk. This dynamic decision problem is modeled in this paper using dynamic programming (DP). Furthermore, a Markov process (MP) is used to model how the DM's belief about the likelihood of the storm striking evolves over time.

3.2.1. Dynamic programming model

Begin by letting $j = N, N\text{-}1,\cdots, 1$ represent the stage at which decisions regarding evacuation can be made, where N is the number of stages until the hurricane will make landfall, which is assumed to be known.[1] A stage is set to six hours, the frequency with which the National Hurricane Center (NHC) provides hurricane forecasts. Although hurricane intensity is uncertain, this formulation begins by letting T_j be the stage-j expected intensity of the hurricane at landfall and t_j be its value. It can be considered as the forecasted landfall intensity that one might see on The Weather Channel, which is implicitly the expectation of the landfall intensity distribution.

By evacuating before the hurricane makes landfall, society suffers a cost C during the evacuation but reduces the loss L in the event of a strike. Let $C_j(t_j)$ be the cost during the evacuation when evacuation is started at stage j and the intensity at landfall is believed to be t_j (this cost being indexed by intensity because stronger storms result in

[1] In reality, the forward movement speed of a storm is variable but the model assumes constant forward movement speed for simplicity.

larger evacuation areas). This cost includes that of individual evacuation, business evacuation, and government evacuation. $L_j(t_j)$ is the loss incurred when evacuation is started at stage j, expected storm intensity at stage 0 is t_j, and the storm strikes the target. $L_j(t_j)$ encompasses loss of life, personal injury, and damage to protectable property. $L_j(t_j)$ does not take into account unprotectable losses not under the DM's control, such as properties that cannot be protected and people who disregard the warning. $L_0(t_j)$ is the loss when the event occurs without action being taken. These costs are summarized in the contingency table shown in Table 1.

Table 1. Cost of evacuation decision under various outcomes.

Observation / Decision	Hit	Not Hit
Evacuate at stage j (> 0)	$C_j(t_j) + L_j(t_j)$	$C_j(t_j)$
Do Not Evacuate	$L_0(t_j)$	0

At each stage, the DM is assumed to have three alternatives: Evacuate, Do Not Evacuate, or Wait One Stage. If the strike probability is s_j at stage j, the expected expense when Evacuate is selected is

$$s_j\left(C_j(t_j)+L_j(t_j)\right)+(1-s_j)C_j(t_j)=C_j(t_j)+s_jL_j(t_j). \tag{1}$$

If the DM chooses Do Not Evacuate, the expected expense is

$$s_jL_0(t_j)+(1-s_j)0=s_jL_0(t_j). \tag{2}$$

Selecting Wait One Stage incurs a cost of deferment γ, which includes the costs of additional information gathering, being prepared for immediate action, etc. In addition to the delay cost, the DM incurs the expected expense at stage $j-1$. If $p_{s_j,s_{j-1}}$ is defined as the transition probability of strike probability from s_j to s_{j-1} and $q_{t_j,t_{j-1}}$ is the transition probability of the expected landfall intensity from t_j to t_{j-1}, the expected expense at stage $j-1$ is

$$\gamma + \sum_{s_{j-1}} \sum_{t_{j-1}} p_{s_j,s_{j-1}} q_{t_j,t_{j-1}} V_{j-1}(s_{j-1},t_{j-1}) \equiv \gamma + \bar{V}_{j-1}(s_j,t_j). \tag{3}$$

It is assumed that s_j is independent of t_j and that beliefs are coherent. Specifically, the revisions are assumed to be such that the expected strike probability and the expected intensity for period j - l are equal to their stage j values. That is,

$$s_j = \sum_{s_{j-1}} p_{s_j,s_{j-1}} s_{j-1}, \quad t_j = \sum_{t_{j-1}} q_{t_j,t_{j-1}} t_{j-1} \quad \forall j.$$

Using Equations (1), (2), and (3), the DP model is

$$\begin{aligned} V_j(s_j,t_j) &= \min\left\{C_j(t_j) + s_j L_j(t_j), s_j L_0(t_j), \gamma + \bar{V}_{j-1}(s_j,t_j)\right\} \\ \bar{V}_{j-1}(s_j,t_j) &\equiv \sum_{s_{j-1}} \sum_{t_{j-1}} p_{s_j,s_{j-1}} q_{t_j,t_{j-1}} V_{j-1}(s_{j-1},t_{j-1}) \\ \bar{V}_0(s_1,t_1) &\equiv s_1 L_0(t_1), \end{aligned} \tag{4}$$

where $V_j(s_j,t_j)$ is expected expense incurred by following the optimal policy at stage j, for which the DM currently believes that the probability of the event is s_j and the intensity of

the event is t_j. The terminal value is $\bar{V}_0(s_1, t_1) = s_1 L_0(t_1)$, given that no action takes place after stage 1.

3.2.2. General features of the model

The model introduced in the previous section has important features about forecast and response improvement. If forecasting about the hazard is improved, i.e., more information is available sooner, the DM can make a good decision earlier.

If response to the hazard is improved, i.e., infrastructure is improved, the DM can defer the decision, which allows more information to be acquired. In this case, same expenses are incurred even with later decision and fewer expenses are incurred even with the same decision timing.

In this model, two different ways of getting more information can be compared. One is getting more information directly by improving the forecast system. The other one is getting more information through buying time by improving the response system.

3.2.3. The value of information and evacuation

The concepts of additional information and increased evacuation speed will be shown here to be closely related. It is assumed that the belief about landfall intensity is fixed and the cost of deferment is negligible.

Value of Perfect Information

Suppose perfect information is available at stage N regarding the path of the hurricane. If it is known that the storm will not strike, then there will be no evacuation. But if the hurricane is going to strike, the evacuation decision depends upon the relative shapes of L_j and C_j:

- If L_j is strictly increasing beginning at $L_N = 0$ and C_j is constant or not decreasing as fast as L_j increases, then evacuation will be as soon as possible. (See below for proof.) Because all loss is avoided by evacuating at stage N, the cost with perfect information is simply the chance the storm will hit, s_N, times the stage-N cost of evacuation, or $s_N C_N$.
- If L_j is strictly increasing, C_j is decreasing (so that $C_j + L_j > C_{j-1} + L_{j-1}$), and evacuation cost is relatively low (so that $L_0 - L_{j-1} > C_{j-1}$), then waiting is called for. The cost with perfect information is the chance that the storm will hit, s_N, times the total expense of evacuating at the next stage, or $s_N(C_{N-1} + L_{N-1})$.
- If L_j is constant or non-increasing and $C_j > 0$, then there should be no evacuation. The cost with perfect information is the chance that the storm will hit, s_N, times the loss level, or $s_N L_0$.

<u>Proof on the value of perfect information</u>

At stage j, if perfect information is available that the storm is going to hit, anticipated expense from selecting Evacuate is $C_j + L_j$, from selecting Do Not Evacuate is L_0, and from selecting Wait is $C_{j-1} + L_{j-1}$. Here, the option Wait means Evacuate at the next stage without revising the belief, because perfect information is already known. The op-

timal decision is Evacuate as long as $C_j + L_j < L_0$ and $C_j + L_j < C_{j-1} + L_{j-1}$. If C_j is constant, the previous sentence holds as long as $C_j + L_j < L_0$ and $L_j < L_{j-1}$. If perfect information is available saying that the storm is not going to hit, anticipated expense from selecting Evacuate is C_j, from selecting Do Not Evacuate is 0, and from selecting Wait is C_j. The optimal decision is Do Not Evacuate as long as $C_j > 0$.

Therefore, with perfect information, Wait can never be optimal as long as $C_j + L_j < L_0$ and $C_j + L_j < C_{j-1} + L_{j-1}$ for all j. If C_j is constant, it holds as long as L_j is strictly increasing. □

Value of Instantaneous Evacuation

If one is at stage N and has the ability to evacuate instantaneously at any stage, then $L_j = 0$ for all $j \geq 0$ since all losses are prevented. In this situation, it is optimal to wait until the final period to act. (See below for proof.) The expected loss is simply the chance of having to evacuate, times the cost of evacuation, or $s_N C_0$.

Proof on the value of instantaneous evacuation

At stage 0, if hurricane landfall is observed, anticipated expense from selecting Evacuate, i.e., instantaneous evacuation, is C_0 and anticipated expense from selecting Do Not Evacuate is L_0. Therefore, the optimal decision is Evacuate as long as $C_0 < L_0$. If the observation is of no hurricane landfall, anticipated expense from selecting Evacuate is C_0 and anticipated expense from selecting Do Not Evacuate is 0. Therefore, the optimal decision is Do Not Evacuate as long as $C_0 > 0$, and the expected expense from selecting the optimal decision at this stage is $s_N C_0$, because it is estimated at stage 0.

At stage 1, anticipated expense from selecting Evacuate is C_1, from selecting Do Not Evacuate is $s_N L_0$, and from selecting Wait is $s_N C_0$. Therefore, the optimal decision is Wait as long as $C_0 < L_0$ and $C_1 > s_N C_0$. The second condition always holds if C_j is constant, because $s_N < 1$.

Likewise, at any stage j from stage 1 backward, Wait is always optimal as long as $C_0 < L_0$ and $C_j > s_N C_0$.

Therefore, with instantaneous evacuation, Wait is optimal for any stage $j > 0$ as long as $C_0 < L_0$ and $C_j > s_N C_0$. If C_j is constant, it holds as long as $C_0 < L_0$.

Thus, the cost with instantaneous evacuation is $s_N C_0$ and the cost with perfect information is $s_N C_N$. These costs are the same when C_j is constant and the value of perfect information equals the value of instantaneous evacuation. If C_j is strictly increasing, then it would be better to have perfect information. On the other hand, if C_j is strictly decreasing, then, with perfect information, it would be optimal to wait until the critical point where $C_j + L_j = C_{j-1} + L_{j-1}$, but not until the final stage because the evacuation speed is finite. In this case, it would be better to have instantaneous evacuation. □

To summarize the results, assuming that C_j and L_j are non-negative linear function of j; $L_N = 0$, $L_j < L_{j-1}$ for all $j > 0$ (strictly increasing); $C_N < L_0$, $C_0 < L_0$; gradient of $C_j >$ - gradient of L_j (C_j not decreasing too fast), then the value of perfect information (VoPI) and the value of instantaneous evacuation (VoIE) has the relationship in Table 2.

Table 2. Value of perfect information vs. value of instantaneous evacuation.

Pattern of C_j	Relationship between VoPI and VoIE
Strictly increasing ($C_N < C_0$)	VoPI > VoIE
Strictly decreasing ($C_N > C_0$)	VoPI < VoIE
Constant ($C_N = C_0$)	VoPI = VoIE

3.2.4. Modeling beliefs

Before adopting the Markov process to model the revision of belief, the conjugate pair distribution approach was tried. This approach is based on the information acquisition and technology adoption model of McCardle (1985). In the conjugate pair distribution approach, it is assumed that the information structure is represented by the conjugate pair Beta-Bernoulli.[2] (See APPENDIX A for more details.) Instead of a Beta-Bernoulli conjugate pair, other conjugate pairs can be used for different information structures. (See APPENDIX B for other conjugate pairs.)

This approach of using a conjugate pair distribution is mathematically convenient but it is not flexible enough to model the improvement of forecast accuracy. Several variants of the Beta-Bernoulli conjugate pair approach were examined to address these issues, but they were determined to be too inflexible. (See APPENDIX A for the variants of the Beta-Bernoulli conjugate pair approach.)

In order to resolve these problems, a Markov process was used to model the revision of the DM's belief. In this approach, the beliefs are represented as state variables and the revision of those beliefs is modeled using state transition probability matrices. Let S_j and T_j be state variables having the specific values s_j and t_j, respectively. s_j and t_j

[2] For background about conjugate pairs, see Raiffa and Schlaifer (1961).

represent the DM's beliefs about the probability of a strike and the expected intensity of the hurricane. These beliefs are revised in a Bayesian fashion at each stage based on the latest information (i.e., forecasts) available to the DM. Different matrices are used for different stages because the pattern of belief revision can change over time. For example, if the impact of information at each stage is ignorable, initial value of the state variable does not change during the transition to the next stage. In this case, the state transition probability matrix at each stage is diagonal, as illustrated in Table 3.

Table 3. Transition probability matrices with ignorable information.

N \ $N-1$	0	1	⋯	9	10
0	1	0	⋯	0	0
1	0	1	⋯	0	0
⋮	⋮	⋮	•	⋮	⋮
9	0	0	⋯	1	0
10	0	0	⋯	0	1

→

j \ $j-1$	0	1	⋯	9	10
0	1	0	⋯	0	0
1	0	1	⋯	0	0
⋮	⋮	⋮	•	⋮	⋮
9	0	0	⋯	1	0
10	0	0	⋯	0	1

If the impact of information at each stage subsides over stages, change in the state variable becomes less likely when approaching the final stage. In this case, the state transition probability matrix becomes closer to a diagonal shape as the stage number decreases, as illustrated in Table 4.

Table 4. Transition probability matrices with subsiding impact of information.

N \ $N-1$	0	1	⋯	9	10
0	0.40	0.20	⋯	0.05	0
1	0.20	0.30	⋯	0.10	0
⋮	⋮	⋮	•	⋮	⋮
9	0	0.10	⋯	0.30	0.20
10	0	0.05	⋯	0.20	0.40

→

j \ $j-1$	0	1	⋯	9	10
0	0.90	0.10	⋯	0	0
1	0.10	0.80	⋯	0	0
⋮	⋮	⋮	•	⋮	⋮
9	0	0	⋯	0.80	0.10
10	0	0	⋯	0.10	0.90

If the impact of information at each stage is constant over stages, the likelihood of the state variable transition does not change over stages. In this case, the state transition probability matrices are identical for all stages, as illustrated in Table 5.

Table 5. Transition probability matrices with constant impact of information.

N \ $N-1$	0	1	⋯	9	10
0	0.40	0.20	⋯	0.05	0
1	0.20	0.30	⋯	0.10	0
⋮	⋮	⋮	•	⋮	⋮
9	0	0.10	⋯	0.30	0.20
10	0	0.05	⋯	0.20	0.40

→

j \ $j-1$	0	1	⋯	9	10
0	0.40	0.20	⋯	0.05	0
1	0.20	0.30	⋯	0.10	0
⋮	⋮	⋮	•	⋮	⋮
9	0	0.10	⋯	0.30	0.20
10	0	0.05	⋯	0.20	0.40

If the impact of information at a given stage increases with each stage, the forecasts represented by the state variables become sharper. Especially when the state variable is the probability of an event, the transition probability distribution becomes more widely distributed and the transition becomes more likely toward 1 or 0 as illustrated in Table 6.

Table 6. Transition probability matrices with increasing impact of information.

N \ $N-1$	0.1	0.2	⋯	0.8	0.9
0.1	0.40	0.20	⋯	0.05	0
0.2	0.20	0.30	⋯	0.10	0
⋮	⋮	⋮	•	⋮	⋮
0.8	0	0.10	⋯	0.30	0.20
0.9	0	0.05	⋯	0.20	0.40

→

j \ $j-1$	0.1	0.2	⋯	0.8	0.9
0.1	0.80	0.05	⋯	0.05	0.10
0.2	0.75	0.05	⋯	0.05	0.20
⋮	⋮	⋮	•	⋮	⋮
0.8	0.20	0.05	⋯	0.05	0.75
0.9	0.10	0.05	⋯	0.05	0.80

→

1 \ 0	0.1	0.2	⋯	0.8	0.9
0.1	0.9	0	⋯	0	0.1
0.2	0.8	0	⋯	0	0.2
⋮	⋮	⋮	•	⋮	⋮
0.8	0.2	0	⋯	0	0.8
0.9	0.1	0	⋯	0	0.9

The Markov process approach is attractive because the state transition at each stage is flexible and the changing pattern of belief revision can be well represented. Despite its drawback of not showing how information works for the state transition at each state, the Markov process approach is adopted here as the main model.

This process is modeled using an MP with transition matrices $\mathbf{P}_j$, which consists of $p_{s_j,s_{j-1}}$ $\left(=\Pr(S_{j-1}=s_{j-1}\mid S_j=s_j)\right)$, and $\mathbf{Q}_j$, which consists of $q_{t_j,t_{j-1}}$ $\left(=\Pr(T_{j-1}=t_{j-1}\mid T_j=t_j)\right)$. At each stage of this example, the state space for S_j consists of 21 possible states (0.00, 0.05,⋯, 0.95, 1.00) and the state space for T_j consists of 6 possible states (0, 1, ⋯, 5). The state transition probabilities $p_{s_j,s_{j-1}}$ and $q_{t_j,t_{j-1}}$ are modeled using a Beta(α, β) distribution.

The Beta distribution was chosen for transition probability matrices for several reasons. First, without such a probability distribution, it is hard or almost impossible to get proper transition probabilities for all possible combinations of states at each stage. Second, the unique pattern of strike probabilities over time needs to be represented. Finally, the distribution makes it convenient to model and control the accuracy improvement of a track forecast (strike probability).

The mean or expected value of the state variable was assumed to be unchanging at every stage even though dispersion (or variance) changes. For example, given a prior state forecast s_j, the expected state forecast should also be s_j for periods j-1, j-2,⋯, 0. That is,

$$s_j=\sum_{s_{j-1}} p_{s_j,s_{j-1}}s_{j-1} \quad \forall j. \tag{5}$$

Under a Beta distribution, the mean of the state transition distribution is $\alpha/(\alpha+\beta)$ = s_j and the variance is $\alpha\beta/((\alpha+\beta)^2(\alpha+\beta+1))$ = σ_j^2 at stage j. Therefore, given s_j and σ_j^2, α and β can be solved for as follows:

$$\alpha = \frac{(1-s_j)s_j^2}{\sigma_j^2} - s_j, \qquad \beta = \frac{s_j(1-s_j)^2}{\sigma_j^2} + s_j - 1.$$

Using the cumulative distribution of the Beta distribution and the discretization of the continuous distribution into discrete states, the transition probability matrices $\mathbf{P}_j$ and $\mathbf{Q}_j$ can be built for each stage.

Modeling the change in the state transition probability matrices over time is based on Figure 3, which appeared in Regnier (2008). Figure 3 displays the NHC's forecasted probability of hurricane strike for New Orleans, LA, conditioned on whether the hurricane struck, i.e., the likelihood function. When many stages are left before landfall, the probability of a strike is low and does not change dramatically with lead-time. As landfall approaches and information increases, the likelihood functions diverge, which leads to sharper strike probability forecasts approaching 1 for striking storms and 0 for non-striking storms. This occurs because the error of forecasted storm track decreases, eventually approaching 0, as the storm moves.

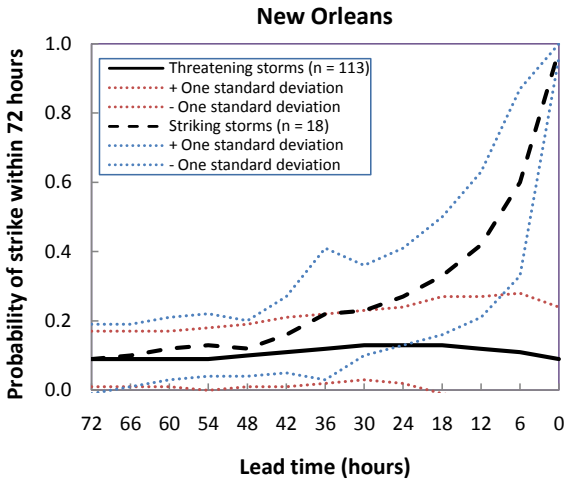

Figure 3. Strike probabilities for striking and threatening (but non-striking) historical hurricanes, as a function of lead-time. Recreated from Regnier (2008).

Based on this data, σ_j^2 or the variance of state transition probability distribution at stage *j* is defined as

$$\sigma_j^2 = \left(\frac{\sigma}{j+\varepsilon} \right)^2 = \frac{\sigma^2}{(j+\varepsilon)^2}, \qquad j \in \{N, N-1, \cdots, 2, 1, 0\}, \tag{6}$$

where σ^2 is a base variance of the state transition probability distribution and ε is a small positive number to prevent too large a variance. At the final stage, $j = 0$, the variance becomes very large and the Beta distribution has a U-shape as shown in Figure 4.

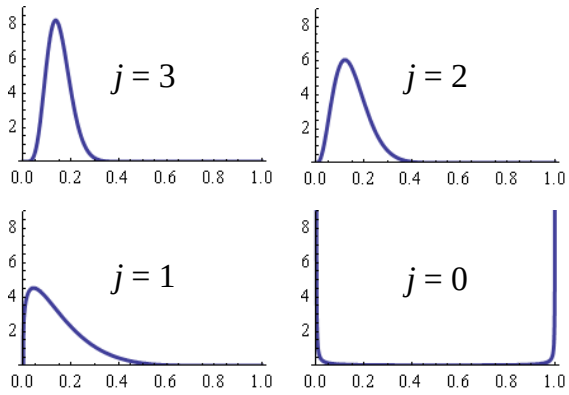

Figure 4. State transition probability distributions at different stages when the mean is 0.15.

The modeling of forecasting ability and its improvements starts with the concept of strike probability and its variance.

Figure 5. Cone of uncertainty (image from The Weather Channel (2008)).

Figure 5 shows the track forecast of a hurricane. This type of graphic is called "forecast cone," "track forecast cone," "cone of uncertainty," "cone of probability," "cone of error," or "cone of death" (Broad, Leiserowitz, Weinkle, & Steketee, 2007).

The cone in the figure covers 67% of possible tracks of the hurricane center. Hereafter, the cone will be referred to as "uncertainty cone" and the cone circle as "uncertainty circle." In the early stages, the range of possible prior values of state variable S_j is limited. Generally, when the hurricane center is far from shore, the strike probability for an onshore target is very low. But if the hurricane center is close to the target and the target is still in the uncertainty cone, the strike probability is much higher. In other words, the strike probability is low when the area of the error circle, where the target is, is large, and it is high when the area is small. Therefore, the strike probability can be roughly defined as a constant times a target area divided by the area of the uncertainty circle. As seen in Figure 5, the radius of each uncertainty circle is almost proportional to the distance from the current hurricane center or the remaining time until strike as shown in Table 7. Because the variance is the square of standard deviation and the area of an uncertainty circle is a constant times the square of the radius, it can be inferred that the variance of strike probability is proportional to the reciprocal of the square of the remaining distance or periods.

Table 7. Radii of NHC forecast cone circles for 2007, based on error statistics from 2002-2007. (Table adapted from NHC.)

Forecast periods (hours)	2/3 Probability Circle, Atlantic Basin (nautical miles)
12	39
24	69
36	99
48	124
72	179
96	252
120	326

Regnier (2008) determined the range of conditional strike probabilities at four different target locations as a function of lead-time. Her graph shows that as lead-time declines, the strike probability of striking storms increases and converges to one and that of non-striking storms decreases to 0. However, a striking storm and a threatening but non-striking storm may have similar initial strike probabilities. Dispersion of strike probability is proportional to the reciprocal of lead-time. When lead-time is great, such as greater than 30 hours, it is usually difficult to determine whether a storm will be striking or non-striking.

On the other hand, the uncertainty cone in Figure 5 can be simplified and compared for different lead-times, as shown in Figure 6.

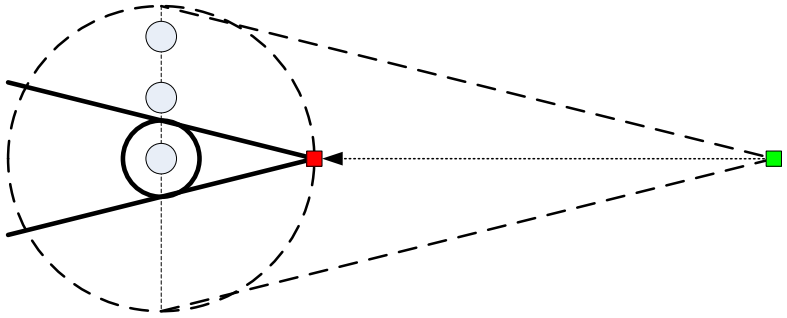

Figure 6. Cone of uncertainty for different lead-times.

In Figure 6, it is assumed that the hurricane moves in a straight line. As the hurricane center approaches the target location, the area of the circle in the corresponding uncertainty cone decreases while the area of the target remains constant. The gray circle is the target location, typically a coastal city within the initial uncertainty cone. Two squares before and after the arrow represent the hurricane center as it moves. The dashed circle represents the possible locations of the hurricane center in four periods from when

the hurricane center is at the square before the arrow. The solid circle represents the possible locations of the hurricane center in one period from when the hurricane center is at the square after the arrow.

Assume that the actual landfall locations are normally distributed around the center of the uncertainty circle along the vertical black dashed line and that the radius of the uncertainty circle is the standard deviation. Then the strike probability p(S) is calculated as

$$p(S) = \int_a^b \frac{1}{\sigma\sqrt{2\pi}} e^{-\frac{(x-\mu)^2}{2\sigma^2}} dx = \Phi\left(\frac{b-\mu}{\sigma}\right) - \Phi\left(\frac{a-\mu}{\sigma}\right),$$

where *a* and *b* are the relative locations of the boundaries of the target area from the center of the uncertainty circle, Φ is the standard normal cumulative distribution, μ is the mean, and σ is the standard deviation of the landfall location distribution. For example, if standard deviation is 4 when lead-time is four periods, standard deviation is 1 when lead-time is one period, and radius of the target is 0.4, the strike probabilities for the target located at the center of the uncertainty circle when lead-time is four periods and one period are calculated as

$$p_4(S) = \int_{-0.4}^{0.4} \frac{1}{4\sqrt{2\pi}} e^{-\frac{(x-0)^2}{2\cdot 4^2}} dx = \Phi\left(\frac{0.4-0}{4}\right) - \Phi\left(\frac{-0.4-0}{4}\right) = 0.079656$$

$$p_1(S) = \int_{-0.4}^{0.4} \frac{1}{1\sqrt{2\pi}} e^{-\frac{(x-0)^2}{2\cdot 1^2}} dx = \Phi\left(\frac{0.4-0}{1}\right) - \Phi\left(\frac{-0.4-0}{1}\right) = 0.310843.$$

Plotting the strike probabilities for all the possible targets in the initial uncertainty circle, in which lead-time is four periods, yields a shape as in Figure 7. When lead-time is four periods, the target in the middle and the one at the boundaries have similar strike probabilities between 0.05 and 0.08. However, when lead-time is one period, strike probability is heavily dependent on the target location. Strike probabilities for the targets that are still in the shrunk uncertainty circle increase noticeably. However, strike probabilities for the targets that are far from the shrunk uncertainty circle approach 0.

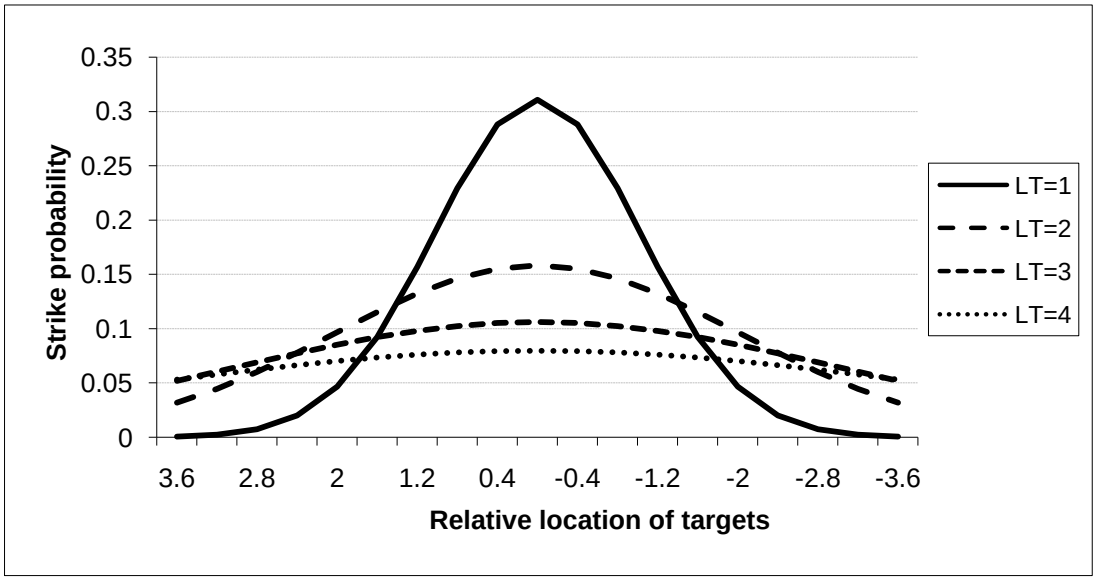

Figure 7. Distribution of strike probabilities over different target locations.

The change of strike probabilities for different target locations is plotted as a function of lead-time in Figure 8. This figure shows that strike probabilities become more widely dispersed as lead-time becomes shorter.

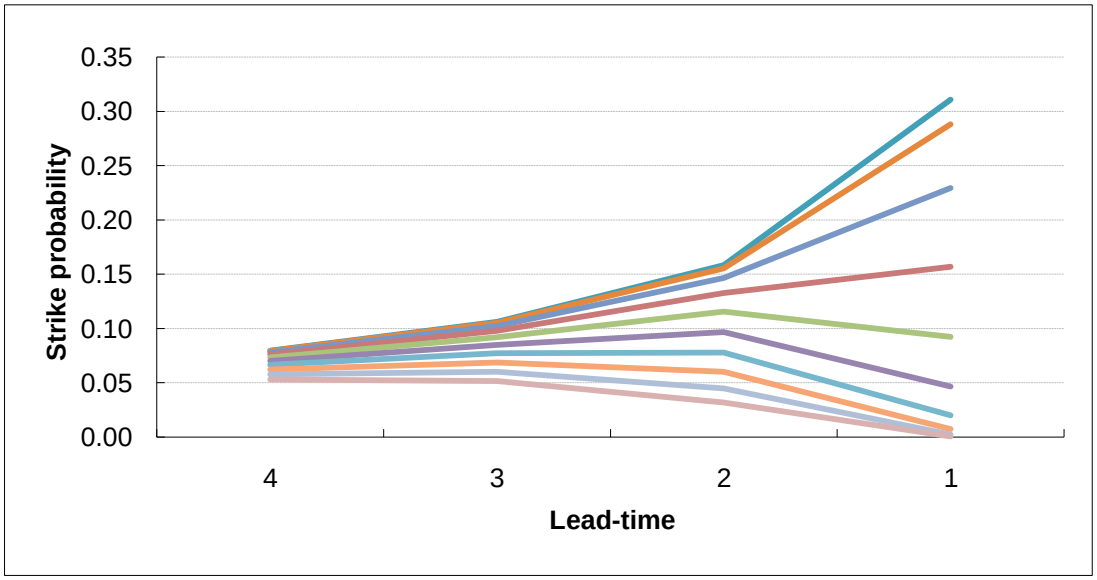

Figure 8. Change of strike probabilities over time for different target locations.

When lead-time is long, the uncertainty circle has a large area, making the target location less significant and implying low chance of strike.[3] When lead-time becomes shorter, the uncertainty circle shrinks, making the target location more significant but not necessarily implying high chance of strike. If the target location is within the final uncertainty cone, like the lowest dot in Figure 6, strike probability grows sharply when landfall is imminent. However, if the target shifts outside the uncertainty cone due to a change in hurricane direction, the strike possibility drops.

As implied from Figure 7 and Figure 8, the variance of strike probabilities for the targets increases sharply as lead-time approaches 0. Figure 9 shows the variance as a function of lead-time. It shows that three-fourths shorter lead-time enlarges variance by over 150 times.

[3] According to the National Hurricane Center (NHC), strike probability is the chance of the center of the hurricane passing within 65 nautical miles or 75 statute miles of the target location.

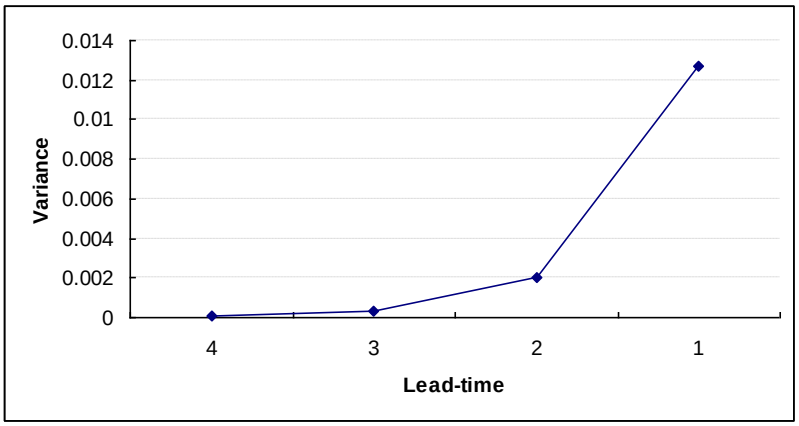

Figure 9. Variance of strike probabilities for the targets.

This result roughly matches the work of Regnier (2008). This observation implies that the variance of strike probability increases as lead-time decreases, even though it varies depending on the location of the target relative to the hurricane track. It also implies that as the strike probability for a target in the cone increases, variance of strike probabilities over all targets also increases. Because the area of the uncertainty circle is proportional to the square of radius and the variance of strike probability is the square of standard deviation, one can infer that the variance of strike probability is proportional to the reciprocal of the square of the uncertainty circle radius. Assuming that the angle of the uncertainty cone does not change as the hurricane moves,[4] the radius of the uncertainty cone is proportional to lead-time before landfall. Then, the variance of strike probabilities at stage *j* can be defined as

$$\sigma_j^2 = \frac{K_S}{(j+\varepsilon)^2}, \qquad j \in \{N, N-1, \cdots, 2, 1, 0\}. \tag{7}$$

[4] This is because the uncertainty cone is made using historical official forecast errors (mean absolute errors) for the past five years, not storm-specific data.

In this definition, σ_j^2 is the variance of strike probability at stage j and K_S is a constant.

The above creates a foundation for modeling forecasting ability and the effect of its improvement on landfall intensity. A landfall intensity forecast uses the same definition of α and β as in strike probability. A DM's estimation of landfall intensity changes over time, but its fluctuation does not change noticeably, as seen in Figure 10 and Figure 11. The former figure shows the transition probability matrices for landfall intensity, which were created from 30 hurricanes and tropical storms before year 2006. If lead-time is four periods and a DM's belief on landfall intensity is Category 1, category would change with probability 0.2 at the next period. If the DM's belief on landfall intensity is Category 3, category would change with probability 0.4 at the next period. No significant pattern of dispersion change over time is observed in the figure.

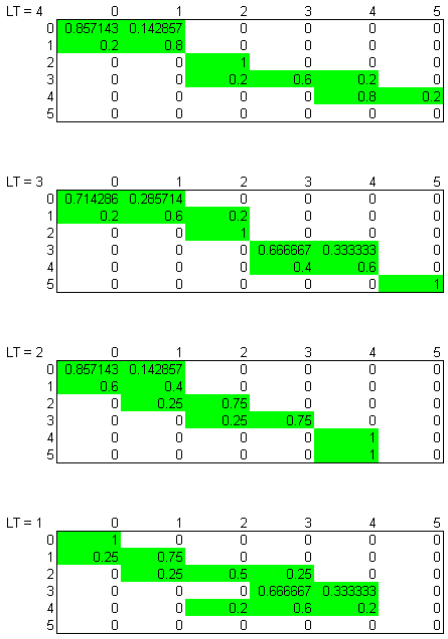

Figure 10. Transition probability matrix of landfall intensity from 30 storms from 1998 to 2005 (built using the data from NHC).

Based on this observation, this model assumes a constant variance of the revision of landfall intensity forecast. Therefore, a constant variance K_T is defined for all stages as

$$\sigma_j^2 = K_T \qquad j \in \{N, N-1, \cdots, 2, 1\}.$$

Because the forecast of landfall intensity does not change dramatically when lead-time approaches 0, transition matrices have a nearly diagonal shape for all stages.

Figure 11 displays the dynamics of the NHC's landfall intensity forecasts from 1998 to 2005. It shows that intensity forecasts do not change appreciably as landfall approaches. Therefore, it is assumed that the variance of transition probability distribution for $\mathbf{Q}_j$ is not a function of the stage.

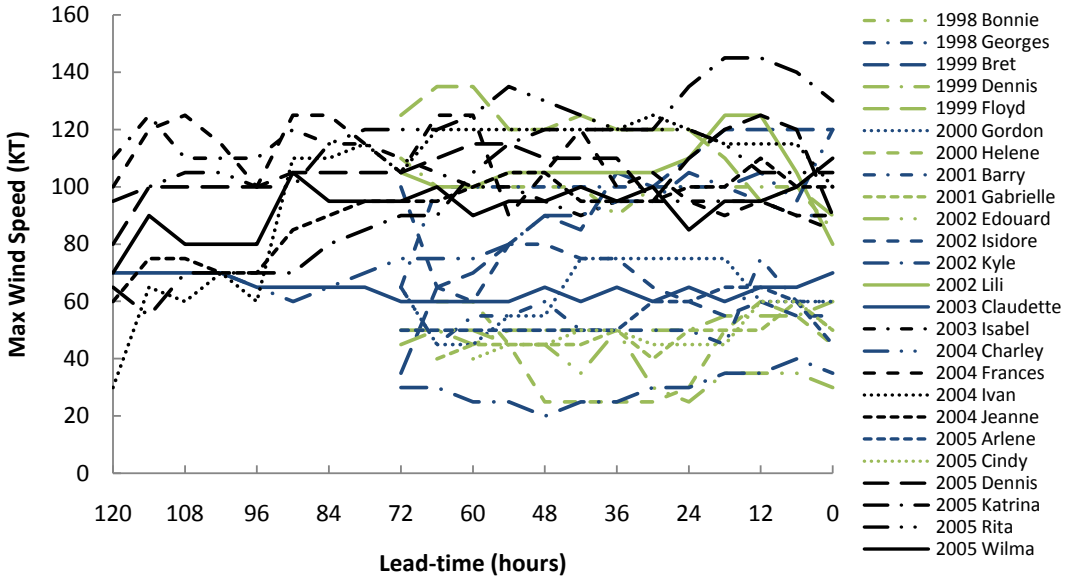

Figure 11. Landfall intensity forecast as a function of lead-time (plotted using data from NHC Tropical Cyclone Advisory Archive 1998-2005).

3.2.5. Cost functions

Figure 12 displays the general shape of the loss function $L_j(t_j)$ considered in this paper, which is a modification of the cost profile in Regnier and Harr (2006). $L_j(t_j)$ represents the level of loss or damage from the hazardous event when the protective action is started at stage j, the intensity of the event is expected to be t_j, and the event really occurs at stage 0. Full protection is possible if the action begins before a critical decision point c. After this point, the action can provide only partial protection. In this figure, m is the minimum time requirement for the protective action to be effective. Action started after stage m does not provide any protection.

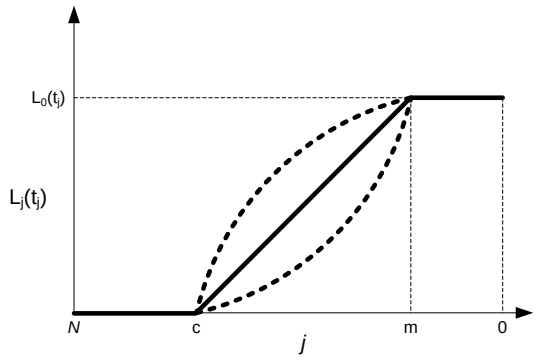

Figure 12. General shape of $L_j(t_j)$.

The general shape of $L_j(t_j)$ in Figure 12 can be formulated as

$$L_j(t_j) = \max\left\{0, L_0(t_j) - a_j(t_j)\max\{0, j-m\}\right\}. \quad (8)$$

In (8), $L_0(t_j)$ is the maximum level of loss, which is incurred when action is not taken until the final stage and the storm strikes. In this equation, $a_j(t_j)$ is the capacity of the infrastructure system, or the protection rate per stage (e.g., the number of vehicles that can be evacuated per hour). The rate $a_j(t_j)$ is a function of stage j and intensity t_j. It is not necessarily constant but can change by t_j because the extent of infrastructure for the protective action can change according to the DM's belief about the landfall intensity. For example, if the landfall intensity is believed to be Category 1, the infrastructure within a small area determines the capacity. However, if the expected landfall intensity is Category 5, people in a much larger area should be protected and the infrastructure therein determines the capacity.

The cost of taking action or evacuating consists of two components: the direct cost of the evacuation (e.g., transportation and housing) and opportunity costs such as

forgone income. It is assumed that the cost of action is a function of landfall intensity and lead-time. $C_j(t_j)$ means the level of cost of protected action when the protective action is started at stage j and the intensity of the event is expected to be t_j. The general form of $C_j(t_j)$ is defined as

$$C_j(t_j) = mC + j \cdot d_j(t_j). \tag{9}$$

mC is minimum cost of action. $d_j(t_j)$ is incremental cost of action per period at stage j when the expected intensity is t_j. Figure 13 displays possible cost functions.

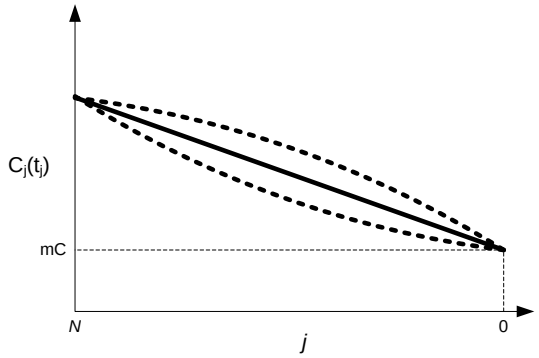

Figure 13. General shape of cost of action.

If $d_j(t_j)$ is a linear function of j, the action cost function will resemble the solid line. If $d_j(t_j)$ is not a linear function of j, the action cost function may resemble one of the dotted lines. If $mC > 0$ and $d_j(t_j) = 0$, the action cost is constant, i.e., fixed cost. The value of t_j can change the slope of the line in Figure 13. This implies that if a higher-category hurricane is going to strike, more people should evacuate and the evacuation cost becomes higher.

3.2.6. Modeling improvements in forecasting ability and evacuation speed

The DM's estimates of the strike probability and of the landfall intensity are revised at each stage, independently of each other. However, the transition matrices will not be identical for all stages if the transition probabilities differ depending on stage or lead-time before landfall. For example, in the early stages, the DM's prior estimate of the strike probability does not change appreciably. Therefore, the variance of the transition distribution is small. However, if landfall is imminent, the DM's prior estimate of the strike probability moves toward 1 or 0 instead of staying close to the prior value.

Track forecast improvement is used here to mean the reduction of the mean absolute error (MAE) of a track forecast. MAE of a track forecast is usually larger for a longer forecast lead-time. By improving forecasting ability, the MAE cone of a track forecast becomes narrower as shown in Figure 14 and strike probability for a target becomes sharper. Thus, the improvement of a track forecast is modeled here such that the standard deviation of its transition probability distribution increases at the same rate for all stages.

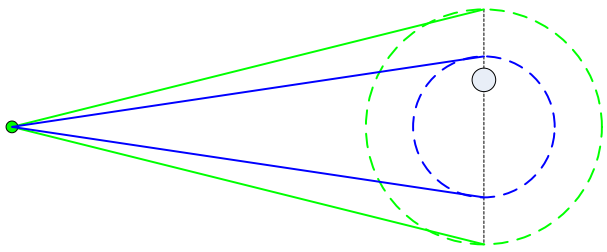

Figure 14. Cone of uncertainty with different track forecast qualities.

This paper addresses only improvements in track forecasting. Improvements in intensity forecasting will be addressed in future research. Therefore, "forecast quality" should be interpreted here as "track forecast quality."

In order to model the improvement in forecasting ability, the parameter r_S is used to redefine the variance of state transition probability distribution for S_j at stage j in (6) as

$$\sigma_j^2 = \left(\frac{\sigma / r_S}{j + \varepsilon} \right)^2 = \frac{(\sigma / r_S)^2}{(j + \varepsilon)^2}. \tag{10}$$

$r_S = 1$ implies the current track forecast quality. $r_S \approx 0$ implies perfect information on the storm track. $r_S \approx \infty$ implies that no information is available on the storm track. Using the revised variance of state transition probability distribution at each stage from N to 0, parameters of the Beta distribution are recalculated and the transition probability matrices for all stages are revised. Thus, the revised transition probability matrices reflect forecast improvement at a constant rate across stages.

The improvement of evacuation speed is modeled such that the slope of the $L_j(t_j)$ curve increases after the critical point, as illustrated in Figure 12. As the evacuation speed is improved, the slope becomes steeper and the critical decision point of evacuation shifts toward the final stage. To model the improvement in evacuation speed, an improvement parameter r_E is introduced into (8). The resulting redefinition of $L_j(t_j)$ is

$$L_j(t_j) = \max\left\{0, L_0(t_j) - \frac{a_j(t_j)}{r_E} \max\{0, j - m\}\right\}. \tag{11}$$

An r_E value equal to 1 implies the current evacuation speed or evacuation capacity. $r_E \approx 0$ implies infinite evacuation capacity. If *m*, the minimum time requirement for evacuation, is 0, $r_E \approx 0$ means instantaneous evacuation. $r_E \approx \infty$ implies that no protective action or evacuation route is available.

The transition probability matrices need to be manipulated to best represent the nature of the revision of a DM's belief. They also need to be controlled to represent improved forecasting. This was done using a Beta distribution, a well-defined flexible probabilistic distribution that can be manipulated by a few parameters. Its pdf function is defined as follows:

$$f(x) = \frac{1}{B(\alpha,\beta)} x^{\alpha-1}(1-x)^{\beta-1}, \quad x \in [0,1],$$

where $B(\alpha,\beta) = \int_0^1 t^{\alpha-1}(1-t)^{\beta-1}dt.$

A Beta density function can take on different shapes depending on the values of parameters α and β. It can be U-shaped, strictly decreasing or increasing, strictly convex or concave, straight line, uniform, or unimodal. In the early stages of hurricane forecasting, as seen in Figure 8, the strike probability remains fairly stable over time and the transition matrix is almost diagonal. At close-to-final stages, the strike probabilities change noticeably toward 0 or 1 rather than in-between, and therefore the transition matrix has a U shape in each row.

Another benefit of the Beta distribution is that it is supported on the bounded interval [0, 1], which means that the model does not have to truncate unnecessary tails of the transition distribution outside the valid range.

New information at near-final stages has a large impact on the state variable s_j, resulting in a more dispersed transition distribution. Therefore, a changing variance that grows faster as it approaches the final stage must be used. To calculate the variance at each stage, a number reciprocally proportional to the square of remaining periods before landfall is used with a scale parameter. In this model, variance at stage j is defined as $K_S/(j+\varepsilon)^2$ as in Equation (7), where K_S is a scale parameter. In an early stage, such as $j = N-1$, the variance grows slowly. However, it grows rapidly as it approaches the final stage, $j = 1$. With the given mean and the calculated variance, the transition distribution of each row of the transition matrix at each stage is defined as a Beta distribution and each transition probability is determined by the discretization of the distribution.

If the prior value of state variable S_j is very close to 0 because the target is far outside the uncertainty cone, or very close to 1 because the target is right on the estimated track of the imminent hurricane, the calculated value of α or β can be non-positive, which is not acceptable for a Beta distribution. To prevent this, our model has absorbing states for state variable S_j. If the value of state variable S_j changes to 0 or 1 after discretization, it cannot leave that state for the remaining stages. Due to the absorbing states, transition probabilities associated with prior states 0 and 1 have special values as

$$p_{0,0} = p_{1,1} = 1$$

$$p_{0,s_j} = 0 \ \forall s_j \neq 0, \qquad p_{1,s_j} = 0 \ \forall s_j \neq 1.$$

Other transition probabilities are defined as

$$p_{s_i,s_j} = \int_{s_j - ds/2}^{s_j + ds/2} f(x)dx .$$

In this equation, s_i is the prior value of the state variable before the transition and s_j is its posterior value after the transition. The interval between the consecutive values of the state variable is *ds*. The pdf of the Beta distribution defined by s_i and the calculated variance is *f*. For example, if *ds* is 0.1, $p_{0.1,0.2}$ is defined as

$$p_{0.1,0.2} = \int_{0.15}^{0.25} f(x)dx .$$

The mean of Beta distribution is 0.1 in this example, and the pdf *f* is defined accordingly.

Likewise, if the prior value of state variable T_j is very close to 0 because the storm is thought to be dissipating, or very close to 5 because the storm is very close to the target and is maintaining maximum strength, the calculated value of α or β can be non-positive, which is not acceptible for a Beta distribution. To prevent this, our model has absorbing states for the state variable T_j.[5] If the value of state variable T_j changes to 0 or 5, it cannot leave that state. Due to the absorbing states, transition probabilities associated with prior state 0 and 5 have special values as

[5] The absorbing states exist because of the simplified categories and the consistency assumption about the expected value of state variables.

$$q_{0,0} = q_{5,5} = 1$$
$$q_{0,t_j} = 0 \ \forall t_j \neq 0, \qquad q_{5,t_j} = 0 \ \forall t_j \neq 5.$$

Other transition probabilities are defined as

$$q_{t_i,t_j} = \int_{t_j - dt/2}^{t_j + dt/2} g(y)dy .$$

In this equation, t_i is the prior value of the state variable before the transition and t_j is its posterior value after the transition. dt is the interval between the consecutive values of the state variable. $g(y)$ is the pdf of the Beta distribution defined by t_i and the calculated variance. For example, if dt is 1, $q_{1,2}$ is defined as follows:

$$q_{1,2} = \int_{1.5}^{2.5} g(y)dy .$$

The mean of the Beta distribution is 1 in this example, and the pdf g is defined accordingly.

In the transition probability matrix of state variable S_j for close-to-final stages, the transition distribution of each row approaches a complete U-shape, which means perfect information, and the calculated value of α or β can be non-positive, which is not acceptable for a Beta distribution. If this is the case, transition probabilities are calculated to maintain the DM's rationality as

$$\begin{aligned} p_{s_i,sj} &= 1 - s_i \quad \text{if } s_j = 0 \\ &= s_i \quad \text{if } s_j = 1 \\ &= 0 \quad \text{otherwise.} \end{aligned}$$

By this definition, $\mathrm{E}\left[S_j \mid S_i = s_i\right] = (1 - s_i)0 + s_i \cdot 1 = s_i$ for all $j < i$ and the mean of transition does not change. Using our Markov chain model, the pattern of the range of the strike probability at each stage roughly matches the work of Regnier (2008), as illustrated in Figure 15. In this example, transition probabilities less than 0.1 are ignored to remove thin tails from each transition distribution. To discretize the value of strike probabilities, this example used 11 categories from 0 to 1. In this figure, a DM's belief about the strike probability starts at 0.1 and remains so in early stages because of the weakness of the new information available at this time. As lead-time decreases, the new information becomes stronger and begins to influence the DM's belief. As the final stage approaches, the new information gains power and the DM becomes more certain about whether the hurricane will strike the target. At the final stage, the DM definitively knows the outcome.

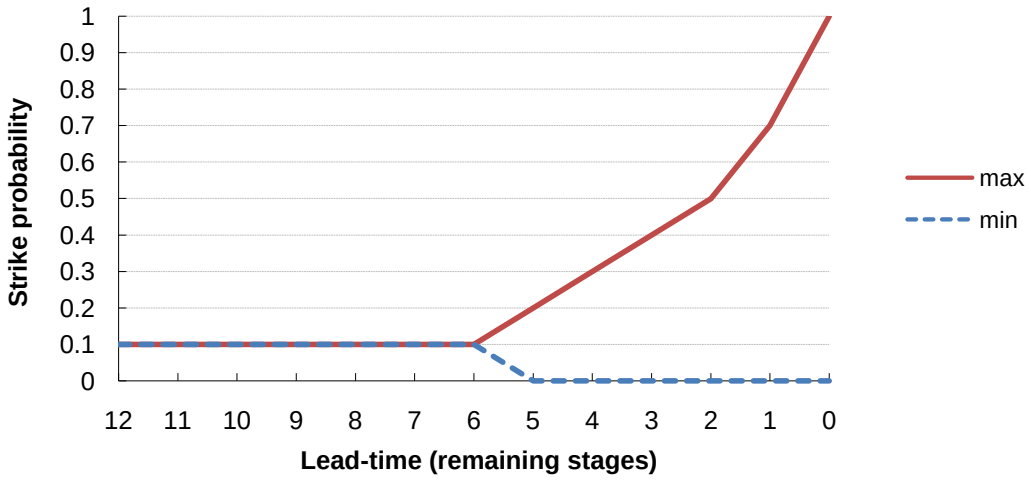

Figure 15. Range of strike probability at each transition.

An example of the optimal policies as a function of stage (j) and strike probability (S_j) is shown in Table 8. In this table, E stands for Evacuate, N stands for Do Not Evacuate, and W stands for Wait. Constant C_j is assumed in this example. As seen in the table, the Wait region is narrowed as the final stage approaches and Wait cannot be an optimal policy after a critical point.

Table 8. An example of optimal policies from the model.

S_j \ j	12	11	10	9	8	7	6	5	4	3	2	1
0	N	N	N	N	N	N	N	N	N	N	N	N
0.05	W	W	W	W	W	W	W	W	W	E	E	E
0.10	W	W	W	W	W	W	W	W	W	E	E	E
0.15	W	W	W	W	W	W	W	W	W	E	E	E
0.20	W	W	W	W	W	W	W	W	E	E	E	E
0.25	W	W	W	W	W	W	W	E	E	E	E	E
0.30	W	W	W	W	W	W	E	E	E	E	E	E
0.35	W	W	W	W	E	E	E	E	E	E	E	E
0.40	E	E	E	E	E	E	E	E	E	E	E	E
0.45	E	E	E	E	E	E	E	E	E	E	E	E
0.50	E	E	E	E	E	E	E	E	E	E	E	E
0.55	E	E	E	E	E	E	E	E	E	E	E	E
0.60	E	E	E	E	E	E	E	E	E	E	E	E
0.65	E	E	E	E	E	E	E	E	E	E	E	E
0.70	E	E	E	E	E	E	E	E	E	E	E	E
0.75	E	E	E	E	E	E	E	E	E	E	E	E
0.80	E	E	E	E	E	E	E	E	E	E	E	E
0.85	E	E	E	E	E	E	E	E	E	E	E	E
0.90	E	E	E	E	E	E	E	E	E	E	E	E
0.95	E	E	E	E	E	E	E	E	E	E	E	E
1	E	E	E	E	E	E	E	E	E	E	E	E

3.3. Risk-averse Decision Maker

To keep the model simple, a risk-neutral DM is assumed. However, if the DM's utility function for the expense generated by the decision and outcome were presumed exponential instead of linear, risk aversion could be captured by recasting the dynamic

programming recursion in terms of certainty equivalents rather than expected values, as in Bickel and Smith (2006). Since all the monetary values in our problem are expenses, an optimal decision is made so that the certainty equivalent of policy is minimized. Therefore, suppose the DM's utility function is u(x) = exp(x/R), where x is the expense and R is the DM's risk tolerance. With this utility function, the certainty equivalent of a policy $\tilde{x}$ is given by CE[$\tilde{x}$] = R·ln(E[exp($\tilde{x}$ /R)]). The recursive calculation of certainty equivalents exploits the "delta property" of the exponential utility function: If a constant Δ is added to all outcomes of a gamble $\tilde{x}$, its certainty equivalent increases by Δ; that is, CE[$\tilde{x}$ + Δ] = CE[$\tilde{x}$] + Δ.

If a Beta-Bernoulli conjugate pair information structure is used, then a dynamic program using the CE from the exponential u-value function is structured as

for counting-up stage k = 0, 1,⋯, N,

$$V_k(p_k) = \min\{CE(\text{ignore}), CE(\text{act}), CE(\text{wait})\}$$
$$= \min\left\{R\ln\left((1-p_k)e^{0/R} + p_k e^{L/R}\right), R\ln\left((1-p_k)e^{C_k/R} + p_k e^{(C_k+L_k)/R}\right), \gamma + R\ln(E[e^{\bar{V}_{k+1}(p_k)/R}])\right\}$$

, for $p_k \in (0,1)$

$$E\left[e^{\bar{V}_{k+1}(p_k)/R}\right] \equiv \sum_{x=0}^{1} p_k{}^x (1-p_k)^{1-x} \exp\left(V_{k+1}\left(\frac{(\alpha+\beta+k)p_k + x}{\alpha+\beta+k+1}\right)/R\right)$$

$$E\left[e^{\bar{V}_N(p_{N-1})/R}\right] = (1-p_{N-1})e^{0/R} + p_{N-1}e^{L/R}$$

or

for counting-down stage j = N, N-1,⋯, 0,

$$V_j(p_j) = \min\{CE(\text{ignore}), CE(\text{act}), CE(\text{wait})\}$$
$$= \min\left\{R\ln\left((1-p_j)e^{0/R} + p_j e^{L/R}\right), R\ln\left((1-p_j)e^{C_j/R} + p_j e^{(C_j+L_j)/R}\right), \gamma + R\ln(E[e^{\bar{V}_{j-1}(p_j)/R}])\right\}$$
$$\text{, for } p_j \in (0,1)$$
$$E\left[e^{\bar{V}_{j-1}(p_j)/R}\right] \equiv \sum_{x=0}^{1} p_j{}^x (1-p_j)^{1-x} \exp\left(V_{j-1}\left(\frac{(\alpha+\beta+N-j)p_j + x}{\alpha+\beta+N-j+1}\right)/R\right)$$
$$E\left[e^{\bar{V}_0(p_1)/R}\right] = (1-p_1)e^{0/R} + p_1 e^{L/R}.$$

However, if a Markov process is used to model the revision of beliefs, then a dynamic program using the CE from the exponential u-value function is structured as

$$V_j(s_j) = \min\{CE(\text{ignore}), CE(\text{act}), CE(\text{wait})\}$$
$$= \min\left\{R\ln\left((1-s_j)e^{0/R} + s_j e^{L/R}\right), R\ln\left((1-s_j)e^{C_j/R} + s_j e^{(C_j+L_j)/R}\right), \gamma + R\ln(E[e^{\bar{V}_{j-1}(s_j)/R}])\right\}$$
$$\text{, for } s_j \in \Omega = \{0, 0.05, \cdots, 0.95, 1\}$$
$$E\left[e^{\bar{V}_{j-1}(s_j)/R}\right] \equiv \sum_{s_{j-1}\in\Omega} p_{s_j, s_{j-1}} \exp\left(V_{j-1}(s_{j-1})/R\right)$$
$$E\left[e^{\bar{V}_0(s_1)/R}\right] = (1-s_1)e^{0/R} + s_1 e^{L/R}.$$

3.4. Modeling the Investment Decision

The investment decision has two cases: mutually exclusive investments and a mix of investments. In the case of mutually exclusive investments, the investment-decision problem is modeled as follows:

$$\begin{aligned} &\arg\min_{(x,y)\in\{(r_S,1),(1,r_E)\}} V_j(s_j,t_j,x,y) \\ &s.t.\ G(r_S) \le B \\ &\quad H(r_E) \le B \\ &\quad 0 \le r_S \le 1 \\ &\quad 0 \le r_E \le 1 \end{aligned} \tag{12}$$

$G(r_S)$ is the investment amount that brings about the forecast accuracy improvement r_S, $H(r_E)$ is the investment amount that brings about the evacuation speed improvement r_E, and B is the budget. $V_j(s_j,t_j,r_S,r_E)$ is the anticipated expense when strike probability is s_j, expected landfall intensity is t_j, forecast accuracy is improved by r_S, and evacuation speed is improved by r_E. Given s_j, t_j, and B, this formulation specifies the better investment between forecast accuracy improvement only and evacuation speed improvement only.

In the case of a mix of investments, the investment-decision problem is modeled as follows:

$$\begin{aligned} &\arg\min_{r_S,r_E} V_j(s_j,t_j,r_S,r_E) \\ &s.t.\ G(r_S)+H(r_E) \le B \\ &\quad 0 \le r_S \le 1 \\ &\quad 0 \le r_E \le 1 \end{aligned} \tag{13}$$

Given s_j and t_j, this formulation specifies an optimal combination of r_S and r_E that minimizes the anticipated expense within budget. The function $V_j(s_j,t_j,r_S,r_E)$ also defines the evacuation-decision problem, as explained in subsequent sections.

4. APPLYING THE MODEL: AN EXAMPLE

One of the most damaging and potentially deadly natural disasters that occur in the US is a hurricane. Of the various effects of a hurricane, storm surge poses the highest threat to life and destruction in many coastal areas throughout the US.[6] In this section, our model is applied to an actual community, San Patricio County, along the Texas Gulf Coast. It is assumed that the natural hazard is a hurricane and the major protective action is population evacuation from the storm surge areas. San Patricio County was selected because of its uncomplicated topography and simple primary evacuation route in comparison to other areas.

In the DP model for the hurricane case, stage j starts at N and ends at 0. Thus, N represents the initial number of remaining stages until landfall. Stage 0 is the stage when the detected hurricane would hypothetically make landfall on a designated target. At this stage, it becomes clear whether the hurricane hits the target. Because the uncertainty of landfall timing is much less than other uncertainties, it is assumed that a DM knows N. "Stage" represents the cycle of the hurricane forecasts as well as the decision points. Because hurricane forecasts are usually made every 6 hours, the interval between the stages is 6 hours and a DM is presumed to make a multi-stage decision every 6 hours. Because the lead-time for a hurricane forecast may be up to 120 hours, the value of N is at most 20. If a tropical storm originates near the coast, the value of N will be much less than 20.

[6] Refer to FEMA (2007) at http://www.fema.gov/hazard/hurricane/hu_hazard.shtm.

At any given stage j, the DM believes that the probability of landfall on the area at stage 0 is $S_j = s_j$ and the hurricane intensity at landfall is $T_j = t_j$. The DM is assumed to accept the hurricane forecasts from the National Hurricane Center (NHC) at face value without adjustment.

The revision of the strike probability at each stage is modeled using a Markov chain, and its transition probability matrix can be built by finding a best-fit matrix using historical forecast data of strike probabilities. Because this would entail collecting large amounts of hurricane forecast data and the focus of this analysis is the value of the improvement rather than current performance, plausible matrices were devised to model the revision of the strike probability.

State variable S_j represents the DM's belief on the strike probability of a detected hurricane on a target at stage 0, and s_j represents its value. State variable T_j represents the DM's belief about the expected storm intensity in terms of the hurricane category along the Saffir-Simpson scale, and t_j represents its value. $t_j = 0$ means an intensity less than Category 1. S_j has 21 states (0, 0.05,⋯, 0.95, 1), and T_j has 6 states (0, 1, 2, 3, 4, 5). Each component of the base DP model is explained in the following sections.

In this section, how the loss level function and its components are built is described starting with the number of vehicles at risk when facing a hurricane. After that, the evacuation cost function and its components are described. And then, how the transition matrices are built is addressed. Next, optimal policies for this area given stage (j), strike probability (s_j), and expected landfall intensity (t_j) are illustrated. And later, sensitivity to each improvement and issues about sectional improvement of infrastructure are

discussed. Finally, the optimal investment decision and cumulative benefit of each investment is shown.

4.1. Vehicles at Risk

$RV_j(t_j)$ is the number of vehicles that remain in risky areas at landfall when the evacuation starts at stage j and the hurricane category at landfall is believed to be t_j. This component is not explicit in the base DP model, but is a key element that is used to calculate $C_j(t_j)$ and $L_j(t_j)$.

$RV_j(t_j)$ is determined by the evacuation demand in the area, capacity of the primary evacuation route (PER), evacuation timing, the intensity of the hurricane, etc. An approximation model was developed to estimate $RV_j(t_j)$ using the model for the number of evacuating vehicles and the evacuation time estimate in Lindell (2008). The value of t_j determines the scope of the evacuation. The areas affected by storm surge from different categories of hurricane are called "risk areas," which are determined by the SLOSH[7] model (Lindell, Prater, & Wu, 2002). For example, if $t_j = 1$, only risk area 1 is influenced and needs to evacuate. If $t_j = 3$, risk areas 1, 2, and 3 are affected and should evacuate. Their model gives different estimates for different risk areas, which are determined by storm-surge level. We simplified this model to remove the risk area factor because it was not needed. $RV_j(t_j)$ is defined as

$$RV_j(t_j) = \max\left\{0, EV(t_j) - \frac{CAPA}{r_E} \times \max\left[0, 6j - 10^{th}\, TGT - \frac{MED(t_j)}{30mph}\right]\right\}. \quad (14)$$

[7] Sea, Lake, and Overland Surge from Hurricanes (SLOSH) is a computerized model developed by the Federal Emergency Management Agency (FEMA), United States Army Corps of Engineers (USACE), and the National Weather Service (NWS) to estimate storm surge depths.

In this equation, $EV(t_j)$ is the total number of evacuating vehicles when the hurricane category at stage 0 is believed to be t_j. *CAPA* is the evacuation capacity of the PER in number of vehicles per hour. r_E is the evacuation improvement parameter. 10^{th} *TGT* is the 10^{th} percentile of trip generation time,[8] which is the necessary time before people actually start evacuation (Lindell et al., 2002). As discussed later, tenth percentile is used rather than mean or other percentile because it gives better approximation of evacuation time estimate.

$MED(t_j)$ is the maximal evacuation distance when the hurricane intensity at stage 0 is believed to be t_j. In this example, the change of r_E cannot reduce trip generation time or time spent on the PER; it only reduces the waiting time until entering the PER. $MED(t_j)$ / 30 mph is the time required for a vehicle to travel at 30 mph from the farthest populated location on the coast to the inland boundary of the appropriate risk area (e.g., risk area 4 for a Category 4 hurricane) and is adopted from Lindell et al. (2002). $MED(t_j)$ or maximum evacuating distance in hurricane intensity t_j is summarized in Table 9 (Lindell, 2008).

Table 9. Maximal evacuation distance in different hurricane intensities (San Patricio County).

Hurricane intensity	CAT 1	CAT 2	CAT 3	CAT 4	CAT 5
Max distance	1	2	31	34	35

$RV_j(c)$ values are calculated as follows. $t = 6j$ is the remaining time before landfall in hours and $RV_j(c)$ is calculated as

[8] How trip generation time is estimated is described in Lindell (2008).

$$RV_j(c) = \max\left\{0, \text{EVc} - \text{CAPA}_{\text{PER}} \max\left\{0, t - 10^{\text{th}}\text{TGT} - \text{MaxDist}/30\text{mph}\right\}\right\}$$
$$RV_j(1) = \max\left\{0, 9401 - 1600 \max\left\{0, t - 1.5 - 1/30\right\}\right\}$$
$$RV_j(2) = \max\left\{0, 14552 - 1600 \max\left\{0, t - 1.5 - 2/30\right\}\right\}$$
$$RV_j(3) = \max\left\{0, 21527 - 1600 \max\left\{0, t - 1.5 - 31/30\right\}\right\}$$
$$RV_j(4) = \max\left\{0, 24536 - 1600 \max\left\{0, t - 1.5 - 34/30\right\}\right\}$$
$$RV_j(5) = \max\left\{0, 25407 - 1600 \max\left\{0, t - 1.5 - 35/30\right\}\right\},$$

where EVc is the total number of evacuating vehicles for a Category *c* hurricane, CAPA_{PER} is capacity of the PER in number of vehicles per hour, 10^{th} TGT is the 10^{th} percentile of trip generation time, and MaxDist is maximum evacuation distance. The results are summarized in Table 10, where the number of evacuating vehicles and PER capacity are taken from Lindell et al. (2002), and max evacuation distance is taken from Lindell (2008).

Table 10. Calculated number of remaining vehicles given evacuation timing and intensity when using the 10th percentile of TGT.

$t = h \cdot j$ (hours)	20	19	18	17	16	15	14	13	12	11	10	9	8	7	6	5	4	3	2	1	0
Cat 1	0	0	0	0	0	0	0	0	0	0	0	0	1135	2735	4335	5935	7535	9135	9401	9401	9401
Cat 2	0	0	0	0	0	0	0	0	0	1486	3086	4686	6286	7886	9486	11086	12686	14286	14552	14552	14552
Cat 3	0	0	0	0	461	2061	3661	5261	6861	8461	10061	11661	13261	14861	16461	18061	19661	21261	21527	21527	21527
Cat 4	0	0	270	1870	3470	5070	6670	8270	9870	11470	13070	14670	16270	17870	19470	21070	22670	24270	24536	24536	24536
Cat 5	0	0	1141	2741	4341	5941	7541	9141	10741	12341	13941	15541	17141	18741	20341	21941	23541	25141	25407	25407	25407

The capacity of the PER in San Patricio County was defined in Lindell et al. (2002). That area has two evacuation routes, each with a capacity of 800 vehicles per hour. Since they are separate routes, the total capacity of the area is the sum of the two capacities, which is 1600 vehicles per hour. Because SH 361 and SH 35 converge to US 181, the capacity of US 181 determines the evacuation capacity of vehicles for this route.

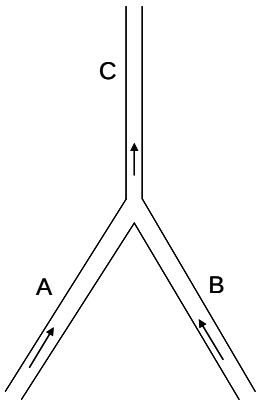

Figure 16. Converging route.

If the structure of the PER forms a network, however, total capacity of the PER is not simply the sum of the separate capacities. Figure 16 illustrates a converging route. Two roads (A and B) start from an area at risk and they converge to one road (C) before it reaches the edge of the area. There is an example of this kind of route in San Patricio County, where SH 361 and SH 35 converge to US 181. If each road has the same capacity, the capacity of this ERS equals that of road C even though the sum of the capacities of road A and road B may be greater than that. Therefore, if the capacity of each road is 1000 vehicles per hour, then the capacity of this system is 1000 vehicles per hour.

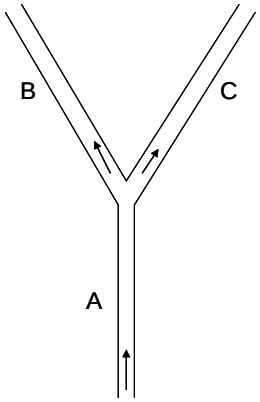

Figure 17. Diverging route.

Figure 17 depicts a diverging route. One road (A) starts from an area at risk and diverges to two roads (B and C) before reaching the edge of the area. If each road has the same capacity, the capacity of this ERS is determined by road A. Therefore, if the capacity of each road is 1000 vehicles per hour, then the capacity of this system is 1000 vehicles per hour.

The systems in Figure 16 and Figure 17 have the same capacity, but a converging route is better in the last-minute evacuation scenario. If a hurricane's movement at sea parallels a coastline and suddenly changes its track toward the coastal area, people in the area have to start evacuation when landfall is imminent. They can reach the junction area, which is less risky than the coast, faster in a converging route than in a diverging route. If the capacity of each road in the two figures is the same, 2000 vehicles can reach the junction area in Figure 16 in the time that 1000 vehicles can reach the junction area in Figure 17. This study, however, does not account for that kind of delicate interaction of the capacities in evacuation routes.

Lindell (2008) showed how to estimate the total number of evacuating residents' vehicles and evacuating transients' vehicles. The present example ignores transients' vehicles because transients are far outnumbered by residents, are especially sensitive to the weather, usually start evacuation even before the evacuation order is issued, and have a much shorter trip generation time than do residents.

This example uses Equation (15), simplified from Lindell (2008), to estimate the number of evacuating vehicles given storm category ($EV(t_j)$) in San Patricio County. The number of residents' vehicles evacuating during a Category *c* hurricane is defined as

$$EV(t_j = c) = (Pop_R D_{Rc}) / PHH_R (1 - TD_R)(EVHH_R + ETHH_R)(1 - S_R)U_R . \quad (15)$$

In this equation, Pop_R is the residential population in all five risk areas, PHH_R is the number of persons per residential household, D_{Rc} is the proportion of residential households deciding to evacuate facing a Category *c* hurricane, and TD_R is the proportion of transit-dependent residential households. $EVHH_R$ is the average number of evacuating vehicles per residential household, $ETHH_R$ is the average number of evacuating trailers per residential household, S_R is the proportion of early residential evacuees (those evacuating before an official warning is issued), and U_R is the proportion of residential households who use the official evacuation route system.

As stated above, EMBLEM2 by Lindell (2008) has been simplified for our use. Lindell (2008) suggested the following equation to estimate the number of residents' vehicles (EV_{Rrsc}) evacuating from a given emergency response planning area ($ERPA_{rs}$) – sector *s* of risk area *r* – during a Category *c* hurricane:

$$EV_{Rrsc} = (Pop_{Rrs} / PHH_R) D_{Rrc} (1 - TD_R)(EVHH_R + ETHH_R)(1 - S_R) U_R$$
$$= (Pop_{Rrs} D_{Rrc}) / PHH_R (1 - TD_R)(EVHH_R + ETHH_R)(1 - S_R) U_R .$$

In this equation, Pop_{Rrs} is the residential population of sector *s* in risk area *r* (summarized in Table 11), PHH_R is the number of persons per residential household, D_{Rrc} is the proportion of residential households in risk area *r* deciding to evacuate in a Category *c* hurricane (summarized in Table 12), and TD_R is the proportion of transit-dependent residential households. Moreover, $EVHH_R$ is the average number of evacuating vehicles per residential household, $ETHH_R$ is the average number of evacuating trailers per residential household, S_R is the proportion of early residential evacuees (those evacuating before an official warning is issued), and U_R is the proportion of residential households who use the official ERS.

Lindell's model gives different estimates for different risk areas, reflecting that their optimal evacuation decisions can be different. His model has been simplified to remove the risk area factor because it is not needed here. The simplified equation to estimate the number of residents' vehicles evacuating from a given emergency response planning area ($ERPA_s$) – sector *s* – during a Category *c* hurricane is

$$EV_{Rsc} = (Pop_{Rs} D_{Rc}) / PHH_R (1 - TD_R)(EVHH_R + ETHH_R)(1 - S_R) U_R ,$$

where D_{Rc} is calculated as

$$Pop_{Rs}D_{Rc} = \sum_{r=1}^{5} PoP_{Rrs}D_{Rrc}$$

$$D_{Rc} = \frac{\sum_{r=1}^{5} PoP_{Rrs}D_{Rrc}}{PoP_{Rs}}$$

and summarized in Table 13, which determines the probability (or proportion) of people staying at home versus on the road when the hurricane category is believed to be CAT.

Table 11. Population in each risk area for San Patricio County (Pop_{Rrs}).

Risk area	Population
1	7710
2	4143
3	30238
4	6803
5	7849
Total	56743

Table 12. Proportion of residential households in risk area *r* deciding to evacuate in Category *c* hurricane (D_{Rrc}).

Risk area	Category 1	Category 2	Category 3	Category 4	Category 5
1	45.9%	63.7%	87.8%	98.2%	100.0%
2	35.9%	53.7%	77.8%	88.2%	91.4%
3	31.1%	48.9%	73.0%	83.4%	86.6%
4	28.2%	46.0%	70.1%	80.5%	83.7%
5	26.5%	44.3%	68.4%	78.8%	82.0%

Table 13. Proportion of residential households deciding to evacuate in Category *c* hurricane (D_{Rc}) for San Patricio County.

Category 1	Category 2	Category 3	Category 4	Category 5
32.48%	50.28%	74.38%	84.78%	87.79%

Using the data for San Patricio County, EV_{Rsc} and EV_{Tsc} (= EV_{T1sc}) are calculated in Table 14.

Table 14. Number of evacuating vehicles for different hurricane categories in San Patricio County.

Variable	Category 1	Category 2	Category 3	Category 4	Category 5
EV_{Rsc}	6985.03	10813.34	15996.61	18233.37	18880.69
EV_{Tsc}	382.85	382.85	382.85	382.85	382.85
$EV_{Rsc} + EV_{Tsc}$	7367.88	11196.19	16379.46	18616.22	19263.54

Following Lindell (2008), the time required for an individual resident or transient household to evacuate after incident initiation can be defined as the sum of four time components,

$$t_T = t_d + t_w + t_p + t_e, \tag{16}$$

where t_T is a household's total clearance time, t_d is the authorities' decision time, t_w is the household's warning receipt time, t_p is the household's evacuation preparation time, and t_e is the household's evacuation travel time.

The evacuation travel (t_e) component is expanded by assuming that evacuating households leave the risk area in three steps: (a) traveling from the home to PERs via collectors and arterials, (b) waiting in queues for access to the PER (which will have duration 0 for the first households to evacuate), and (c) traveling from the queues onto the PER and out of the risk area. That is,

$$t_e = t_c + t_q + t_h,$$

where t_e is an evacuating vehicle's evacuation travel time (from Equation (16)), t_c is the time spent traveling from home to the PER, t_q is the time spent in a queue awaiting access to the PER, and t_h is the time spent traveling on the highway (i.e., the PER). If

ERPAs are sufficiently small, t_c will be negligible because evacuating vehicles need to travel only a short time to reach the PER. Therefore, Equation (16) can be expanded as

$$t_T = t_d + t_w + t_p + t_c + t_q + t_h .$$

Warning time and preparation time can be represented by cumulative distribution functions of the form

$$p_t = 1 - \exp(-at^b),$$

where p_t is the proportion of households that have been warned at time t and exp denotes the base of the natural logarithm (e), which is multiplied by the coefficient a and raised to the b power. This is a Weibull distribution with parameters $k = b$ and $\lambda = (1/a)^{1/b}$. Its mean is $\lambda\Gamma\left(1+1/k\right) = (1/a)^{1/b}\Gamma\left(1+1/b\right)$. If the values of a and b applied to Lindell (2008) are used, the mean warning time is 0.5 hour and the mean preparation time if the residents are at home is 2.33406 hours. Following Lindell et al. (2002), preparation times were calculated on the assumption that risk area residents would be at home.

Lindell et al. (2002) showed that there are two evacuation routes used in San Patricio County and the capacity of each evacuation route is 800 vehicles per hour. Because they are separate routes, the total capacity of the area is the sum of the two capacities, which is 1600 vehicles per hour. In this area, SH 361 and SH 35 converge to US 181 and the capacity of this route is determined by the capacity of US 181.

In sparsely populated counties where queues will not develop, the ETE is the trip generation time for the 98th percentile household plus the time required to travel the max distance at 30 mph (Lindell et al., 2002).

Assuming that t_d, t_c, and t_q are negligible, ETEs in San Patricio County are roughly:

$$\text{Mean TGT} + (\text{total number of evacuating vehicles}) / \text{capacity} + \text{max dist.} / 30\,\text{mph}$$
$$0.5 + 2.33406 + 9401/1600 + 1/30 = 8.74302 \ (> 8) \text{ for CAT 1 hurricane,}$$
$$0.5 + 2.33406 + 14552/1600 + 2/30 = 11.99573 \ (> 11) \text{ for CAT 2 hurricane,}$$
$$0.5 + 2.33406 + 21527/1600 + 31/30 = 17.32177 \ (> 15) \text{ for CAT 3 hurricane,}$$
$$0.5 + 2.33406 + 24536/1600 + 34/30 = 19.30239 \ (> 17) \text{ for CAT 4 hurricane, and}$$
$$0.5 + 2.33406 + 25407/1600 + 35/30 = 19.88010 \ (> 18) \text{ for CAT 5 hurricane.}$$

These estimates are longer than the ETEs in Lindell et al. (2002). Because total number of evacuating vehicles divided by capacity is the estimate of the time duration between the first and last evacuating vehicles entering the PER, there is some overlap between mean trip generation time and the time interval just mentioned. In other words, some evacuating vehicles enter the PER even before other vehicles leave home.

To reduce this overlap, the 10^{th} percentile household is used rather than the mean trip generation time, which changes the estimate to

$$\text{ETE}_c = 10^{\text{th}} \text{ percentile of TGT} + (\text{total number of evacuating vehicles}) / \text{capacity} + \text{max dist.} / 30\,\text{mph}$$
$$\text{ETE}_{\text{CAT1}} = 1.5 + 9401/1600 + 1/30 = 7.40896 \ (< 8)$$
$$\text{ETE}_{\text{CAT2}} = 1.5 + 14552/1600 + 2/30 = 10.66167 \ (< 11)$$
$$\text{ETE}_{\text{CAT3}} = 1.5 + 21527/1600 + 31/30 = 15.98771 \ (> 15)$$

$$\mathrm{ETE}_{\mathrm{CAT4}} = 1.5 + 24536/1600 + 34/30 = 17.96833 \quad (> 17)$$
$$\mathrm{ETE}_{\mathrm{CAT5}} = 1.5 + 25407/1600 + 35/30 = 18.54604 \quad (> 18).$$

This shows that 10th percentile of TGT produces less mean error and gives better approximation than mean TGT.

Lindell (2008) provided the proportion of residential households in risk area *r* deciding to evacuate in a Category *c* hurricane (D_{Rrc}). D_{Rc} is the average of D_{Rrc} for hurricane Category *c* weighted by the population of risk areas.[9]

In San Patricio County, PHH_R is 2.94, TD_R is 8%, $EVHH_R$ is 1.6, $ETHH_R$ is 0.3, S_R is 25%, and U_R is 85% (Lindell, 2008). Numbers of evacuating residents' vehicles calculated using Equation (15) are summarized in Table 15.

Table 15. Evacuating residents' vehicles by hurricane intensity in San Patricio County.

Hurricane category (c)	CAT 1	CAT 2	CAT 3	CAT 4	CAT 5
Evacuating vehicles ($EV(c)$)	6984	10813	15998	18234	18880

4.2. Lives at Risk

$RL_j(t_j)$ is the number of people who remain in risky areas at landfall when a mandatory evacuation order is issued at stage *j* and the hurricane category at stage 0 is believed to be t_j. $RL_j(t_j)$ can be estimated as the number of vehicles at risk divided by the average number of vehicles per household multiplied by the average number of people in a household as formulated in the following equation:

[9] The improvement in forecast quality could influence D_{Rrc} or D_{Rc} because people feel less likely that the evacuation will turn out to be a false alarm. However, our model assumes that the proportions are unaffected by the improvement in forecast quality.

$$RL_j(t_j) = RV_j(t_j) / EVHH_R \times PHH_R .$$

4.3. Loss from Hurricane Landfall

Loss from a hurricane includes the cost from injury and the cost from loss of human lives. Therefore, $L_j(t_j)$ is defined as the sum of injury cost and life loss cost as

$$L_j(t_j) = IC_j(t_j) + LLC_j(t_j) . \quad (17)$$

In this equation, $IC_j(t_j)$ is the cost of injury and $LLC_j(t_j)$ is life loss cost when the evacuation order is issued at stage j and the hurricane category at landfall is believed to be t_j.

4.3.1. Injury cost

Cost of injury $IC_j(t_j)$, calculated as the per capita expected cost of not evacuating multiplied by the number of people who remain in the risky area when the hurricane strikes, is defined as

$$IC_j(t_j) = ICPC(t_j) \times RL_j(t_j),$$

where $ICPC(t_j)$ is the injury cost per non-evacuating capita when the storm category is believed to be t_j. To estimate $ICPC(t_j)$ requires the cost of each injury case and the probability of injury. Cost of injury differs by its severity and is summarized in Table 16. Probability of injury differs by hurricane category, as shown in Table 17.

Table 16. Cost of injuries (Czajkowski, 2007).

Severity	Cost (2004 dollars)	Cost (2007 dollars)[10]
Minor	$6,303	$6,918
Moderate	$51,471	$56,495
Serious	$189,076	$207,530
Severe	$619,748	$680,235
Critical	$2,521,008	$2,767,058

Table 17. Hypothesized probability of injury (Czajkowski, 2007).

CAT	Prob. of injury
0	0.00%
1	0.05%
2	0.20%
3	0.45%
4	0.85%
5	0.95%

The injury cost per capita given intensity ($ICPC(t_j)$) is calculated as

$$\begin{aligned} ICPC(t_j) &= \sum_{\text{severity}} \text{P(severity}|t_j)\text{Cost}_{\text{severity}} \\ &= \sum_{\text{severity}} \text{P(severity|injury)}\,\text{P(injury}|t_j)\text{Cost}_{\text{severity}} \\ &= \text{P(injury}|t_j) \sum_{\text{severity}} \text{P(severity|injury)}\text{Cost}_{\text{severity}} \end{aligned}.$$

Due to the limitation stemming from the available data, it is assumed that all injury severities are equally likely. Given this and $\sum_{\text{severity}} \text{P(severity|injury)} = 1$, P(severity|injury) = 1/5 for all severities.

[10] Inflation rate from 2004 to 2007 is 9.76% (Consumer Price Index at http://www.bls.gov/CPI/).

4.3.2. Life loss cost

To calculate the life loss cost requires an estimate of the value of life. Assigning an economic value to human life is problematic. Some research shows that the value of life can change by different factors (Viscusi, 2004). However, we assume that the value is unaffected by age, sex, race, occupation, religion, or location. We adopt the value of statistical life (VSL) from Hoffer et al. (1998), which is $3 million per life.

$LLC_j(t_j)$ can be calculated as VSL multiplied by the expected number of lives lost as

$$LLC_j(t_j) = VSL \times ELL_j(t_j), \tag{18}$$

where $ELL_j(t_j)$ is the expected number of lives lost when the evacuation starts at stage j and the hurricane intensity at landfall is believed to be t_j.

A constant can be assigned to VSL, but $ELL_j(t_j)$ changes by location, population, hurricane intensity, evacuation timing, how the evacuation is controlled, etc. For example, people living on the beach are more likely to be killed by the hurricane if it strikes. If a risky area is highly populated, the expected number of lives lost would be greater. If the hurricane intensity is high, it will influence more area and thus more people. If people start evacuation earlier, fewer lives will be lost. Also, effective evacuation planning can reduce the loss.

Our model defines $ELL_j(t_j)$ as the number of people remaining in the risky areas at stage 0 multiplied by fatality rates, or

$$ELL_j(t_j) = RL_j(t_j) \times FR_{t_j}, \tag{19}$$

where FR_{t_j} is the fatality rate or the percentage of people staying in the risky areas who are killed by the event when the hurricane category at landfall is t_j.

Fatality rate (FR) can be affected by the vulnerability of the area where people live, wind speed, whether people are at home or on the road, and many other factors. Our model defines FR as a function of risk area and hurricane category, assuming that the people are on the road when the storm strikes. The FR matrix is shown in Table 18. These FRs explain only fatalities from storm surge, which are determined by the surge level over ground elevation.[11] Table 18 shows the risk of being killed on the road in risky areas. As seen in this table, FR is 0 if risk area level is higher than hurricane category. FR is higher for higher hurricane category and lower risk area.

Table 18. Hypothesized hurricane fatality rate on the road ($FR_{c,r}$).

		Hurricane intensity				
		CAT 1	CAT 2	CAT 3	CAT 4	CAT 5
Risk area	RA1	2%	20%	100%	100%	100%
	RA2	0%	2%	20%	100%	100%
	RA3	0%	0%	2%	20%	100%
	RA4	0%	0%	0%	2%	20%
	RA5	0%	0%	0%	0%	2%

In the Hurricane Contingency Planning Guide (2001), RISK stands for Risk of Inhabitants Staying in residences being Killed. RISK tables are based on two threats to life: storm surge and wind. Projections of deaths from storm surge are based upon the reasoning that victims could escape their dwellings (or find safety on the roof) if the

[11] This follows the procedure of the Hurricane Contingency Planning Guide (2001) by the Hazard Reduction & Recovery Center at Texas A&M University.

surge is up to 10 feet above ground elevation. But if the surge is 10 to 15 feet above ground elevation, a much larger percentage could drown—especially in mobile homes. Surges 15 to 20 feet above ground elevation would result in substantial casualties in single and multi-family structures and 100 percent casualties in mobile homes. Nearly 100 percent casualties would be expected above 20 feet of surge. This leads to the expected percent of fatalities by surge depth and housing type, shown in Table 20.

Table 19 shows the rough relationship among ground elevation, storm surge, and fatality rate. It implies that the storm surge has a substantial level of life threat only when the storm surge is higher than the ground elevation.

Table 19. Fatality rates by ground elevation and storm surge.

Storm intensity (storm surge) / Risk area (ground elevation)	CAT 1 (5±Δ ft above sea level)	CAT 2 (10±Δ ft above sea level)	CAT 3 (15±Δ ft above sea level)	CAT 4 (20±Δ ft above sea level)	CAT 5 (25±Δ ft above sea level)
RA1 (< 5 ft above sea level)	Low	Medium	High	High	High
RA2 (5~10 ft above sea level)	0%	Low	Medium	High	High
RA3 (10~15 ft above sea level)	0%	0%	Low	Medium	High
RA4 (15~20 ft above sea level)	0%	0%	0%	Low	Medium
RA5 (20~25 ft above sea level)	0%	0%	0%	0%	Low

In Table 20, if risk area 2 faces a Category 1 hurricane, storm surge over land can be 0 ~ 5 feet and the fatality rate is 0% for all housing types. If risk area 2 faces a Category 2 hurricane, storm surge over land can be 5 ~ 10 feet and fatality rate for mobile homes is 2%.

Table 20. Expected percentage of fatalities by surge depth and housing type.

Feet of surge over land	Expected percentage of fatalities by housing type		
	Single family	Multi-family	Mobile home
0.00 – 5.00	0.0	0.0	0.0
5.01 – 10.00	1.0	1.0	2.0
10.01 – 15.00	10.0	10.0	20.0
15.01 – 20.00	50.0	50.0	100.0
20.01 – 30.00	90.0	90.0	100.0

The fatality rate is needed to calculate the loss of lives in the vehicles on the road, but the fatalities in the table pertain to those staying at home. Because evacuating vehicles on the road are as vulnerable as mobile homes to storm surge, it is assumed that the same fatality rate applies to both situations.

RISK tables are based on two threats to life, the other being wind. Because the RISK table for San Patricio County was incompatible with our research and because fatalities by wind speed are a function of hurricane category as well as distance from the coast, only the fatality rates by storm surge are used here. Based on the above reasoning and assumptions, fatality rates by hurricane category and risk area for evacuating vehicles on the road ($FR_{c,r}$) are summarized in Table 18.

People opting to stay at home rather than evacuate may have lower risk of being killed than those who are on the road. However, our model does not take into account those staying at home, because the decision of issuing an evacuation order does not change their risk. Although that proportion of people could be estimated using DRc and included in our model, it has been excluded because it does not change the optimal policies.

Once people leave their homes, they may not still be in the same risk area as their home. However, our model assumes that if people start evacuation and are still in risky areas at landfall, their risk areas have not changed. The model uses the average of FR given t_j weighted by population in the area.

In our model, expected number of lives lost given evacuation timing and hurricane intensity is defined as the number of remaining lives multiplied by the average FR weighted by the population in each risk area as

$$\begin{aligned} ELL_j(t_j) &= \sum_{r=1}^{5} RL_j(t_j)\frac{Pop_r}{Pop} FR_{t_j,r} \\ &= \frac{RL_j(t_j)}{Pop}\left(\sum_{r=1}^{5} Pop_r FR_{t_j,r}\right) \\ &= RL_j(t_j)\left(\sum_{r=1}^{5} \frac{Pop_r}{Pop} FR_{t_j,r}\right). \end{aligned} \tag{20}$$

In this equation, the part in the large parentheses is the average of the FRs weighted by the population of each risk area. *Pop* is the combined population of the five risk areas, and Pop_r is the population of risk area *r*. $FR_{t_j,r}$ is the FR on the road in risk area *r* when the storm category at landfall is believed to be t_j.

4.3.3. Injury cost and life loss cost

Economic damage to protectable lives due to the hurricane is the sum of injury cost and life loss cost. From Equation (17), the calculated $L_j(t_j)$ values are plotted in Figure 18. This matches the general shape of $L_j(t_j)$ in Figure 12. It is also a special case of

the definition of $L_j(t_j)$ in Equation (8) with decreasing function of j, $a_j(t_j)$, and a short minimum time requirement, m.

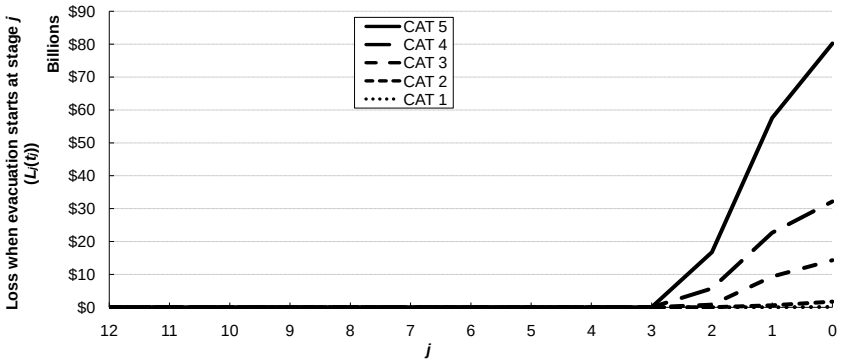

Figure 18. The loss incurred when evacuation is started at stage *j*, expected storm intensity at landfall is currently (at stage *j*) believed to be t_j, and the storm strikes the target.

Figure 18 can be represented as a function of remaining hours (t) instead of stage (j), as in Figure 19. This figure shows that minimum required time for evacuation does not change for different intensities but that loss prevention rate changes by intensity because the FR and injury rate are affected.

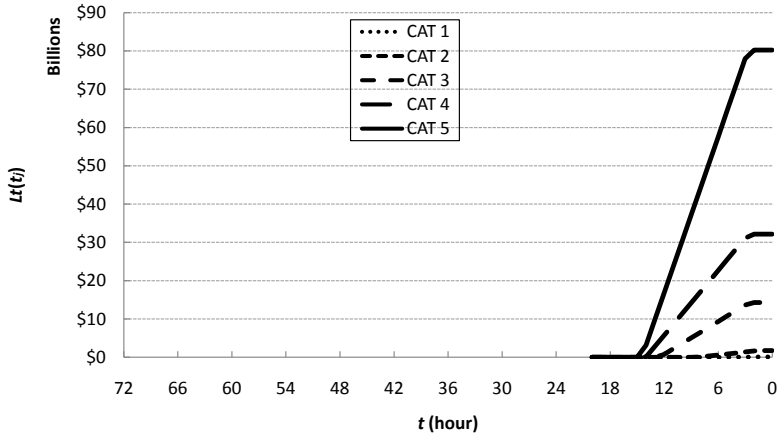

Figure 19. The loss incurred when evacuation is started at *t* hours before the final stage, expected storm intensity at landfall is currently (at stage *j*) believed to be t_j, and the storm strikes the target.

4.4. Cost of Action

The cost of evacuation from a hurricane includes three components (Lindell & Prater, 2007) as follows:

$$C_j(t_j) = REC_j(t_j) + CEC_j(t_j) + GEC_j(t_j).$$

Given intensity t_j when the protective action is taken at stage j, $REC_j(t_j)$ is residential households' evacuation cost, $CEC_j(t_j)$ is commercial evacuation cost, and $GEC_j(t_j)$ is governmental evacuation cost.

$REC_j(t_j)$ consists of direct evacuation cost and lost income. For the present study, evacuation cost was adopted from a survey result about Hurricane Lili, \$112.21 per household per day in 2002 dollars (Lindell, Prater, Lu, Arlikatti, Zhang, & Kang, 2004). This is \$129.32 in 2007 dollars.[12] Per capita income in this area is \$21,215[13] in 2002 dollars, or \$24,450 in 2007 dollars.[14] Therefore, the lost income cost for San Patricio County is \$24,450/365 ≈ \$67 per day per capita in 2007 dollars, and $REC_j(t_j)$ can be calculated as

$$REC_j(t_j) = (N - j)/4 \times (\$129.32 + \$67 PHH_R) \sum_{r=1}^{t_j} \left(\frac{Pop_r}{PHH_R} \right) D_{R,t_j}.$$

[12] Inflation rate from 2002 to 2007 is 15.25% (Consumer Price Index at http://www.bls.gov/CPI/).
[13] Refer to the State and Metropolitan Area Data Book: 2006 by the U.S. Census Bureau at http://www.census.gov/prod/2006pubs/smadb/smadb-06.pdf.
[14] Inflation rate from 2002 to 2007 is 15.25% (Consumer Price Index at http://www.bls.gov/CPI/).

The average business loss was $20,599 in 2006 dollars (NBO, 2008), which is $21,185.70 in 2007 dollars, and the number of businesses in San Patricio County is 1,013 (establishments of private nonfarm businesses in 2002).[15] Because no data were available about numbers of businesses located in various risk areas, it was assumed that the businesses are distributed at the same rate as the population in different risk areas. This yielded 138 San Patricio County businesses in risk area 1, 74 in risk area 2, 540 in risk area 3, 121 in risk area 4, and 140 in risk area 5. Average days people stay away from their homes during evacuation was 2.34 (Lindell et al., 2004), and commercial evacuation cost per business per day was assumed to be $21,185.70/2.34 = $9,053.72. Because commercial evacuation cost is a function of hurricane intensity and evacuation timing, $CEC_j(t_j)$ can be expressed as

$$CEC_j(t_j) = (N - j)/4 \times \$9,053.72 \sum_{r=1}^{t_j} Bus_r. \quad (21)$$

In this equation, Bus_r is the number of businesses in risk area r. It is assumed that all businesses in the corresponding risk areas evacuate. Because $GEC_j(t_j)$ is hard to estimate, it is assumed to be 0.

The value of $C_j(t_j)$ using the data in San Patricio County is plotted in Figure 20. This matches the general shape of $C_j(t_j)$ in Figure 13. It's a special case of the definition of $C_j(t_j)$ in Equation (9) with constant $d_j(t_j)$ and $mC = 0$.

[15] Refer to the State and Metropolitan Area Data Book: 2006 by the U.S. Census Bureau at http://www.census.gov/prod/2006pubs/smadb/smadb-06.pdf.

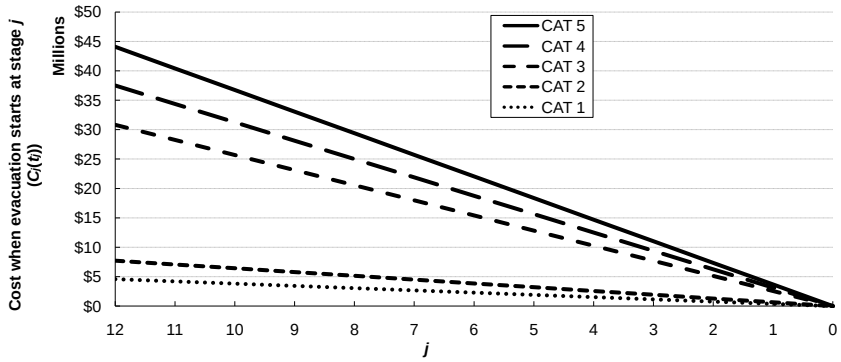

Figure 20. The cost of starting evacuation at stage *j*, where the expected landfall intensity is t_j.

State transition probability matrices $\mathbf{P}_j$'s were constructed based on Section 3.2. Base values of $\sigma^2 = 0.03$ and $\varepsilon = 0.5$ were used in Equation (6). Prior states and the calculated variances of transition probability distribution at different stages were used to generate the corresponding Beta distribution. By discretizing the Beta distribution into 21 states, from 0 to 1 by 0.05, each of the transition probabilities was obtained. To take an extreme case, if the prior state of $\mathbf{P}_j$ is 0, then all subsequent transition probabilities $p_{0,s_{j-1}\neq 0}$ equal 0. Likewise, if the prior state of $\mathbf{P}_j$ is 1, then all subsequent transition probabilities $p_{1,s_{j-1}\neq 1}$ equal 0. As discussed earlier, transition probability distributions for $\mathbf{P}_j$ are more widely dispersed in later stages, as shown in Table 21 and Table 22, which depict portions of the transition probability matrices.

Table 21. Portion of transition probability matrix P_j from stage 12 to stage 11.

s_{12} \ s_{11}	0	0.05	0.10	0.15	0.20	0.25	0.30	· · ·
0	1	0	0	0	0	0	0	· · ·
0.05	0.017	0.935	0.048	0	0	0	0	· · ·
0.10	0	0.028	0.930	0.042	0	0	0	· · ·
0.15	0	0	0.031	0.929	0.040	0	0	· · ·
0.20	0	0	0	0.032	0.929	0.039	0	· · ·
0.25	0	0	0	0	0.033	0.929	0.038	· · ·
0.30	0	0	0	0	0	0.034	0.929	· · ·
⋮	⋮	⋮	⋮	⋮	⋮	⋮	⋮	•

Table 22. Portion of transition probability matrix P_j from stage 1 to stage 0.

s_1 \ s_0	0	0.05	0.10	0.15	0.20	0.25	0.30	· · ·
0	1	0	0	0	0	0	0	· · ·
0.05	0.722	0.102	0.049	0.031	0.022	0.017	0.013	· · ·
0.10	0.326	0.243	0.141	0.093	0.064	0.044	0.031	· · ·
0.15	0.091	0.222	0.195	0.153	0.114	0.081	0.055	· · ·
0.20	0.015	0.112	0.171	0.179	0.159	0.126	0.091	· · ·
0.25	0.001	0.035	0.100	0.152	0.171	0.161	0.133	· · ·
0.30	0	0.007	0.040	0.093	0.141	0.166	0.163	· · ·
⋮	⋮	⋮	⋮	⋮	⋮	⋮	⋮	•

Table 23 shows the change in the distribution of strike probability after each transition in the model. Initial strike probability at stage 12 is 0.1, 0.15, or 0.2, all equally likely. Unlike Figure 3, this table does not distinguish striking storms from non-striking storms. If the data in Figure 3 are weighted to reflect that there were 113 non-striking storms and only 18 striking storms, the overall pattern is similar to that of Table 23.

Table 23. Distribution of strike probabilities generated by our model as a function of stage when initial strike probability at stage 12 is 0.1, 0.15, or 0.2.

$S_i \backslash j$	12	11	10	9	8	7	6	5	4	3	2	1	0
1.00	0.000	0.000	0.000	0.000	0.000	0.000	0.000	0.000	0.000	0.000	0.000	0.000	0.051
0.95	0.000	0.000	0.000	0.000	0.000	0.000	0.000	0.000	0.000	0.000	0.000	0.000	0.018
0.90	0.000	0.000	0.000	0.000	0.000	0.000	0.000	0.000	0.000	0.000	0.000	0.000	0.013
0.85	0.000	0.000	0.000	0.000	0.000	0.000	0.000	0.000	0.000	0.000	0.000	0.000	0.011
0.80	0.000	0.000	0.000	0.000	0.000	0.000	0.000	0.000	0.000	0.000	0.000	0.000	0.009
0.75	0.000	0.000	0.000	0.000	0.000	0.000	0.000	0.000	0.000	0.000	0.000	0.001	0.009
0.70	0.000	0.000	0.000	0.000	0.000	0.000	0.000	0.000	0.000	0.000	0.000	0.001	0.008
0.65	0.000	0.000	0.000	0.000	0.000	0.000	0.000	0.000	0.000	0.000	0.000	0.003	0.008
0.60	0.000	0.000	0.000	0.000	0.000	0.000	0.000	0.000	0.000	0.000	0.000	0.006	0.008
0.55	0.000	0.000	0.000	0.000	0.000	0.000	0.000	0.000	0.000	0.000	0.001	0.011	0.008
0.50	0.000	0.000	0.000	0.000	0.000	0.000	0.000	0.000	0.000	0.001	0.004	0.018	0.008
0.45	0.000	0.000	0.000	0.000	0.000	0.000	0.000	0.000	0.001	0.003	0.011	0.028	0.008
0.40	0.000	0.000	0.000	0.000	0.000	0.000	0.000	0.002	0.004	0.011	0.024	0.040	0.009
0.35	0.000	0.000	0.000	0.000	0.001	0.002	0.005	0.010	0.018	0.031	0.047	0.052	0.009
0.30	0.000	0.000	0.001	0.004	0.010	0.018	0.029	0.042	0.056	0.070	0.078	0.065	0.010
0.25	0.000	0.017	0.037	0.057	0.077	0.094	0.108	0.117	0.123	0.122	0.111	0.076	0.011
0.20	0.333	0.319	0.302	0.283	0.265	0.247	0.229	0.213	0.194	0.170	0.135	0.084	0.012
0.15	0.333	0.335	0.334	0.329	0.319	0.303	0.281	0.254	0.223	0.186	0.142	0.088	0.015
0.10	0.333	0.316	0.297	0.277	0.257	0.239	0.222	0.205	0.186	0.161	0.130	0.089	0.019
0.05	0.000	0.013	0.029	0.047	0.066	0.083	0.098	0.107	0.112	0.113	0.108	0.094	0.032
0.00	0.000	0.000	0.001	0.002	0.006	0.014	0.028	0.051	0.084	0.132	0.208	0.344	0.724

As discussed in Section 3.2, the dispersion of the transition probability distribution for $\mathbf{Q}_j$ does not change significantly as it approaches the final stage. Therefore, the same transition probability matrix was used for all stages, as shown in Table 24. States from 0 to 5 were rescaled as from 0 to 1, and constant variance of 0.0045 was assumed for the transition probability distribution. Prior states and a constant variance of transition probability distribution were used to generate the corresponding Beta distribution. The transition probabilities were obtained by discretizing the Beta distribution into six states (0 to 5). To take an extreme case, analogous to the transition probability matrix $\mathbf{P}_j$, if the prior state of $\mathbf{Q}_j$ is 0, then all subsequent transition probabilities $q_{0,t_{j-1}\neq 0}$ equal 0. Likewise, if the prior state of $\mathbf{Q}_j$ is 5, then all subsequent transition probabilities $q_{5,t_{j-1}\neq 5}$ equal 0.

Table 24. Transition probability matrix Q_j for all $j \geq 1$.

t_j \ t_{j-1}	0	1	2	3	4	5
0	1	0	0	0	0	0
1	0.101	0.786	0.113	0	0	0
2	0	0.107	0.783	0.110	0	0
3	0	0	0.110	0.783	0.107	0
4	0	0	0	0.113	0.786	0.101
5	0	0	0	0	0	1

4.5. Optimal Policies at Low Level

Suppose that a tropical storm is detected and is estimated to make landfall in 72 hours (12 periods) in San Patricio County with probability 0.15.[16] Based on the forecasted maximum wind speed, the storm will become a Category 1[17] hurricane at landfall (Blake, Rappaport, & Landsea, 2007). The cost of deferring the decision is assumed to be the small amount \$100. Table 28 shows the optimal policies for stages 12, 3, 2, and 1. The stage 12 optimal policy is Wait One Stage. The expected expense of following the optimal policy is $V_{12}(0.15, 1)$ = \$1.5 million. Table 28 displays the optimal policies for the San Patricio County example. Stage 4 and earlier stages have the same optimal policies.

A strike probability of 0.15 and a landfall intensity of 1 were selected because they constitute climatological averages. For the distribution of hurricane intensities, historical data in Texas were used. Table 25 shows the frequency of hurricane strike from 1851 to 2006 on the US mainland coastline and Texas, by Saffir-Simpson category

[16] Regnier (2008) showed that strike probabilities when lead-time is 72 hours for four different locations are 18/(113+18) = 0.137, 25/(164+25) = 0.132, 36/(186+36) = 0.162, and 18/(209+18) = 0.079, respectively. Their average is 0.128, which is closest to 0.15 in our state space.

[17] Mean category of Texas landfalling tropical storms from 1851 to 2006 is 1.14 (Blake, Rappaport et al. 2007), which is closest to 1 in our state space.

(Blake et al., 2007). Total number of hurricane strikes in San Patricio County is 14 from 1900 to 2007, averaging 0.12963 per year.[18]

Table 25. Frequency of hurricane strike on the U.S. mainland coastline and Texas by Saffir-Simpson category.

Area	Category					All	Major hurricanes	Mean category	Freq. per year
	1	2	3	4	5				
U.S. (Texas to Maine)	110 (39%)	73 (26%)	75 (27%)	18 (6%)	3 (1%)	279 (100%)	96	2.04	1.78846
Texas	23 (38%)	18 (30%)	12 (20%)	7 (12%)	0 (0%)	60 (100%)	19	2.05	0.38462

Of the 455 tropical storms in the Atlantic, Caribbean, and Gulf of Mexico from 1966 to 2006 (11.1 per year), 253 (55.6%) became hurricanes (6.17 per year) (Blake et al., 2007). Thus, Table 25 can be modified to yield Table 26.

Table 26. Frequency of hurricane strike on the U.S. mainland coastline and Texas by Saffir-Simpson category including Category 0.

Area	CAT						All	Mean category	Freq. per year
	0	1	2	3	4	5			
U.S. (Texas to Maine)	44.4%	21.9%	14.5%	14.9%	3.6%	0.6%	502 (100%)	1.13	3.21666
Texas	44.4%	21.3%	16.7%	11.1%	6.5%	0.0%	108 (100%)	1.14	0.69176

Regnier (2008) showed strike probabilities for striking and threatening (but non-striking) historical hurricanes as a function of lead-time for four different locations. Their average strike probabilities when lead-time is 72 hours are 18/(113+18) = 0.137, 25/(164+25) = 0.132, 36/(186+36) = 0.162, and 18/(209+18) = 0.079. These average 0.128, which is used as the climatological average for our model, i.e., $m(s_0) = 0.128$ when $N = 12$. It is assumed that the initial distribution of S_j at stage 12 (i.e., 12 stages

[18] Refer to Figure 5 in "Tropical Cyclone Climatology" at http://www.nhc.noaa.gov/pastprofile.shtml.

before landfall) is Normal with mean of 0.128 and standard deviation of 0.09, which is the average of the four standard deviations in Regnier (2008) as

$$S_0 \sim \mathrm{N}(0.128, 0.09).$$

By discretizing the normal distribution, the distribution of S_0 (strike probability at stage 0, or 12 periods before landfall) to be used in our model is given in Table 27.

Table 27. Distribution of state variable S_0.

s_0	$\mu(s_0)$	s_0	$\mu(s_0)$	s_0	$\mu(s_0)$
0.00	0.126	0.35	0.011	0.70	0
0.05	0.152	0.40	0.003	0.75	0
0.10	0.209	0.45	0	0.80	0
0.15	0.213	0.50	0	0.85	0
0.20	0.160	0.55	0	0.90	0
0.25	0.089	0.60	0	0.95	0
0.30	0.037	0.65	0	1.00	0

Lacking any new information about hurricane intensity and because the mean hurricane category in the US is given as 1.13 in Table 26, it is assumed that hurricane intensity is currently (at stage 0 or 12 periods before the landfall) believed to be 1.

As expected, Table 28 shows that the optimal policy is Do Not Evacuate whenever $s_j = 0$ or $t_j = 0$—meaning it is known that the storm will not strike or will be of negligible intensity. Up to stage 4, which is 24 hours before landfall, the DM should defer ordering evacuation (i.e., Wait One Stage) because the evacuation can be cheaper at later stages. This also allows maximum time for the threat to become negligible in either strike probability or landfall intensity. At stage 3, if the intensity at landfall is believed to be greater than Category 1, optimal policy is Evacuate. If the landfall intensity is be-

lieved to be Category 1, the critical decision point is one period later than that of higher intensities. From stage 2 forward, Wait One Stage is no longer an attractive option and the optimal decision is always Evacuate. The optimal policy is Evacuate even for low non-zero strike probabilities and low non-zero landfall intensities because the monetary value of human-life loss mitigation has an expected value greater than the evacuation cost.

Table 28. Optimal policies before improvement (E: Evacuate, N: do Not evacuate, W: Wait one stage).

j = 12 ~ 4

s_i \ t_j	0	1	2	3	4	5
0	N	N	N	N	N	N
0.05	N	W	W	W	W	W
0.10	N	W	W	W	W	W
0.15	N	W	W	W	W	W
0.20	N	W	W	W	W	W
0.25	N	W	W	W	W	W
0.30	N	W	W	W	W	W
0.35	N	W	W	W	W	W
0.40	N	W	W	W	W	W
0.45	N	W	W	W	W	W
0.50	N	W	W	W	W	W
0.55	N	W	W	W	W	W
0.60	N	W	W	W	W	W
0.65	N	W	W	W	W	W
0.70	N	W	W	W	W	W
0.75	N	W	W	W	W	W
0.80	N	W	W	W	W	W
0.85	N	W	W	W	W	W
0.90	N	W	W	W	W	W
0.95	N	W	W	W	W	W
1	N	W	W	W	W	W

j = 3

s_i \ t_j	0	1	2	3	4	5
0	N	N	N	N	N	N
0.05	N	W	E	E	E	E
0.10	N	W	E	E	E	E
0.15	N	W	E	E	E	E
0.20	N	W	E	E	E	E
0.25	N	W	E	E	E	E
0.30	N	W	E	E	E	E
0.35	N	W	E	E	E	E
0.40	N	W	E	E	E	E
0.45	N	W	E	E	E	E
0.50	N	W	E	E	E	E
0.55	N	W	E	E	E	E
0.60	N	W	E	E	E	E
0.65	N	W	E	E	E	E
0.70	N	W	E	E	E	E
0.75	N	W	E	E	E	E
0.80	N	W	E	E	E	E
0.85	N	W	E	E	E	E
0.90	N	W	E	E	E	E
0.95	N	W	E	E	E	E
1	N	W	E	E	E	E

j = 2

s_i \ t_j	0	1	2	3	4	5
0	N	N	N	N	N	N
0.05	N	E	E	E	E	E
0.10	N	E	E	E	E	E
0.15	N	E	E	E	E	E
0.20	N	E	E	E	E	E
0.25	N	E	E	E	E	E
0.30	N	E	E	E	E	E
0.35	N	E	E	E	E	E
0.40	N	E	E	E	E	E
0.45	N	E	E	E	E	E
0.50	N	E	E	E	E	E
0.55	N	E	E	E	E	E
0.60	N	E	E	E	E	E
0.65	N	E	E	E	E	E
0.70	N	E	E	E	E	E
0.75	N	E	E	E	E	E
0.80	N	E	E	E	E	E
0.85	N	E	E	E	E	E
0.90	N	E	E	E	E	E
0.95	N	E	E	E	E	E
1	N	E	E	E	E	E

j = 1

s_i \ t_j	0	1	2	3	4	5
0	N	N	N	N	N	N
0.05	N	E	E	E	E	E
0.10	N	E	E	E	E	E
0.15	N	E	E	E	E	E
0.20	N	E	E	E	E	E
0.25	N	E	E	E	E	E
0.30	N	E	E	E	E	E
0.35	N	E	E	E	E	E
0.40	N	E	E	E	E	E
0.45	N	E	E	E	E	E
0.50	N	E	E	E	E	E
0.55	N	E	E	E	E	E
0.60	N	E	E	E	E	E
0.65	N	E	E	E	E	E
0.70	N	E	E	E	E	E
0.75	N	E	E	E	E	E
0.80	N	E	E	E	E	E
0.85	N	E	E	E	E	E
0.90	N	E	E	E	E	E
0.95	N	E	E	E	E	E
1	N	E	E	E	E	E

4.6. Perfect Information and Instantaneous Evacuation

This example has assumed that the evacuation speed can be improved only by increasing the capacity of the PER. Yet, some portions of total evacuation time cannot be reduced by increasing capacity, including the time the evacuees spend until they reach

the PER and the time the evacuating vehicles spend on the PER when going 30 mph. Therefore, infinite capacity is meant here as an extreme increase in capacity rather than instantaneous evacuation.

Following the logic in Section 3.2.2, with fixed value of t_j, the cost with perfect information at stage N is $s_N C_N$ and the cost with instantaneous evacuation is $s_N C_0$. In the example, where C_j is strictly decreasing, instantaneous evacuation has lower cost than perfect information. For example, if $s_N = 0.15$ and $t_N = 1$, the cost with free instantaneous evacuation is $0.15 \times \$0 = \$0$, which means there is no loss. Because current anticipated expense is \$1.5 million, the value of instantaneous evacuation as compared to the original evacuation speed is \$1.5 million at stage N. With C_j neither strictly increasing nor constant, having perfect information without instantaneous evacuation means that evacuation begins sometime between stage 12 and stage 0.

The value of perfect information is higher when it is available earlier, as shown in Figure 21, which displays this value when $s_j = 0.15$, $t_j = 1$, and the average strike probability is 0.128.[19] Because later availability of perfect information reduces the available time for evacuation, its benefit is diminished, whereas the value of instantaneous evacuation does not decrease as the hurricane approaches.

[19] Regnier (2008) showed that when lead-time is 72 hours, strike probabilities for four different locations are 18/(113+18) = 0.137, 25/(164+25) = 0.132, 36/(186+36) = 0.162, and 18/(209+18) = 0.079. Their average is 0.128.

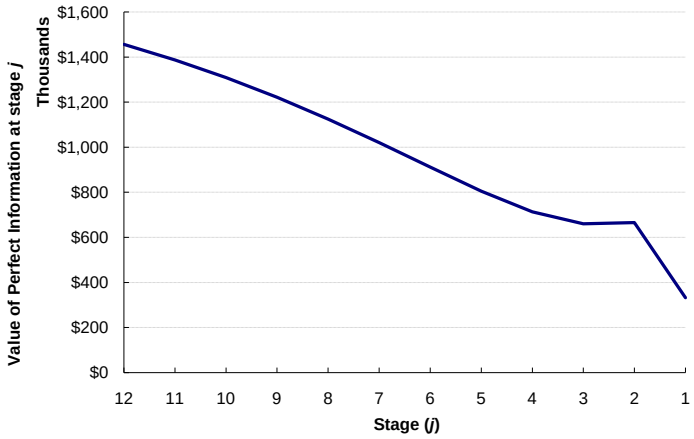

Figure 21. Value of perfect information on the storm track as a function of stage.

4.7. Sensitivity to the Improvements

Figure 22 shows the sensitivity of $V_{12}(s_j,t_j)$ to track-forecast improvement by plotting V_{12} values while r_S decreases from 1 toward 0. Anticipated expenses are seen to change smoothly as the track forecast improves. Consider a hurricane detected at stage 12, where strike probability in San Patricio County is 0.15 and hurricane intensity at landfall is believed to be Category 2. Anticipated expense from following the optimal policy is $3.4 million. If the mean error of track forecast decreases to 90% of current mean error, the anticipated expense decreases to $3.2 million. If the mean error decreases to 10% of current mean error, the anticipated expense decreases to $0.6 million.

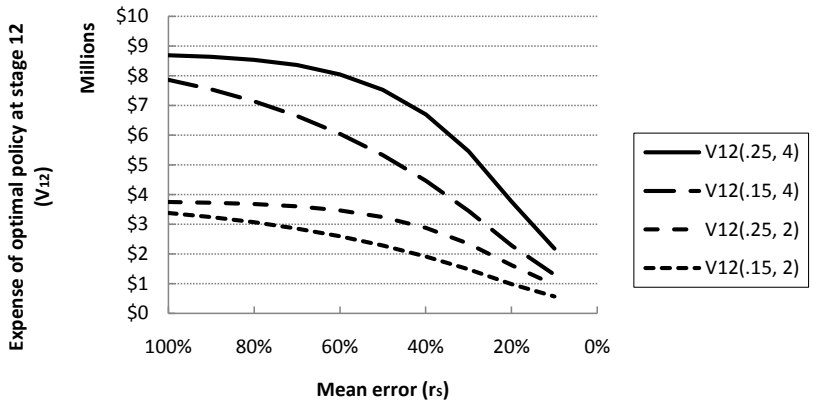

Figure 22. Sensitivity of V_{12} to track-forecast mean error.

Figure 23 shows the sensitivity of $V_{12}(s_j,t_j)$ to evacuation speed improvement as a function of evacuation time, by plotting V_{12} values as r_E decreases from 1 toward 0. Unlike track forecast improvement, increasing evacuation speed does not bring about steady change in anticipated expense. Figure 23 shows three plateaus within which V_{12} does not change noticeably. Improvement of evacuation speed shifts the optimal action timing toward the final stage and, due to the possible action timings being discrete, anticipated expense drops drastically at some points. Decreasing evacuation time by more than 75% is unnecessary because the anticipated expense will have reached a minimum.

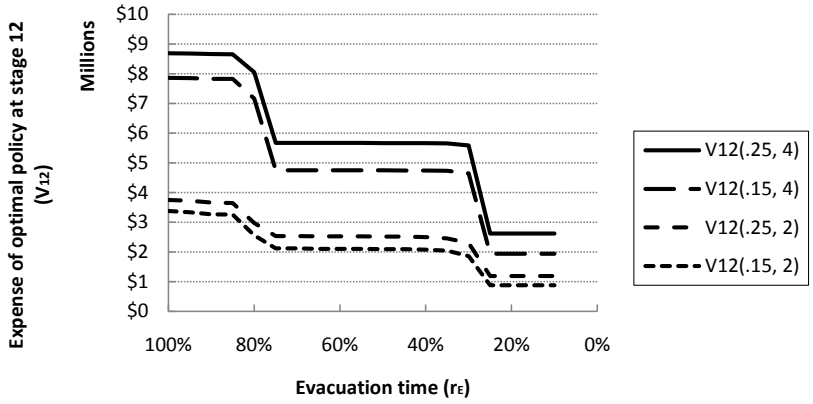

Figure 23. Sensitivity of V_{12} to evacuation time.

4.8. Sectional Improvement of Road Capacity

Improvement of evacuation speed may be deceptive because it depends on which part of the infrastructure receives the investment as well as the amount invested. If investment is in radar for better forecast quality, the improvement affects risk areas 1 through 5. However, investment in the infrastructure or the primary evacuation route (PER) does not always affect all the risk areas as illustrated in Figure 24.

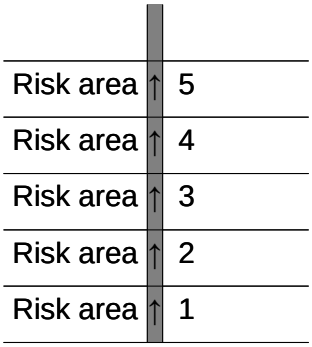

Figure 24. Risk areas with a single evacuation route.

Improving only one section of the PER does not change the capacity of the entire PER. However, it can be beneficial to the people in some areas.

When a Category 1 hurricane is going to make landfall, the PER in risk area 1 is critical. In this case, improvement in the other parts of the PER does not provide any benefit. Investing in the PER, but only in risk area 1, changes the capacity of the critical section of the PER. It provides benefit to risk area 1 in case of a Category 1 hurricane. When a Category 1 hurricane is imminent, people in risk area 2 can more quickly reach the inland edge of risk area 1. When a Category 2 or higher hurricane approaches, people in risk area 1 can reach a safer area faster but cannot complete the evacuation faster.

When a Category *c* hurricane is going to make landfall and *c* is 2, 3, or 4, the PER in risk areas 1 through *c* is critical. In this case, improvement in the other parts of the PER does not provide any benefit. Investing in the PER only in risk area *c* does not change the capacity of the critical section of the PER, although it provides benefit to risk area *c* in case of a Category *c* hurricane. When a Category *c* hurricane is imminent, people in risk area *c* can more quickly reach the inland edge of risk area *c*. When a Category *c*+1 or higher hurricane approaches, people in risk area *c* can reach a less risky area faster but cannot complete the evacuation faster.

When a Category 5 hurricane is going to landfall, the PER in risk areas 1, 2, 3, 4, and 5 is critical. In this case, investing in the PER only in risk area 5 does not change the capacity of the critical section of the PER. It benefits risk area 5 in case of a Category 5 hurricane. When a Category 5 hurricane is imminent, people in risk area 5 can more quickly reach the inland edge of risk area 5.

Assuming that a Category c hurricane is going to make landfall, define $CAPA_{CER,c}$ as the capacity of the critical evacuation route (CER), N_c as the number of vehicles that are supposed to evacuate, $N_{t,c}$ as the number of vehicles that escape the risky areas until time t, and T_c as the time for all the vehicles in risky areas to escape.

Suppose that improving a section of the PER doubles the capacity of the road and that all the sections of the PER have a capacity of 1,000 vehicles per hour. If a Category 1 hurricane is going to make landfall, the CER consists solely of the RA1 section of the PER because people have only to move outside that section. If a Category c hurricane is going to make landfall and c is 2, 3, or 4, the CER consists of the RA1 through RAc sections of the PER because people have only to move outside those sections. If a Category 5 hurricane is going to make landfall, the CER consists of the RA1, RA2, RA3, RA4, and RA5 sections of the PER because people have to move outside those sections. Given the population of each risk area and the capacity of each section of the PER, $N_{t,c}$ can be calculated using a table format. For a Category 3 hurricane, $N_{t,3}$ without any improvement is calculated in Table 29.

Table 29 assumes 1000 vehicles in each risk area and a PER capacity of 1000 vehicles per hour in each section. When assuming that a Category 3 hurricane is going to make landfall, risk areas 4 and 5 are disregarded.[20] The table also assumes that vehicles that entered a risk area cannot leave the area within the same period. For this reason, Lc can exceed neither Vc nor Ec + Vc. In each row, L3 is added to N_t of the previous period.

[20] In reality, there exists an evacuation shadow. That is, when facing a Category 3 hurricane, some portion of people in risk areas 4 and 5 will evacuate.

L2 equals E3, and L1 equals E2. L3 is determined by the capacity of the PER in RA3, but it cannot exceed V3. Therefore, at period *t*, L3 can be defined as

$$L3 = \min\left\{V3,\ CAPA_{RA3}\left(t-\left(t-0.5\right)\right)\right\}$$

and L2 and L1 are defined analogously.

Table 29. Remaining vehicles in different risk areas over time for a Category 3 hurricane when infrastructure is not improved.

Risk Area	RA1 (1000/H)			RA2 (1000/H)				RA3 (1000/H)				RA4 (1000/H)				RA5 (1000/H)				
t (hour)	V1	L1	V1 – L1	E2	V2	L2	E2 + V2 – L2	E3	V3	L3	E3 + V3 – L3	E4	V4	L4	E4 + V4 – L4	E5	V5	L5	E5 + V5 – L5	*Nt*
0.0	1000		1000		1000		1000		1000		1000		1000		1000		1000		1000	0
0.5	1000	500	500	500	1000	500	1000	500	1000	500	1000									500
1.0	500	500	0	500	1000	500	1000	500	1000	500	1000									1000
1.5	0	0	0	0	1000	500	500	500	1000	500	1000									1500
2.0	0	0	0	0	500	500	0	500	1000	500	1000									2000
2.5	0	0	0	0	0	0	0	0	1000	500	500									2500
3.0	0	0	0	0	0	0	0	0	500	500	0									3000

Vc: net number of vehicles in risk area c at the end of the previous period (*t*–0.5)
Ec: number of vehicles that entered risk area c for the latest period ((*t*–0.5) ~ *t*)
Lc: number of vehicles that left risk area c for the latest period ((*t*–0.5) ~ *t*)
Ec + Vc – Lc: net number of vehicles in risk area c at the end of the current period (*t*)

Table 29 shows that when a Category 3 hurricane is going to make landfall, finishing the evacuation of all 3000 vehicles in the risky areas takes 3 hours. Assuming no infrastructure improvements, $N_{t,c}$ and T_c for different hurricane categories are summarized in Table 30. For a Category 5 hurricane, $N_{t,3}$ with sectional improvement in risk areas 4 and 5 is calculated in Table 31. This table shows that time necessary for evacuation is 4 hours in this case.

Table 30. Vehicles that evacuate over time and total evacuation time for different hurricane categories when infrastructure is not improved.

t (hour)	CAT 1	CAT 2	CAT 3	CAT 4	CAT 5
	$N_{t,1}$	$N_{t,2}$	$N_{t,3}$	$N_{t,4}$	$N_{t,5}$
0.0	0	0	0	0	0
0.5	500	500	500	500	500
1.0	1000	1000	1000	1000	1000
1.5		1500	1500	1500	1500
2.0		2000	2000	2000	2000
2.5			2500	2500	2500
3.0			3000	3000	3000
3.5				3500	3500
4.0				4000	4000
4.5					4500
5.0					5000
T_c	1.0 H	2.0 H	3.0 H	4.0 H	5.0 H

Table 31. Remaining vehicles in different risk areas over time for a Category 5 hurricane when infrastructure is not improved.

Risk Area	RA1 (1000/H)			RA2 (1000/H)				RA3 (1000/H)				RA4 (2000/H)				RA5 (2000/H)				
t (hour)	V1	L1	V1 – L1	E2	V2	L2	E2 + V2 – L2	E3	V3	L3	E3 + V3 – L3	E4	V4	L4	E4 + V4 – L4	E5	V5	L5	E5 + V5 – L5	N_t
0.0	1000		1000		1000		1000		1000		1000		1000		1000		1000		1000	0
0.5	1000	500	500	500	1000	500	1000	500	1000	500	1000	500	1000	1000	500	1000	1000	1000	1000	1000
1.0	500	500	0	500	1000	500	1000	500	1000	500	1000	500	500	500	500	500	1000	1000	500	2000
1.5	0	0	0	0	1000	500	500	500	1000	500	1000	500	500	500	500	500	500	500	500	2500
2.0	0	0	0	0	500	500	0	500	1000	500	1000	500	500	500	500	500	500	500	500	3000
2.5	0	0	0	0	0	0	0	0	1000	500	500	500	500	500	500	500	500	500	500	3500
3.0	0	0	0	0	0	0	0	0	500	500	0	500	500	500	500	500	500	500	500	4000
3.5	0	0	0	0	0	0	0	0	0	0	0	0	500	500	0	500	500	500	500	4500
4.0	0	0	0	0	0	0	0	0	0	0	0	0	0	0	0	0	500	500	0	5000

Due to the relationship between risk areas and hurricane categories, N_c values are

$$N_1 = 1000,\ N_2 = 2000,\ N_3 = 3000,\ N_4 = 4000,\ N_5 = 5000\,.$$

Suppose that only the RA1 section of the PER is improved. Facing a Category 1 hurricane, the CER consists of section 1 and its capacity is 2000/hr. Facing a Category 2 hurricane, the CER consists of sections 1 and 2 and its capacity is 1000/hr, where section

2 is the bottleneck. For any Category $c \geq 2$, the CER consists of sections 1 through c and its capacity is 1000/hr, where sections 2 through c are bottlenecks. Facing a Category 4 hurricane, the CER consists of sections 1, 2, 3, and 4 and its capacity is 1000/hr, where sections 2, 3, and 4 are bottlenecks. Facing a Category 5 hurricane, the CER consists of sections 1, 2, 3, 4, and 5 and its capacity is 1000/hr, where sections 2, 3, 4, and 5 are bottlenecks. Capacity of the CER given hurricane category is summarized as

$$\begin{aligned}
\text{CAPA}_{\text{CER},1} &= 2000 / \text{hr} \\
\text{CAPA}_{\text{CER},2} &= 1000 / \text{hr} \\
\text{CAPA}_{\text{CER},3} &= 1000 / \text{hr} \\
\text{CAPA}_{\text{CER},4} &= 1000 / \text{hr} \\
\text{CAPA}_{\text{CER},5} &= 1000 / \text{hr}.
\end{aligned}$$

Accordingly, $N_{t,c}$ and T_c are calculated and presented in Table 32.

Table 32. Vehicles that evacuate over time and total evacuation time for different hurricane categories when the infrastructure only in risk area 1 is improved.

t (hour)	CAT 1	CAT 2	CAT 3	CAT 4	CAT 5
	$N_{t,1}$	$N_{t,2}$	$N_{t,3}$	$N_{t,4}$	$N_{t,5}$
0.0	0	0	0	0	0
0.5	1000	500	500	500	500
1.0		1000	1000	1000	1000
1.5		1500	1500	1500	1500
2.0		2000	2000	2000	2000
2.5			2500	2500	2500
3.0			3000	3000	3000
3.5				3500	3500
4.0				4000	4000
4.5					4500
5.0					5000
T_c	0.5 H	2.0 H	3.0 H	4.0 H	5.0 H

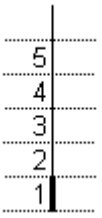

Suppose that only the RA4 and RA5 sections of the PER are improved. Capacity of the CER given hurricane category becomes

$$\text{CAPA}_{\text{CER},1} = 1000 / \text{hr}$$
$$\text{CAPA}_{\text{CER},2} = 1000 / \text{hr}$$
$$\text{CAPA}_{\text{CER},3} = 1000 / \text{hr}$$
$$\text{CAPA}_{\text{CER},4} = 1000 / \text{hr}$$
$$\text{CAPA}_{\text{CER},5} = 1000 / \text{hr}.$$

Accordingly, $N_{t,c}$ and T_c are calculated and presented in Table 33.

Table 33. Vehicles that evacuate over time and total evacuation time for different hurricane categories when infrastructure only in risk areas 4 and 5 is improved.

t (hour)	CAT 1	CAT 2	CAT 3	CAT 4	CAT 5
	$N_{t,1}$	$N_{t,2}$	$N_{t,3}$	$N_{t,4}$	$N_{t,5}$
0.0	0	0	0	0	0
0.5	500	500	500	1000	1000
1.0	1000	1000	1000	1500	2000
1.5		1500	1500	2000	2500
2.0		2000	2000	2500	3000
2.5			2500	3000	3500
3.0			3000	3500	4000
3.5				4000	4500
4.0					5000
4.5					
5.0					
T_c	1.0 H	2.0 H	3.0 H	3.5 H	4.0 H

Suppose that all sections of the PER are improved. Capacity of the CER given hurricane category is

$$CAPA_{CER,1} = 2000 / hr$$
$$CAPA_{CER,2} = 2000 / hr$$
$$CAPA_{CER,3} = 2000 / hr$$
$$CAPA_{CER,4} = 2000 / hr$$
$$CAPA_{CER,5} = 2000 / hr.$$

Accordingly, $N_{t,c}$ and T_c are calculated and presented in Table 34.

Table 34. Vehicles that evacuate over time for different hurricane categories when all parts of infrastructure are improved.

t (hour)	CAT 1	CAT 2	CAT 3	CAT 4	CAT 5
	$N_{t,1}$	$N_{t,2}$	$N_{t,3}$	$N_{t,4}$	$N_{t,5}$
0.0	0	0	0	0	0
0.5	1000	1000	1000	1000	1000
1.0		2000	2000	2000	2000
1.5			3000	3000	3000
2.0				4000	4000
2.5					5000
3.0					
3.5					
4.0					
4.5					
5.0					
T_c	0.5 H	1.0 H	1.5 H	2.0 H	2.5 H

All other possible sectional improvements can be calculated in the same way, and the benefit from the sectional capacity increase of the PER is summarized in Table 35. Shaded areas mean the non-critical sections of the PER given hurricane category. "+" means that the capacity increase benefits the people in the area. "0" means that the capacity increase does not benefit the people in the area.

Table 35. Benefit from the sectional capacity increase of the PER.

Hurricane category	CAT 1	CAT 2	CAT 3	CAT 4	CAT 5
Capacity increase in risk area 1 (RA1)	+	0	0	0	0
Capacity increase in risk area 2 (RA2)	0	+	0	0	0
Capacity increase in risk area 3 (RA3)	0	0	+	0	0
Capacity increase in risk area 4 (RA4)	0	0	0	+	0
Capacity increase in risk area 5 (RA5)	0	0	0	0	+

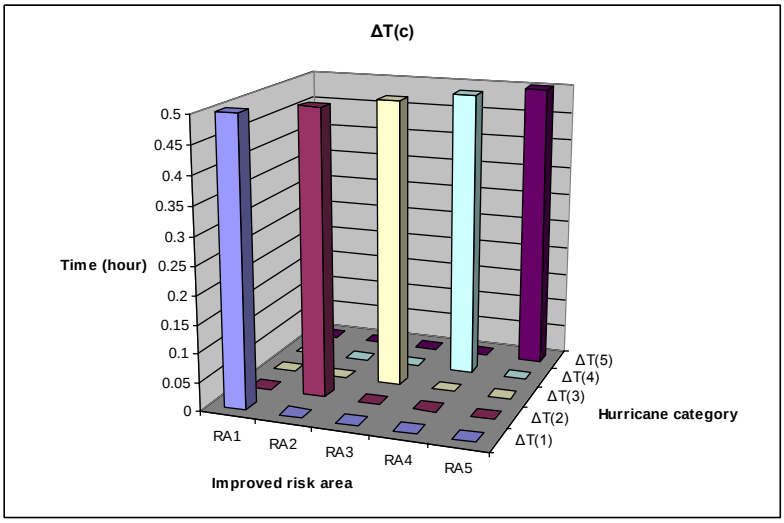

Figure 25. Improvement of evacuation time estimate.

Figure 25 shows the improvement in the evacuation time estimate (ETE) when one of five sections of the PER is improved. If the capacity of the RA1 section of the PER is doubled, evacuation from a Category 1 hurricane can be completed half an hour earlier than before the improvement. However, if the hurricane is other than Category 1, ETE does not improve. If the capacity of the RA2 section of the PER is doubled, evacuation from a Category 2 hurricane can be completed half an hour earlier than before the improvement. However, ETE does not improve for the other categories. Likewise for other sections of the PER. Increasing RA1 capacity or RA5 capacity results in the same ETE improvement, but the impact of these improvements can differ. A 0.5 hour im-

provement due to an RA1 capacity increase benefits 1000 vehicles, whereas a 0.5 hour improvement due to an RA5 capacity increase benefits 5000 vehicles.

Using Figure 25, the expected improvement of ETE can be calculated as

$$\Delta T(c)_{RA1} = 0.5 \times P(CAT1)$$
$$\Delta T(c)_{RA2} = 0.5 \times P(CAT2)$$
$$\Delta T(c)_{RA3} = 0.5 \times P(CAT3)$$
$$\Delta T(c)_{RA4} = 0.5 \times P(CAT4)$$
$$\Delta T(c)_{RA5} = 0.5 \times P(CAT5).$$

If the categories of hurricane are uniformly distributed, the expected improvement of ETE will be 0.1 for all sectional improvements. If lower category is more likely, capacity increase in RA1 is more beneficial. If higher category is more likely, capacity increase in RA5 is more beneficial.

Benefit from different ranges (starting from the lowest RA) of sectional capacity increase of the PER is summarized in Table 36. Benefit from different ranges (starting from the highest RA) of sectional capacity increase of the PER is summarized in Table 37.

Table 36. Benefit from different ranges (from the lowest RA) of sectional capacity increase of the PER.

Hurricane category	CAT 1	CAT 2	CAT 3	CAT 4	CAT 5
Capacity increase in RA1	+	0	0	0	0
Capacity increase in RA1 thru RA2	+	+	0	0	0
Capacity increase in RA1 thru RA3	+	+	+	0	0
Capacity increase in RA1 thru RA4	+	+	+	+	0
Capacity increase in RA1 thru RA5	+	+	+	+	+

Table 37. Benefit from different ranges (from the highest RA) of sectional capacity increase of the PER.

Hurricane category	CAT 1	CAT 2	CAT 3	CAT 4	CAT 5
Capacity increase in RA5	0	0	0	0	+
Capacity increase in RA4 thru RA5	0	0	0	+	+
Capacity increase in RA3 thru RA5	0	0	+	+	+
Capacity increase in RA2 thru RA5	0	+	+	+	+
Capacity increase in RA1 thru RA5	+	+	+	+	+

Budget constraints may preclude increasing PER capacity in all sections. If the population in each risk area is identical and the hurricane categories are uniformly distributed, Table 36 and Table 37 show that investing from the lowest risk area is the best decision because greater capacity in those areas is most beneficial in case of last-minute evacuation.

Table 35, Table 36, and Table 37 show that the benefit from the sectional capacity increase in the PER is not additive. The capacity increase in a given section of the PER benefits only one combination of risk area and hurricane category, whereas the capacity increase in all the sections of the PER benefits all risk areas for all hurricane categories except non-critical sections of the PER, i.e., 15 combinations of risk area and hurricane category.

Because such considerations are beyond the scope of this research, it is assumed that the improvement of evacuation speed is proportional to the amount of investment and that sectional improvement is not considered in regard to investment in infrastructure.

4.9. Tradeoff between the Improvements

Pairs of equivalent improvements in track forecast and evacuation time are plotted in Figure 26 for $V_{12}(0.15,2)$. Improvement parameter values corresponding to the improvement percentages are shown in parentheses.[21] For example, if the track forecast is improved by 10%, $V_{12}(0.15,2)$ equals \$3.2 million. The same value of $V_{12}(0.15,2)$ is obtained if the evacuation speed is improved by 15.36%. When only one of the two improvements can be made, evacuation speed yields greater benefit than forecast quality if their incremental improvement percentages are the same. While this provides some insight, the costs of these percentage improvements also need to be considered.

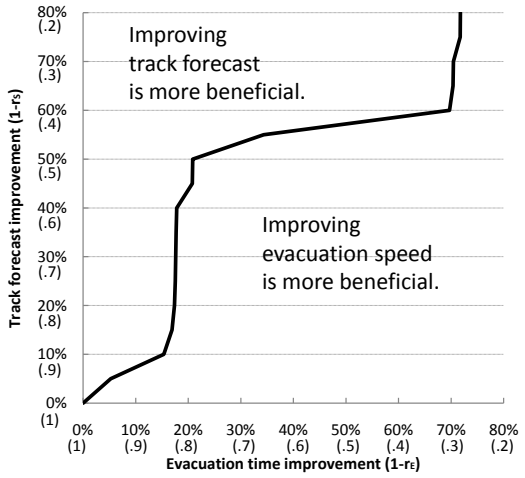

Figure 26. Pairs of equivalent mutually exclusive improvements.

The mixtures of improvements that yield the same benefit are illustrated in Figure 27. Improvement parameter values corresponding to the improvement percentages are in parentheses.

[21] The values in the figure were found numerically using Mathematica.

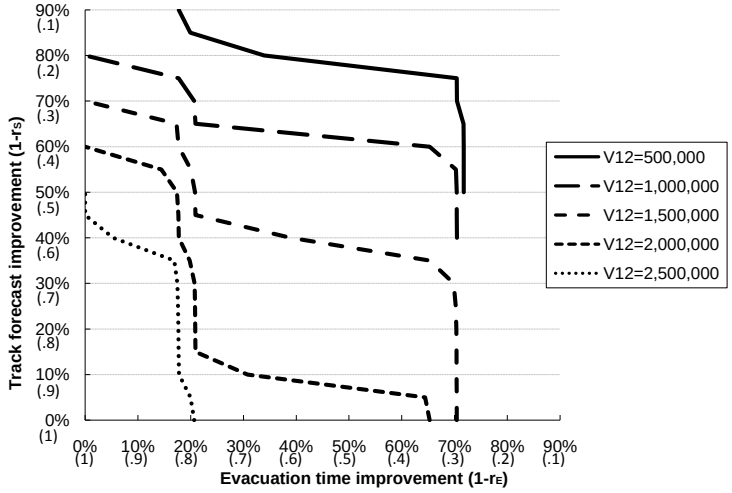

Figure 27. Mixtures of improvements that yield the same benefit.

4.10. Finding the Optimal Mix of Investments

It is vital to know the relationship between the improvement and the investment required to achieve it. A linear relationship is assumed here for simplicity.

According to the Washington State Department of Transportation (2002), the cost to construct a single lane-mile of highway averages $2.3 million ($2.7 million in 2007 dollars).[22] In this example, adding one lane to the existing primary evacuation route, which totals 53 miles,[23] costs approximately $143 million.[24]

If the improvement is depicted as a percentage of evacuation time, adding a one-lane route reduces the time to finish evacuation by 50% (15.88 hours → 7.94 hours) by

[22] Inflation rate from 2002 to 2007 is 15.25% (Consumer Price Index at http://www.bls.gov/CPI/).

[23] In San Patricio County, maximum evacuation distance via US Highway 181 is about 18 miles and maximum evacuation distance via FM 136 / FM 1360 / FM 2441 is 35 miles. Therefore, total length of the PER is 18 + 35 = 53 miles.

[24] It implies that the evacuation capacity improves at the same rate regardless of the hurricane intensity. If the evacuation capacity is not expanded in all risk areas, the benefit from the improvement can change according to the hurricane intensity. This is left for future research.

doubling the capacity of the primary evacuation route (PER) (1600 vehicles per hour → 3200 vehicles per hour). Therefore, reducing evacuation time by 50% costs $143 million.[25] This is equivalent to $2.8 million per unit percent or 0.35% per $1 million. However, this rate is not constant over the range of the improvement. Reducing current evacuation time by 50% costs $143 million, but eliminating that last 50% costs far more because zero evacuation time implies unlimited evacuation capacity of the PER. Adding a second one-lane route still leaves 33.33% of the original evacuation time.

The cost of forecast improvement is hard to estimate, but the FY 2009 budget proposal for the National Oceanic and Atmospheric Administration (NOAA) provides a rough estimate (NBO, 2008). By investing $4.3 million for FY 2009, for a total of approximately $57 million, the National Weather Service (NWS) claimed it could reduce forecast track and wind speed errors by 50% and 30%, respectively. Therefore, it is assumed here that reducing forecast track error by 50% costs $57 million, which is equivalent to 0.87% per $1 million or $1.1 million per unit percent. It is also assumed that the cost of track forecast improvement increases exponentially because 100% improvement is impossible to achieve even with unlimited investment. Because no improvement (x = 0) incurs no cost ($F(x) = 0$), the cost of track forecast improvement ($F(x)$) is defined as follows:

$$F(x) = b(e^{ax} - 1),$$

[25] 53 miles × $2.688 million per lane-mile = $142,464,000.

where *a* and *b* are constants and *x* is the percentage improvement of the track forecast. If \$5 million of investment is assumed to improve the track forecast by 10%, based on \$57 million of investment being thought to improve the track forecast by 50%, the cost of track forecast improvement as a function of r_S is defined as

$$F(r_S) = \$11,793,107.64\left(e^{3.53(1-r_S)} - 1\right).$$

For example, 10% improvement in the track forecast (r_S = 0.9) is equivalent to approximately \$5 million in investment. Converting the improvement percentage into the equivalent investment amount facilitates selecting between mutually exclusive improvements expressed as investment amounts, as shown in Figure 28. If the point representing a pair of competing investments is mapped to the lower right area, investment in evacuation speed is more beneficial, whereas a pair of competing investments being mapped to the upper left area implies that investment in forecast quality is more beneficial. For example, \$70 million investment in track forecast improvement provides almost the same benefit as \$70 million investment in evacuation speed improvement.

Figure 28 shows the graphical solution to Formulation (12) with j = 12, s_{12} = 0.15, and t_{12} = 2 as follows:

$$\begin{aligned} &\underset{(x,y)\in\{(r_S,1),(1,r_E)\}}{\arg\min} \quad V_{12}(0.15, 2, x, y) \\ &s.t.\ G(r_S) = B \\ &\quad H(r_E) = B \\ &\quad 0 \le r_S \le 1 \\ &\quad 0 \le r_E \le 1 \end{aligned}$$

The figure shows how the optimal investment mix of the two improvements changes as the budget varies from 0 up to $200 million.

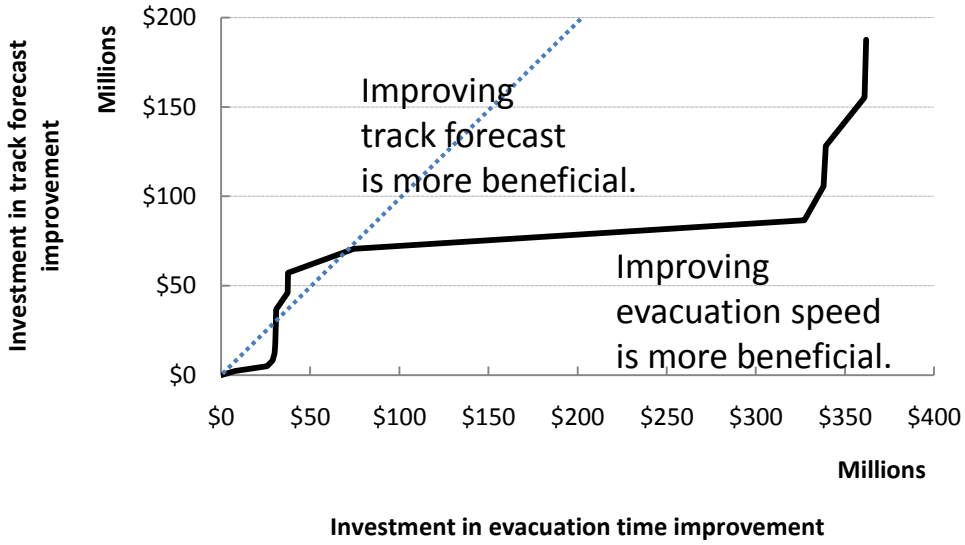

Figure 28. Pairs of equivalent mutually exclusive improvements.

Figure 29 displays the optimal mix of investments when they are not mutually exclusive. The optimal mix is at the point where V_0 is minimized within the budget constraint area. For example, if the budget is $140 million, V_0 reaches its minimum of $1 million when $105 million is invested in track forecast improvement and $35 million is invested in evacuation speed improvement. If the budget is $45 million, V_0 reaches its minimum of $2 million when $5 million is invested in track forecast and $40 million is invested in evacuation speed improvement. If the budget is less than approximately $70 million, more money should be invested in evacuation speed improvement than in forecast improvement. However, if the budget is larger than that, more money should be invested in forecast improvement than in evacuation speed improvement.

Figure 29 shows the graphical solution to Formulation (13) with $j = 12$, $s_{12} = 0.15$, and $t_{12} = 2$ as follows:

$$\begin{aligned} &\arg\min_{r_S, r_E} \; V_{12}(0.15, 2, r_S, r_E) \\ &s.t. \; G(r_S) + H(r_E) \le B \\ &\quad 0 \le r_S \le 1 \\ &\quad 0 \le r_E \le 1 \end{aligned}$$

The figure shows that if the budget allows investing in both improvements, the optimal mix of the investments is noticeably affected by the budget.

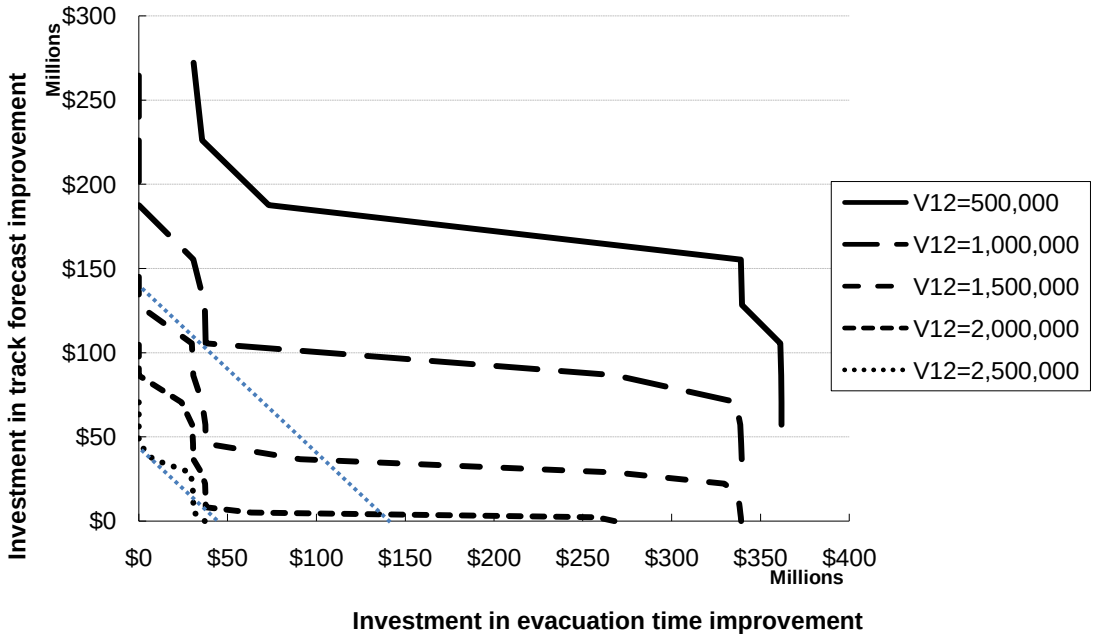

Figure 29. Mixtures of improvements (investments) that yield the same benefit.

Improving track forecasting would arguably apply across the US, whereas improving evacuation speed would apply only to the local area. Therefore, expanding the study area will affect the tradeoff.

4.11. Cumulative Benefit

Because 55.6% of detected tropical storms become hurricanes when the lead-time is 72 hours and the average number of hurricanes making landfall in this area has been shown to be 0.12963 per year, the average number of detected tropical storms when lead-time is 72 hours can be estimated as 0.12963/.556 = 0.233147 per year. Therefore, the benefit of perfect information is 0.233147 × ΔVoPI_0 = \$240,036.90 per year and the benefit of infinite capacity is 0.233147 × ΔVoIC_0 = \$215,771.99 per year.

Using the definition of ΔVoPI, the benefit of 50% improvement in track forecast mean error (ΔVoII(50%)) can be defined as follows (N = 12):

$$\begin{aligned}
&\Delta\text{VoII}(50\%) = \text{Value w/ imperfect } (50\%) \text{ info} - \text{Value w/ current info} \\
&= -\left(\sum_{s_N} \mu(s_N) V_N(s_N, t_N = 1, r_S = 0.5) - \sum_{s_N} \mu(s_N) V_N(s_N, t_N = 1, r_S = 1) \right) \\
&= -(825{,}298.31 - 1{,}183{,}179.82) \\
&= \$357{,}881.51
\end{aligned}$$

This is equivalent to 0.233147 × \$357,881.51 = \$83,439.00 per year. Based on the cost of 50% improvement in track forecast being \$57.253 million, the cumulative benefit over time is plotted in Figure 30.

The benefit of 50% improvement in evacuation time in PER (ΔVoBC(50%)) can be defined as follows (N=12):

$$\begin{aligned}
&\Delta\text{VoBC}(50\%) = \text{Value w/ 50\% faster evacuation} - \text{Value w/ current evacuation} \\
&= -\left(\sum_{s_N} \mu(s_N) V_N(s_N, t_N = 1, r_E = .5) - \sum_{s_N} \mu(s_N) V_N(s_N, t_N = 1, r_E = 1) \right) \\
&= -(767,497.31 - 1,183,179.82) \\
&= \$415,682.51
\end{aligned}$$

This is equivalent to 0.233147 × $415,682.51 = $96,915.13 per year. Based on the cost of 50% improvement in evacuation time being $142,464,000, the cumulative benefit over time is plotted in Figure 30. This figure assumes that evacuation speed improvement always covers all five risk areas. If this assumption does not hold, the benefit will be different and more complicated. For example, if the evacuation speed improvement applies only to risk area 1, the benefit occurs only for Category 1 hurricanes. If the evacuation speed improvement applies to risk areas 1 and 2, the benefit only occurs for hurricanes of Categories 1 or 2. If the evacuation speed improvement applies only to risk area 2, then the benefit will be very limited. In addition, the graph could be segmented into five hurricane categories. This example does not address this sectional improvement, which is left for future research.

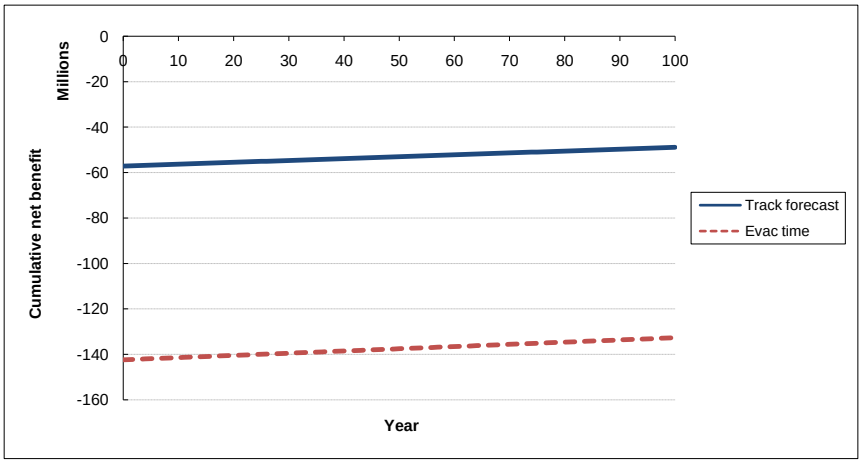

Figure 30. Cumulative benefit of 50% improvements.

This figure shows that neither of the cumulative benefits becomes positive in the near future. For forecast investment, this is because the benefit outside San Patricio County is not taken into account and other benefits not directly related to the hurricane are not properly captured. For road investment, this is because the benefits during non-hurricane situation are not properly captured.

5. PROBABILITY ASSESSMENT AND VERIFICATION[26]

In a decision situation with any uncertainty, probability assessment and its verification are crucial for making a good decision. This section shows our previous work that includes an example of probability assessment and verification on the probability of precipitation forecasts by The Weather Channel (Bickel & Kim, 2008).

5.1. Introduction

The Weather Channel (TWC) is a leading provider of weather information to the general public via its cable television network and interactive Web site (see http://www.weather.com/). TWC's cable network is available in 95% of cable TV homes in the United States and reaches more than 87 million households. Their Internet site, providing weather forecasts for 98,000 locations worldwide, averages over 20 million unique users per month and is among the top 15 news and information Web sites, according to Nielsen/NetRatings (more information is available online at http://press.weather.com/company.asp).

The public uses TWC's forecasts to make decisions as mundane as whether to carry an umbrella or as significant as whether to seek shelter from an approaching storm. How accurate are these forecasts? Are they free from bias? Should the public accept TWC forecasts at face value or do they need to be adjusted to arrive at a better forecast?

[26] Reprinted with permission from "Verification of The Weather Channel Probability of Precipitation forecasts" by J. Eric Bickel and Seong Dae Kim, 2008. *Monthly Weather Review*, Vol. 136, Issue 12, pp 4867-4881, Copyright [2008] by the American Meteorological Society.

In this paper, we analyze the reliability of probability of precipitation (PoP) forecasts provided by TWC (via weather.com) over a 14-month period (2 November 2004–16 January 2006), at 42 locations across the United States. Specifically we compare *n*-day-ahead PoP forecasts, where *n* ranges from 0 (same day) to 9, with actual precipitation observations.

This paper is organized as follows. In the next section, we describe our verification approach and review the associated literature. In section 3 we summarize our data collection procedure. In section 4 we present the reliability results and discuss the implications. In section 5 we present our conclusions.

5.2. Verification of Probability Forecasts

The literature dealing with forecast verification and value is extensive (e.g., for an overview see Katz and Murphy (1997); Jolliffe and Stephenson (2003)). In this paper, we adopt the distribution-oriented framework proposed by Murphy and Winkler (1987), (1992).

5.2.1. Distributional measures

Let F be the finite set of possible PoP forecasts $f_i \in [0,1]$, i = 1 to m. Here X is the set of precipitation observations, which we assume may obtain only the value $x = 1$ in the event of precipitation and $x = 0$ otherwise. The empirical relative frequency distribution of forecasts and observations given a particular lead-time l is $p(f,x|l)$ and completely describes the performance of the forecasting system. A perfect forecasting sys-

tem would ensure that $p(f, x| l) = 0$ when $f \neq x$. In the case of TWC, l may obtain integer values ranging from 0 (same day) to 9 (the last day in a 10-day forecast). Since

$$p(f, x | l) = p(f | l)\, p(x | f, l) = p(x | l)\, p(f | x, l),$$

two different factorizations of $p(f, x| l)$ are possible and each facilitates the analysis of forecasting performance.

The first factorization, $p(f, x| l) = p(f | l)p(x| f, l)$ is known as the calibration-refinement (CR) factorization. Its first term, $p(f | l)$, is the marginal or predictive distribution of forecasts and its second term, $p(x| f, l)$, is the conditional distribution of the observation given the forecast. For example, $p(1| f, l)$ is the relative frequency of precipitation when the forecast was f and the lead-time was l. The forecasts and observations are independent if and only if $p(x|f, l) = p(x|l)$. A set of forecasts is well *calibrated* (or reliable) if $p(1| f, l) = f$ for all f. A set of forecasts is perfectly *refined* (or sharp) if $p(f) = 0$ when f is not equal to 0 or 1 (i.e., the forecasts are categorical). Forecasting the climatological average or base rate will be well calibrated, but not sharp. Likewise, perfectly sharp forecasts generally will not be well calibrated.

The second factorization, $p(f, x| l) = p(x| l)p(f | x, l)$, is the likelihood-base rate (LBR) factorization. Its first term, $p(x| l)$, is the climatological precipitation frequency. Its second term, $p(f | x, l)$, is the likelihood function (also referred to as discrimination). For example, $p(f | 1, l)$ is the relative frequency of forecasts when precipitation occurred, and $p(f | 0, l)$ is the forecast frequency when precipitation did not occur. The likelihood

functions should be quite different in a good forecasting system. If the forecasts and observations are independent, then $p(f \mid x, l) = p(f \mid l)$.

5.2.2. Summary measures

In addition to the distributional comparison discussed above, we will use several summary measures of forecast performance. The mean forecast given a particular lead-time is

$$\bar{f}_l = \sum_F \sum_X f \; p(f, x \mid l) = E_{F,X|l}[f],$$

where $E[\,]$ is the expectation operator. Likewise, the climatological frequency of precipitation, indexed by lead-time, is

$$\bar{x}_l = E_{F,X|l}[x].$$

The mean error (ME) is

$$\mathrm{ME}(f, x \mid l) = \bar{f}_l - \bar{x}_l$$

and it is a measure of unconditional forecast bias. The mean-square error (MSE) or the Brier score (Brier 1950) is

$$\mathrm{MSE}(f, x \mid l) = E_{F,X|l}[(f - x)^2]. \tag{22}$$

The climatological skill score (SS) is

$$\mathrm{SS}(f, x \mid l) = 1 - \mathrm{MSE}(f, x \mid l) / \mathrm{MSE}(\bar{x}_l, x \mid l).$$

Note that

$$\mathrm{MSE}(\bar{x}_l, x \mid l) = E_{F,X|l}[(\bar{x} - x)^2] = \sigma_x^2,$$

where σ_x^2 is the variance of the observations. Therefore,

$$\mathrm{SS}(f, x \mid l) = \frac{\sigma_x^2 - \mathrm{MSE}(f, x \mid l)}{\sigma_x^2}, \tag{23}$$

and we see that SS measures the proportional amount by which the forecast reduces our uncertainty regarding precipitation, as measured by variance.

In addition to these scoring measures, we will also investigate the correlation between the forecasts and the observations, which is given by

$$\rho(f, x \mid l) = \frac{\mathrm{cov}(f, x \mid l)}{(\sigma_x^2 \sigma_f^2)^{1/2}},$$

where cov is the covariance and σ_f^2 is the variance of the forecasts.

5.3. Data Gathering Procedure

5.3.1. PoP forecasts

We collected TWC forecasts from 2 November 2004 to 16 January 2006. [These data were collected from http://www.weather.com/, which provides a 10-day forecast that includes forecasts from the same day (0-day forecast) to 9 days ahead.] Figure 31 displays a representative 10-day forecast from 2007. These forecasts are available for any zip code or city and include probability of precipitation, high/low temperature, and verbal descriptions or weather outcomes such as "partly cloudy." The forecasts are updated on a regular basis and are freely available to the public.

TWC's PoP forecasts cover a 12-h window during the daytime (0700–1900 local time), rather than a complete 24-h day. The 12-h PoP is the maximum hourly PoP estimated by TWC during the forecast window. PoPs are rounded and must adhere to local rules relating PoPs to weather outcomes (B. Rose 2007, personal communication).[27]

[27] Bruce Rose is a meteorologist and software designer for TWC based in Atlanta, Georgia. The authors worked closely with Dr. Rose to understand TWC's forecasting process.

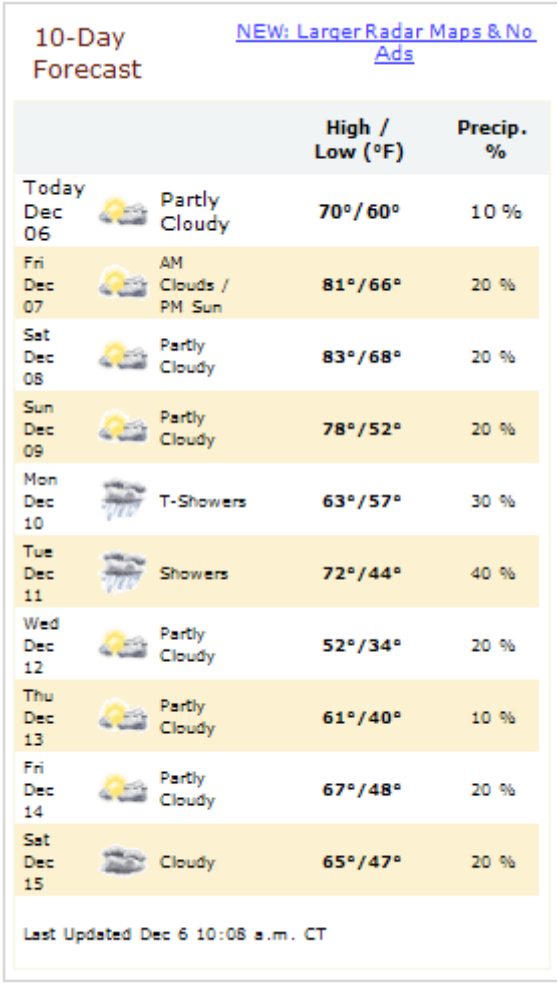

10-Day Forecast

NEW: Larger Radar Maps & No Ads

		High / Low (°F)	Precip. %
Today Dec 06	Partly Cloudy	70°/60°	10 %
Fri Dec 07	AM Clouds / PM Sun	81°/66°	20 %
Sat Dec 08	Partly Cloudy	83°/68°	20 %
Sun Dec 09	Partly Cloudy	78°/52°	20 %
Mon Dec 10	T-Showers	63°/57°	30 %
Tue Dec 11	Showers	72°/44°	40 %
Wed Dec 12	Partly Cloudy	52°/34°	20 %
Thu Dec 13	Partly Cloudy	61°/40°	10 %
Fri Dec 14	Partly Cloudy	67°/48°	20 %
Sat Dec 15	Cloudy	65°/47°	20 %

Last Updated Dec 6 10:08 a.m. CT

Figure 31. Example of 10-day forecast available at the TWC Web site.

We selected 50 locations in the United States, one in each state. Within each state we selected a major city. Within each city we selected the lowest zip code, excluding P.O. boxes. See Table 38 for a list of the cities and zip codes included in this study.

Since TWC's forecasts are not archived, we recorded the forecasts daily. We automated this collection using a Web query and a macro in Microsoft Excel. The macro gathered forecast data directly from Web pages, such as that shown in Figure 31. This process worked well, but was not completely automatic. In some cases, we experienced

temporary problems with certain zip codes (e.g., http://www.weather.com/ data being unavailable) or faced Internet outages. These errors were generally discovered at a point at which forecast data could still be acquired. However, on some days (though fewer than 5%), we were unable to retrieve the PoP forecasts, and these data have been excluded from the analysis. While we did record high and low temperature in addition to PoP, we do not analyze temperature forecasts in this paper.

Because the archival process required intervention, we decided upon a single collection time. This timing is important because the forecasts are updated frequently and not archived. To ensure that we did not collect same-day forecasts before they were posted in our westernmost zip codes (Hawaii and Alaska) we established a collection time of 1130 central standard time (CST), which corresponds to 0730 Hawaii–Aleutian standard time, 0830 Alaska standard time, 0930 Pacific standard time, 1030 mountain standard time, and 1230 eastern standard time (EST). During daylight saving time (DST), we archived forecasts at 1130 central daylight time (CDT; 1030 CST). TWC builds their forecasts at 0100, 0300, 0900, 1100, 1810, and 2300 EST [or eastern daylight time (EDT); B. Rose 2007, personal communication]. These forecasts reach TWC's Web site approximately 15 min later. Therefore, our forecasts represent TWC's view at 1000 CST (or CDT). On rare occasions, TWC amends forecasts during the day, but we do not try to account for this.

5.3.2. Precipitation observations

The observed records of daily precipitation and high/low temperature of the current and previous month are available online at the TWC Web site. However, the Web

site only archives daily precipitation observations, whereas we require hourly observations because the PoP forecast is for the 12-h window during the daytime. Therefore, we obtained hourly precipitation observation data from the National Climatic Data Center (NCDC; available online at www.ncdc.noaa.gov). Using NCDC's database, we selected the observation station that was closest to our forecast zip code.[28] Table 38 lists the observation stations used in this study and both the distance and elevation difference between the forecast zip code and the observation station. Most stations were within 20 km of the forecast zip code. However, eight stations were more than 20 km from the forecast area (i.e., Alaska, California, Colorado, Idaho, New Mexico, Oklahoma, Pennsylvania, and Vermont). In addition, one forecast–observation pair was separated by more than 500 m in elevation (i.e., Alaska). We have therefore removed these eight locations from our analysis, leaving 42 locations.[29] The average distance and elevation between observation stations and our zip codes for these 42 locations are approximately 7 km and 18 m, respectively. The maximum distance and elevation difference between forecast–observation pairs are 16 km and 181 m, respectively. We also verified that the surface conditions between the observation–forecast pairs for the 42 remaining stations are similar.

[28] We considered an NCDC observation of less than 0.01 in. of precipitation as an observation of no precipitation.

[29] In hindsight, we should have selected forecasts that correspond to observation stations. However, we initially thought we would be able to use TWC's observation data, only later realizing that these observations do not cover the same length of time as the forecasts.

Table 38. Forecast zip codes and observation stations.

State	City	Forecast zip code	Observation station (call sign)	Distance between forecast and observation (km)	Elev diff between forecast and observation (m)
Alabama	Montgomery	36104	Montgomery Regional Airport (MGM)	13	16
Alaska	Valdez	99686	M. K. Smith Airport (CDV)	72	1571
Arizona	Phoenix	85003	Phoenix Sky Harbor International Airport (PHX)	5	7
Arkansas	Little Rock	72201	Adams Field Airport (LIT)	5	15
California	Stanford	94305	Hayward Executive Airport (HWD)	24	15
Colorado	Denver	80002	Denver International Airport (DEN)	29	11
Connecticut	Hartford	06101	Hartford–Brainard Airport (HFD)	5	7
Delaware	Newark	19702	New Castle County Airport (ILG)	11	2
Florida	Tallahassee	32306	Tallahassee Regional Airport (TLH)	5	2
Georgia	Atlanta	30303	Hartsfield–Jackson Atlanta Intl AP (ATL)	11	12
Hawaii	Honolulu	96813	Honolulu International Airport (HNL)	8	17
Idaho	Idaho Falls	83401	Idaho Falls Regional ARPT (IDA)	32	246
Illinois	Chicago	60601	Chicago Midway International ARPT (MDW)	11	5
Indiana	Indianapolis	46201	Indianapolis International Airport (IND)	16	7
Iowa	Des Moines	50307	Des Moines International Airport (DSM)	6	21
Kansas	Wichita	67202	Colonel James Jabara Airport (AAO)	8	34
Kentucky	Frankfort	40601	Capital City Airport (FFT)	8	10
Louisiana	New Orleans	70112	Louis Armstrong New Orleans Intl AP (MSY)	16	1
Maine	Augusta	04330	Augusta State Airport (AUG)	5	66
Maryland	Baltimore	21201	Baltimore–Washington International Airport (BWI)	13	19
Massachusetts	Cambridge	02139	Logan International Airport (BOS)	8	1
Michigan	Detroit	48201	Detroit City Airport (DET)	6	4
Minnesota	Minneapolis	55401	Minneapolis–St. Paul International AP (MSP)	11	13
Mississippi	Jackson	39201	Jackson International Airport (JAN)	10	17
Missouri	Springfield	65802	Springfield–Branson Regional Airport (SGF)	5	6
Montana	Helena	59601	Helena Regional Airport (HLN)	14	14
Nebraska	Lincoln	68502	Lincoln Municipal Airport (LNK)	8	6
Nevada	Reno	89501	Reno–Tahoe International Airport (RNO)	3	24
New Hampshire	Manchester	03101	Manchester Airport (MHT)	6	14
New Jersey	Trenton	08608	Trenton Mercer Airport (KTTN)	6	45
New Mexico	Santa Fe	87501	Santa Fe Municipal Airport (SAF)	32	215
New York	New York	10001	Central Park (NYC)	5	30
North Carolina	Raleigh	27601	Raleigh–Durham International AP (RDU)	16	39
North Dakota	Fargo	58102	Hector International Airport (FAR)	2	0
Ohio	Columbus	43085	Port Columbus International Airport (CMH)	16	29
Oklahoma	Oklahoma City	73102	Wiley Post Airport (PWA)	21	23
Oregon	Portland	97201	Portland International Airport (PDX)	10	182
Pennsylvania	Pittsburgh	15201	Pittsburgh International Airport (PIT)	24	73
Rhode Island	Providence	02903	T. F. Green State Airport (PVD)	10	9
South Carolina	Charleston	29401	Charleston AFB/International Airport (CHS)	14	9
South Dakota	Sioux Falls	57103	Joe Foss Field Airport (FSD)	3	30
Tennessee	Memphis	38103	Memphis International Airport (MEM)	11	5
Texas	College Station	77843	Easterwood Airport (KCLL)	2	8
Utah	Salt Lake City	84101	Salt Lake City International Airport (SLC)	6	2
Vermont	Newport	05855	Morrisville–Stone St. ARPT (MVL)	48	3
Virginia	Richmond	23219	Richmond International Airport (RIC)	10	3
Washington	Seattle	98101	Seattle–Tacoma International Airport (SEA)	14	68
West Virginia	Charleston	25301	Yeager Airport (CRW)	3	95
Wisconsin	Madison	53703	Dane County Regional–Truax Field Airport (MSN)	6	4
Wyoming	Cheyenne	82001	Cheyenne Airport (CYS)	3	11

The hourly data for each observation station is archived according to local standard time (LST). We used a 12-h observation window from 0700 to 1900 LST for each location to calibrate the PoP forecast data, which corresponds to the TWC's PoP definition. Because the observations are always archived according to LST, during DST we slide our observation window up 1 h (0600–1800 LST) except in Arizona and Hawaii.

The verification of the same day PoP forecasts is more complicated than other PoP forecasts because the timing of the forecast collection determines which hours of observation data should be included. For example, in the eastern time zone, we only want to include precipitation observations between 1100 and 1900 EST (or between 1000 and 1800 EST during DST). Therefore, we removed hourly precipitation observations that occurred before the forecast time for the same-day forecasts at each location.

5.3.3. Data summary

Before beginning our analysis, we summarize our forecast and observation data in Table 39. We collected between 15 742 and 17 338 PoP forecasts, depending on the lead-time (169 163 PoPs in total). Precipitation was observed approximately 21% of the time. The frequency of precipitation for same-day forecasts is lower (18%) because these forecasts span less than a 12-h window for some time zones. TWC's average PoP forecast varied over the lead-times, ranging from a low of 0.198 (7 day) to a high of 0.265 (8 day). All but one lead-time exhibits a positive mean error between the forecast and the observation, suggesting some degree of positive bias in TWC's PoP forecasts. The same-day bias is 0.052.

Table 39. Summary of forecast and observation data.

Lead-time (days)	No. of forecasts	Precipitation observations (x = 1)	Avg PoP forecast	Frequency of precipitation	ME
0	17,338	3121	0.232	0.180	0.052
1	17,231	3651	0.245	0.212	0.034
2	17,161	3636	0.243	0.212	0.031
3	17,075	3610	0.242	0.211	0.031
4	16,975	3605	0.237	0.212	0.025
5	16,914	3550	0.231	0.210	0.021
6	16,909	3588	0.231	0.212	0.019
7	16,849	3580	0.198	0.212	-0.015
8	16,815	3577	0.265	0.213	0.052
9	15,742	3283	0.230	0.209	0.021

Table 40 details the number of forecasts by PoP and lead-time. TWC forecast a 0.2 PoP 4930 times for their same-day forecast. Overall, a 0.0 PoP was forecast 24 382 times, while a PoP of 1.0 was forecast 410 times. The italic values identify forecasts that were made fewer than 40 times, which we exclude from further analysis.[30]

Table 40. Number of probability of precipitation forecasts by lead-time.

Lead-	PoP											
time	0	0.1	0.2	0.3	0.4	0.5	0.6	0.7	0.8	0.9	1	Subtotal
0	4316	2469	4930	2065	799	909	602	234	606	175	233	17338
1	4169	2312	4537	2215	907	833	877	272	794	193	122	17231
2	2285	2989	5435	3366	900	457	936	389	246	113	45	17161
3	1084	2103	7212	4076	1486	231	720	93	70	*30*	*10*	17115
4	1047	2164	7215	4116	1570	244	545	74	*29*	*9*	*0*	17013
5	1053	2395	7106	4152	1541	232	435	*33*	*17*	*5*	*0*	16969
6	1142	2465	6768	4220	1618	228	468	*13*	*1*	*2*	*0*	16925
7	2737	3390	5344	3485	1266	63	564	*3*	*0*	*2*	*0*	16854
8	3395	3271	2907	1810	1255	95	4082	*0*	*0*	*0*	*0*	16815
9	3154	3456	3155	2218	1348	105	2306	*0*	*0*	*0*	*0*	15742
Subtotal	24382	27014	54609	31723	12690	3397	11535	1111	1763	529	410	169163

[30] A cutoff of 40 is common in hypothesis testing. The variance of a binomial distribution is $Np(1 - p)$. The normal approximation to the binomial is very good when this variance is greater than 10. Thus, if $p = ½$ then N should be greater than 40.

5.4. Forecast Verification

5.4.1. Calibration-refinement factorization

Figure 32 displays a calibration or attributes diagram (Hsu & Murphy, 1986) for TWC's 0-day PoP forecasts. The line at 45°, labeled "perfect," identifies PoPs that are perfectly calibrated [i.e., $p(1|f, l) = f$]. The horizontal line labeled "no resolution" identifies the case where the frequency of precipitation is independent of the forecast. The line halfway between no resolution and perfect is labeled "no skill." Along this line the skill score is equal to 0 and according to Equation (23), the forecast does not reduce uncertainty in the observation. Points above (below) this line exhibited positive (negative) skill.

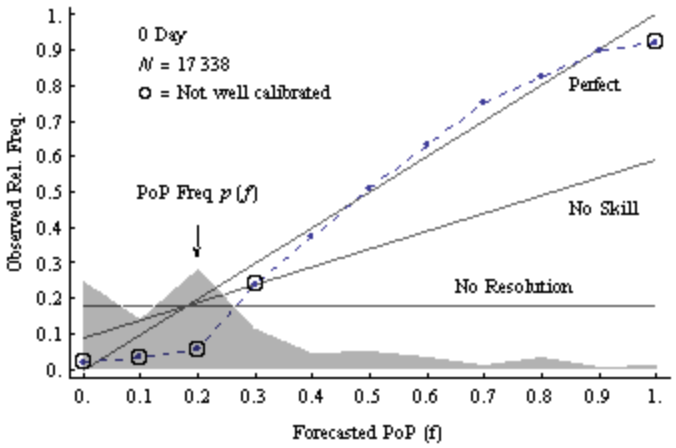

Figure 32. Calibration diagram for TWC's same-day PoP forecasts.

The gray area in Figure 32 presents the frequency with which different PoPs are forecast [i.e., $p(f)$]. We notice peaks at PoPs of 0.0 and 0.2, each being forecast more than 20% of the time.

We identified a probability interval around the line of perfect calibration, based on the number of forecasts, which determines whether we identify a PoP as being not well calibrated. Based on the normal approximation to the binomial distribution, we establish a 99% credible interval, in which case there is a 1% chance a forecast–observation pair would be outside this interval (0.5% chance of being above and 0.5% chance of being below). For example, if the PoP was truly *f*, then there is a 99% chance that the actual relative frequency of precipitation would be within

$$f \pm \Phi^{-1}(0.995)\left[\frac{f(1-f)}{N}\right]^{1/2}, \tag{24}$$

where Φ^{-1} is the inverse of the standard normal cumulative [$\Phi^{-1}(0.995) = 2.576$] and N is the number of forecasts. This range forms an envelope around the line of perfect calibration, the width of which is determined by Equation (24). If a forecast–observation pair lies outside this range, then the forecast is not well calibrated.5 PoPs of 0.0, 0.1, 0.2, 0.3, and 1.0 are not well calibrated. PoPs of 0.0 and 1.0 will not be well calibrated if even a single contrary event occurs, which is a good reason to restrict PoP forecasts to the open interval (0, 1).

The 0.3 PoP is not well calibrated and exhibits no skill. PoPs below 0.3 are quite poor: they are miscalibrated, exhibit negative skill, and are biased. For example, when TWC forecast a 0.2 chance of precipitation for the same day, precipitation occurred only 5.5% of the time.

PoPs of 0.4 and above, excluding 1.0, can be taken at face value and used directly in decision making. However, PoPs of 0.3 and below or 1.0 require adjustment—sometimes significant.

Figure 33 presents the calibration diagrams for lead-times of 1–9 days. The 1-day forecasts exhibit the same behavior as the 0-day forecasts: PoPs from 0.0 to 0.2 and 1.0 are miscalibrated. The calibration of midrange PoPs begins to degrade with lead-time. Performance decreases markedly beginning with the 7-day forecasts. For example, most of the PoP forecasts lay along the no skill line for lead-times of 7 days or longer. While predictability does decrease with lead-time, calibration performance should not; a forecast of *f* should occur *f* × 100% of the time whether it was a forecast for the next hour or the next year.

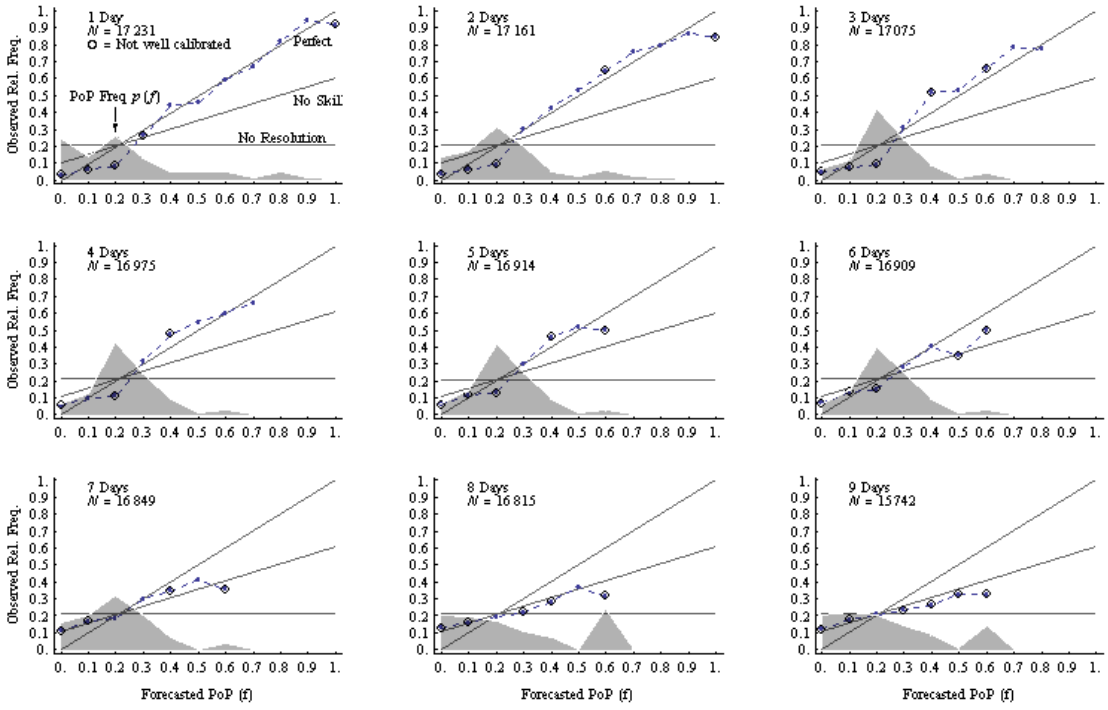

Figure 33. Calibration diagrams for 1- to 9-day lead-times.

These phenomena can be explained in part by TWC's forecasting procedure (B. Rose 2007, personal communication). The meteorologists at TWC receive guidance from a mixture of numerical, statistical, and climatological inputs provided by computer systems. The human forecasters rarely intervene in forecasts beyond 6 days. Thus, the verification results of the 7–9-day forecasts represent the "objective" machine guidance being provided to TWC's human forecasters. In this respect, the human forecasters appear to add considerable skill, since the 0–6-day calibration performance is so much better.

However, when humans do intervene, they introduce considerable bias into the low-end PoP forecasts. This bias could be a by-product of the intervention tools used by the human forecasters. The forecasters do not directly adjust the PoPs, but instead change what is known as the sensible weather forecast. For example, they might change partly cloudy to "isolated thunder." When this change is made, a computer algorithm determines the "smallest" change that must be made in a vector of weather parameters to make them consistent with the sensible weather forecast. A PoP of 29% is the cutoff for a dry forecast and therefore, it appears as though this intervention tool treats all "dry" PoPs as being nearly equivalent. This also might explain the curious dip in forecast frequency at 0.1 in both the 0- and 1-day forecasts.

The frequency of forecasts highlights additional challenges with the machine guidance. The most likely 8- and 9-day forecasts are 0.0 and 0.6, with a forecast of 0.5 being very unlikely. TWC appears to avoid forecasts of 0.5. We can even see the "ghost" of the 0.6 peak in the shorter-term human-adjusted forecasts. Forecasts as extreme as 0.0

or 0.6 are difficult to justify far into the future. For example, the frequency of precipitation conditional on the forecast ranges from 0.12 to 0.32 for the 9-day forecast. It appears that TWC's forecasts would need to be constrained to this range if they were intended to be well calibrated.

Table 41 presents several summary measures of forecasting performance. The mean-square error [Equation (22)] ranges from 0.095 to 0.188. The variance of the forecasts is less than the variance of the observations, but much less stable. The correlation between the forecasts and the observations begins at 0.615 and declines quickly with lead-time. The same-day skill score is approximately 36% and declines with lead-time. The 8- and 9-day computer forecasts exhibit negative skill—using the computer forecasts directly induces more error than using climatology. For comparison, Murphy and Winkler (1977) found an overall SS for a sample of National Weather Service forecasts, averaged over all lead-times, of approximately 31%.

Table 41. Summary measures.

		Variance			
Lead-time	MSE	Forecasts	Observations	Correlation	Skill score
0	0.095	0.053	0.148	0.615	35.9%
1	0.113	0.055	0.167	0.575	32.4%
2	0.127	0.036	0.167	0.499	24.2%
3	0.140	0.019	0.167	0.416	16.1%
4	0.147	0.016	0.167	0.352	11.8%
5	0.152	0.014	0.166	0.289	8.1%
6	0.158	0.015	0.167	0.243	5.4%
7	0.167	0.019	0.167	0.177	0.4%
8	0.188	0.049	0.167	0.176	–12.0%
9	0.179	0.038	0.165	0.158	–8.2%

5.4.2. Likelihood-base-rate factorization

Figure 34 displays the likelihood functions (or discrimination plots), $p(f \mid 1, l)$ and $p(f \mid 0, l)$ for TWC's 0-day PoP forecasts. Given that precipitation did not occur, it is likely TWC forecast a PoP of either 0.0 or 0.2. Likewise, it is unlikely that PoPs greater than 0.6 were forecast in this situation. However, if precipitation did occur, a range of PoPs from 0.3 to 0.8 were almost equally likely to have been forecast. Ideally, one would hope to see $p(f \mid 1, l)$ peak at high PoPs and decline to the left.

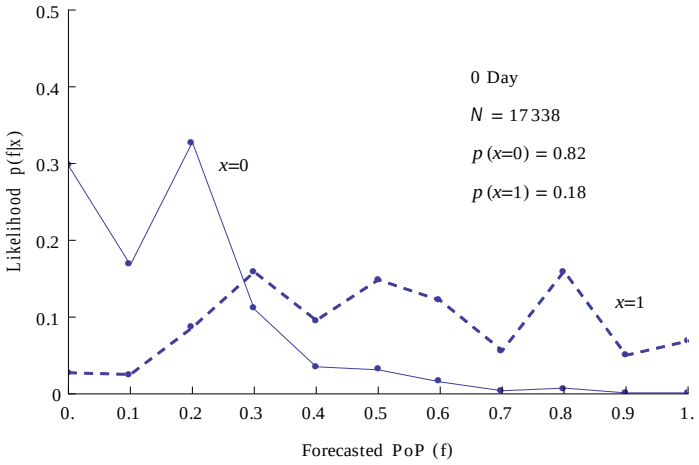

Figure 34. Likelihood function for TWC same-day forecasts.

Figure 35 displays likelihoods for the remainder of lead-times. The degree of overlap between the likelihood functions increases rapidly with lead-time, as the forecasts lose their ability to discriminate and skill scores fall. The peaks at a PoP of 0.6 are even more pronounced in the likelihood graphs.

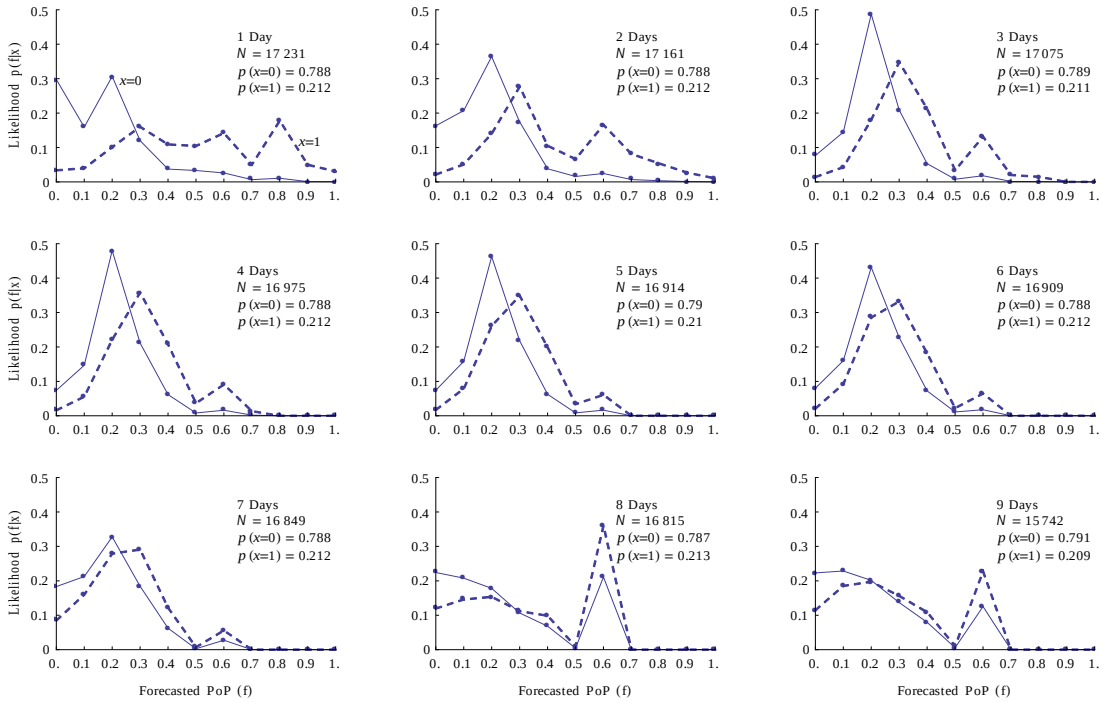

Figure 35. Likelihood diagrams for 1–9-day lead-times.

5.4.3. Warm and cool seasons

Following Murphy and Winkler (1992), we gain additional insight into TWC's forecasts by analyzing their performance during warm (April–September) and cool (October–March) months. Table 42 summarizes the forecast and observation data by season. Approximately 60% of our dataset covers the cool season because we gathered data from 2 November 2004 to 16 January 2006. The sum of the number of forecasts for the cool and warm seasons is lower than the totals presented in Table 39 because we have excluded PoPs that were forecast fewer than 40 times. For example, a same-day PoP of 0.9 was forecast only 26 times during the warm-season and has therefore been excluded from the warm-season analysis (17,388 – 10,374 – 6,938 = 26).

Table 42. Summary of forecast and observation data for cool and warm seasons.

Cool season					
Lead-time (days)	No. of forecasts	Precipitation observations (x = 1)	Avg PoP forecast	Frequency of precipitation	ME
0	10374	1877	0.210	0.181	0.029
1	10374	2232	0.229	0.215	0.014
2	10296	2204	0.231	0.214	0.017
3	10256	2212	0.237	0.216	0.022
4	10216	2196	0.232	0.215	0.017
5	10170	2164	0.224	0.213	0.011
6	10149	2201	0.225	0.217	0.008
7	10117	2199	0.190	0.217	-0.027
8	10080	2188	0.243	0.217	0.026
9	8998	1904	0.239	0.212	0.027
Warm season					
Lead-time (days)	No. of forecasts	Precipitation observations (x = 1)	Avg PoP forecast	Frequency of precipitation	ME
0	6938	1222	0.262	0.176	0.086
1	6765	1341	0.262	0.198	0.064
2	6799	1380	0.252	0.203	0.049
3	6789	1381	0.248	0.203	0.044
4	6745	1404	0.244	0.208	0.036
5	6744	1386	0.240	0.206	0.035
6	6760	1387	0.240	0.205	0.035
7	6722	1377	0.209	0.205	0.004
8	6695	1373	0.296	0.205	0.091
9	6709	1371	0.216	0.204	0.012

The frequency of precipitation was lower during the warm season than during the cool season. Yet, TWC forecast higher PoPs during the warm season, resulting in a larger mean error. For example, the 0-day warm season PoP was 0.086 too high on average.

Figure 36 compares the 0-day PoP calibration in the cool and warm seasons. The most likely forecast in the cool season was 0.0, even though precipitation occurred more frequently than during the warm season. The cool season is not well calibrated for low (0.0–0.2) or high (0.8–1.0) PoPs, whereas the lower half of the PoP range performs poorly during the warm season—TWC overforecasts PoPs below 0.5 during the warm season. Overall, the warm season is not as well calibrated as the cool.

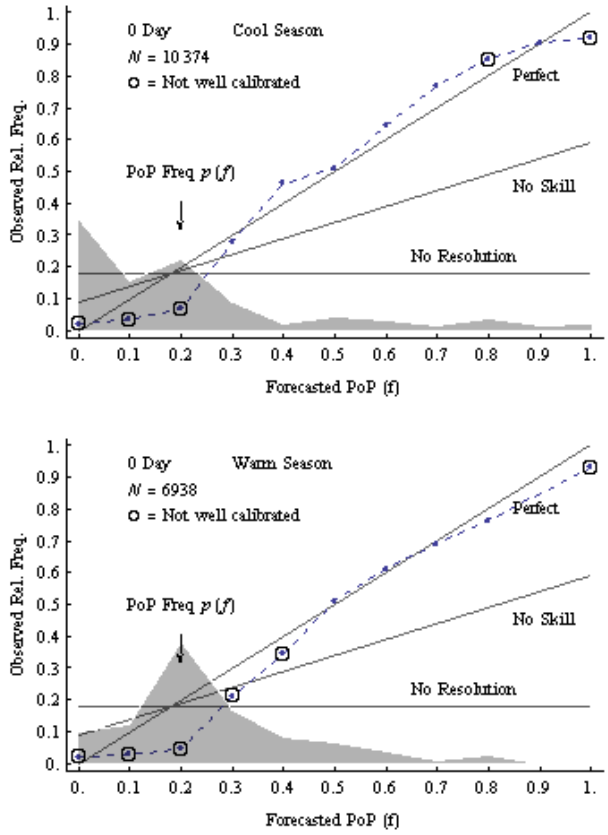

Figure 36. Same-day PoP calibration in warm and cool seasons.

Figure 37 contrasts the cool and warm calibration for 1–9-day forecasts. The calibration performance between the two seasons is similar. However, the cool-season PoPs tend to be sharper because they forecast 0.0 more frequently. One noticeable difference in forecast behavior is the increased frequency of 0.3 PoPs during the warm season.

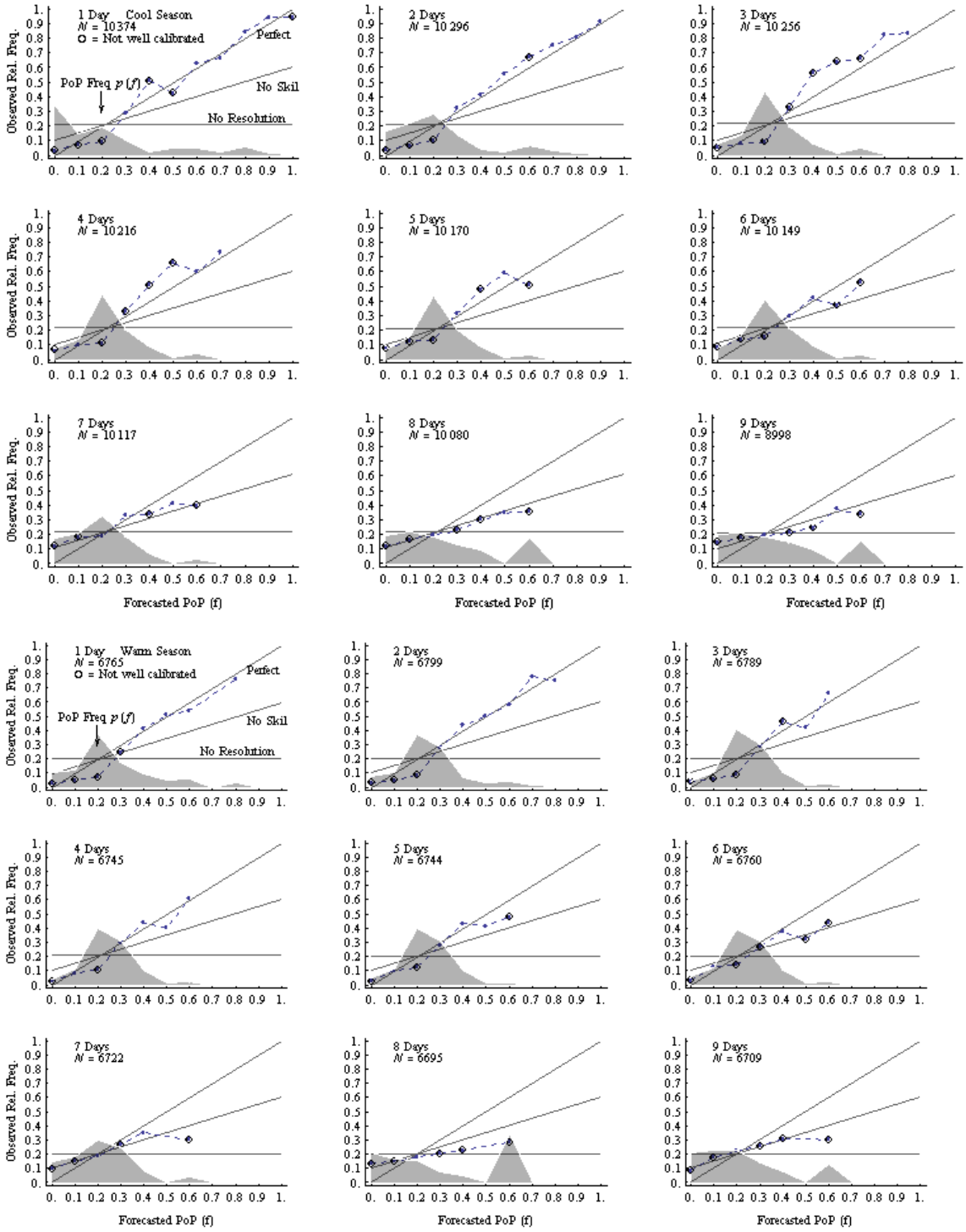

Figure 37. Comparison of PoP calibration in cool (top three rows) and warm (bottom three rows) seasons for 1–9-day lead-times.

Table 43 compares the skill scores and correlations between the two seasons. Warm-season forecasts are about half as skillful as the cool season. Cool-season skill scores begin at about 44% and decline to 0% by day 7. Warm-season skill scores are about 50% lower. For comparison, Murphy and Winkler (1992) found skill scores of 57%, 38%, and 30% for the 0-, 1-, and 2-day forecasts during the cool season and 37%, 24%, and 21% during the warm season, respectively. TWC's performance is on par with these earlier studies in the cool season, if somewhat worse for same-day forecasts. Warm-season performance appears to lag previous studies.

Table 43. Comparison of cool- and warm-season summary measures.

Cool season					
Lead time	MSE	Variance		Correlation	Skill Score
		Forecasts	Observations		
0	0.083	0.064	0.148	0.670	44.3%
1	0.103	0.067	0.169	0.627	39.2%
2	0.119	0.042	0.168	0.543	29.1%
3	0.137	0.021	0.169	0.450	19.0%
4	0.146	0.018	0.169	0.376	13.7%
5	0.153	0.016	0.168	0.300	8.9%
6	0.159	0.016	0.170	0.254	6.1%
7	0.169	0.019	0.170	0.184	0.7%
8	0.179	0.042	0.170	0.199	-5.3%
9	0.183	0.040	0.167	0.150	-9.8%
Warm season					
Lead time	MSE	Variance		Correlation	Skill Score
		Forecasts	Observations		
0	0.112	0.034	0.145	0.527	22.5%
1	0.128	0.032	0.159	0.468	19.4%
2	0.137	0.022	0.162	0.413	15.4%
3	0.144	0.013	0.162	0.360	11.2%
4	0.150	0.013	0.165	0.317	9.1%
5	0.152	0.012	0.163	0.276	6.9%
6	0.156	0.013	0.163	0.229	4.1%
7	0.163	0.019	0.163	0.171	-0.2%
8	0.200	0.058	0.163	0.152	-22.7%
9	0.172	0.035	0.163	0.170	-5.9%

We can better understand the drivers of the difference between warm and cool seasons by decomposing the MSE given in Equation (22) as follows (Murphy & Winkler, 1992):

$$\mathrm{MSE}(f,x\,|\,l) = \sigma_x^2 + E_{F|l}[(f - p(x\,|\,f,l)]^2 - E_{F|l}[(\overline{x}_l - p(x\,|\,f,l)]^2. \qquad (25)$$

The second term on the rhs of Equation (25) is a measure of calibration or refinement. The last term is the resolution (Murphy and Daan 1985). Figure 38 plots the MSE for the cool and warm seasons according to this factorization. Note that we have displayed the negative of the resolution (the lowest area) so that higher resolution lowers the MSE, as in Equation (25). We see that cool-season forecasts have better resolution (more negative) than the warm season. In addition the cool season exhibits better calibration for near-term (2 days or less) and long-term (7 days or more) PoP forecasts. The variance of the observations is slightly lower in the warm season.

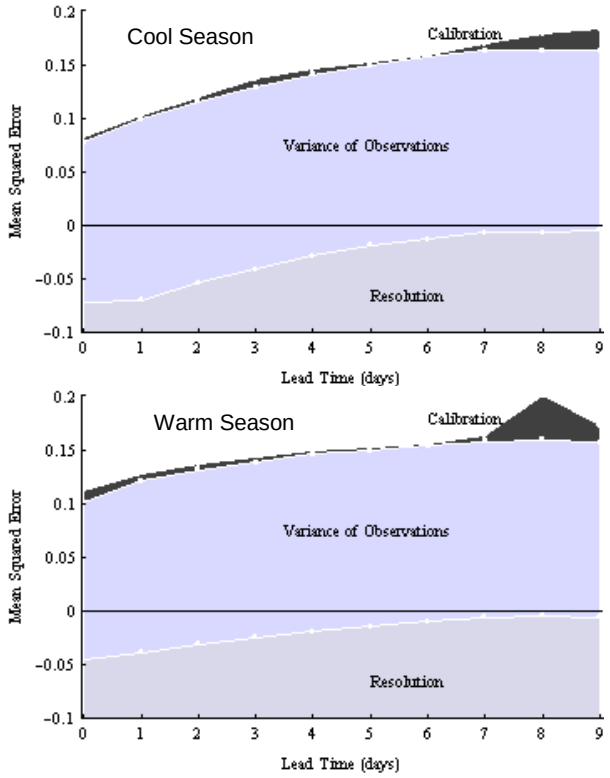

Figure 38. MSE decomposition for cool and warm seasons.

The best measure of a probability distribution's sharpness is its entropy *H* (Cover & Thomas, 1991), which is given by

$$H(p) = -\sum_i p_i \log(p_i).$$

The logarithm can be to any base, but we will use base 2. Entropy is at a minimum in the case of certainty and at a maximum when the probabilities are uniform. In the case of binary forecasts, the maximum entropy is $\log_2(2) = 1$. Entropy can also be thought of as a measure of the amount of information contained in a probability assessment, with lower entropies conveying greater information content.

Suppose a forecaster provides a PoP of *f*. The entropy of this forecast is $-[f \log_2(f) + (1 - f) \log_2(1 - f)]$. We can therefore associate an entropy to each of TWC's forecasts. Figure 39 plots the average entropy of TWC forecasts for the cool and warm seasons as a function of lead-time. In addition, the entropy of a climatological forecast, based on Table 42, is also displayed. In the case of the cool season, we see that TWC forecasts have less entropy (more information) than climatology. The 0- and 1-day forecasts are much narrower than forecasts based solely on climatology because a PoP of 0.0 is forecast often. Entropy increases with lead-time as one would expect, but suddenly drops for lead-times of 7–9 days. Because these forecasts are not calibrated, we see this drop in entropy as not a result of superior information. Rather, the long-term forecasts are too sharp. The warm season entropies are closer to climatology, but also drop significantly after 6 days.

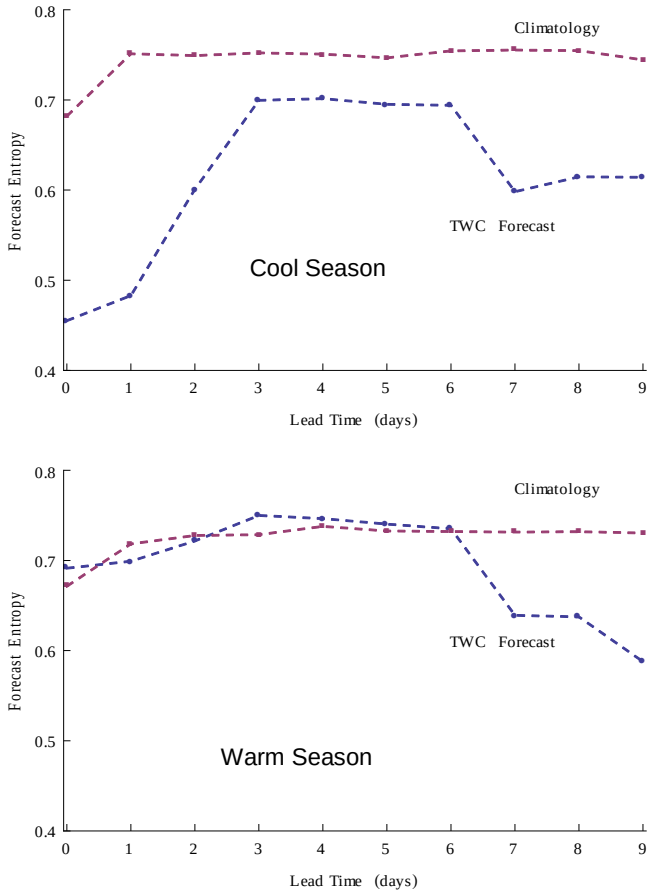

Figure 39. Forecast entropy for cool and warm seasons.

The 0-day likelihood functions for the cool and warm seasons are compared in Figure 40. Given that precipitation was not observed, the most likely forecast during the cool season was 0.0, whereas it was 0.2 during the warm season. If precipitation was observed, it was much more likely that a lower PoP was forecast during the warm season than during the cool season. We also notice peaks at 0.8 in the event of precipitation. Figure 41 compares the likelihoods for the remaining lead-times. The overlap between the likelihood functions is greater during the warm season. We also observe peaks at particular probabilities. For example, if precipitation occurred during the warm season, it is

almost certain that TWC did not forecast a PoP of 0.7 1-day ahead. Likewise, the 0.6 peaks are prominent in both seasons. Again, one would hope to see the likelihood function given precipitation peak at high PoPs and monotonically decline to the left. TWC's forecasts are good at identifying a lack of precipitation, but are not particularly strong at identifying precipitation—especially during the warm season.

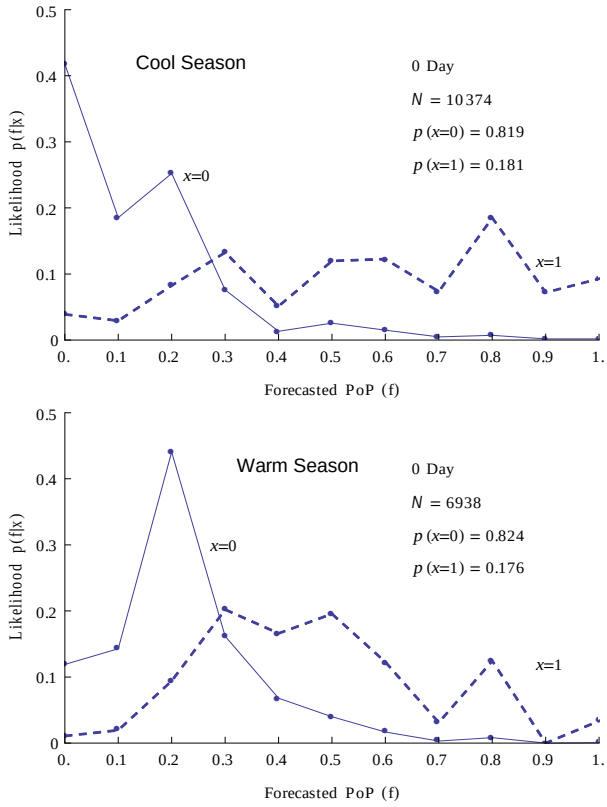

Figure 40. Cool- and warm-season same-day likelihood functions.

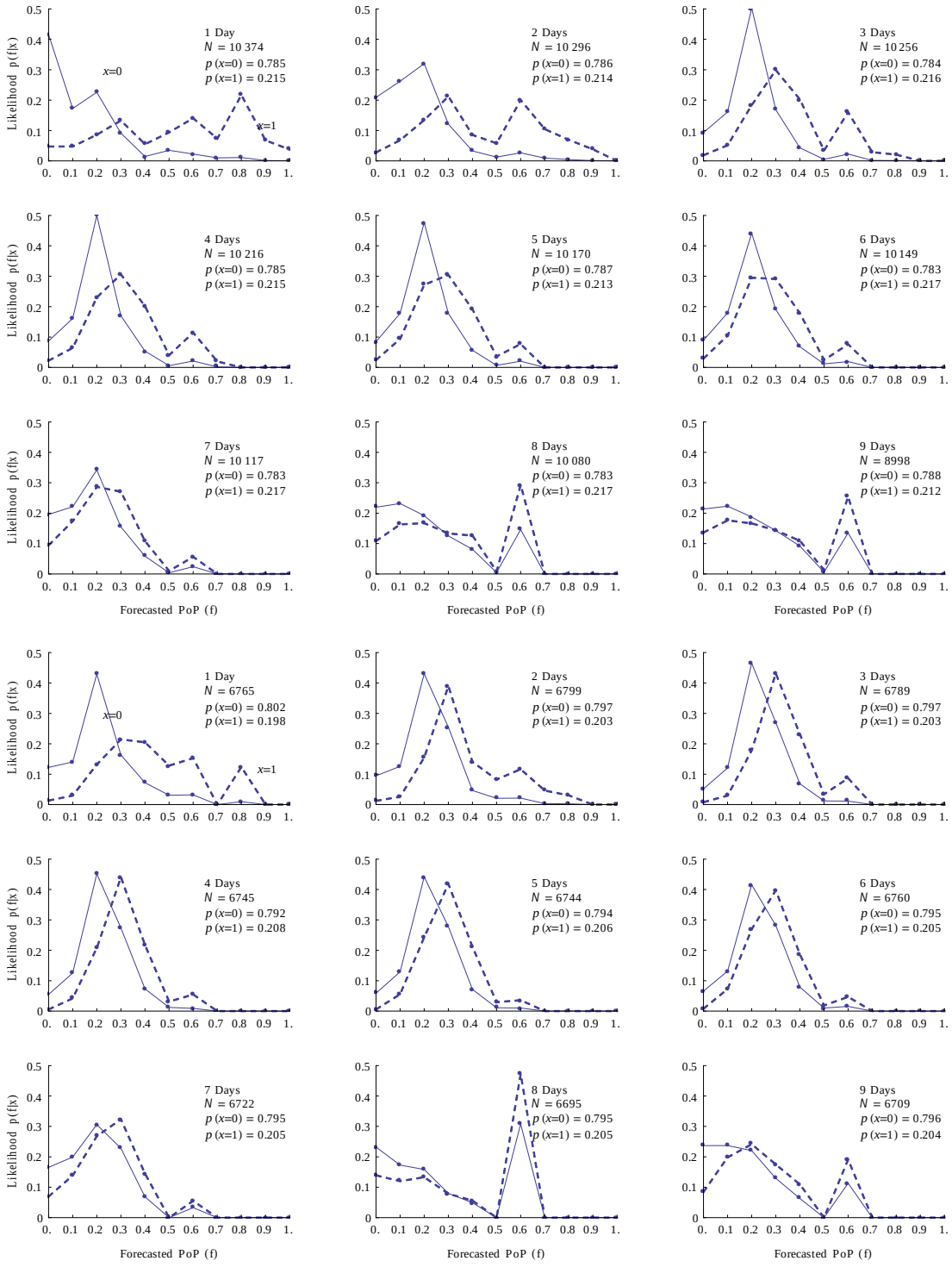

Figure 41. Likelihood functions for cool and warm season for 1–9-day lead-times.

5.5. Conclusions

TWC's forecasts exhibit positive skill for lead-times less than 7 days. Midrange PoPs tend to be well calibrated, but performance decreases with lead-time and worsens during the warm season. PoPs below 0.3 and above 0.9 are miscalibrated and biased. Overall, almost all lead-times exhibit positive bias and the same-day bias is significant, especially during the warm season.

As discussed previously, there is no reason, per se, that calibration performance should decrease with lead-time. Rather, the difficulty of the forecasting task should be reflected in the sharpness of the forecasts. TWC's long-term forecasts are too sharp. Apparently, one cannot reasonably forecast a 0% or 60% chance of precipitation 8 or 9 days from now, much less provide these forecasts nearly 40% of the time.

There seem to be two primary areas in which TWC could improve its forecasts: the machine guidance provided to human forecasters and the intervention tool used by these forecasters to arrive at sensible forecasts. The long-term forecasts, which are unedited by humans, exhibit a tendency to provide extreme forecasts and to artificially avoid 0.5. Perhaps revisions/additions to these models could improve performance. If not, TWC might want to consider intervening in these forecasts as well. The intervention of human forecasters increases skill, but also introduces bias. The intervention tool uses a least squares procedure to adjust underlying weather variables. Perhaps other approaches, such as the application of maximum entropy techniques (Jaynes, 1957), would improve performance. Maximum entropy techniques would avoid producing narrow and biased forecasts.

Performance during the warm season is noticeably worse; even though the variance of the observations is lower (see Table 43). This suggests that TWC should concentrate its attention on improving PoPs during this time. In addition, providing PoPs at 0.05 intervals (i.e., 0.05, 0.10, . . . , 0.95) might be helpful and enable TWC to avoid forecasts of 0.0 and 1.0, which will not be well calibrated.

6. CONCLUSION

This study showed how improvements in forecast accuracy and evacuation speed can be valued using dynamic programming (DP) and Markov processes (MPs). The benefit from forecast quality improvement monotonically increases. However, the benefit from evacuation speed improvement varies considerably.

Our San Patricio County example implies that the optimal investment decision is affected by the range of possible improvements and by budget. Given an unlimited budget and the choice between improving evacuation speed and improving forecast quality, the former provides a greater benefit. This is consistent with the comparison between the value of perfect information and the value of instantaneous evacuation with strictly increasing loss level and strictly decreasing evacuation cost. However, when the cost of improvement is considered, evacuation speed improvement loses much of its advantage. The non-exclusive case, where a combination of evacuation speed improvements and forecast quality improvements may be considered, yields mixed conclusions. If the budget is smaller than some threshold, more money should be invested in evacuation speed improvement than in forecast improvement. However, if the budget is larger than the threshold, more money should be invested in forecast improvement. This is because evacuation speed improvement can at best delay the critical decision until one stage before landfall, beyond which no more investment is beneficial.

Improvement of evacuation speed is more expensive than forecast improvement if there is no way to make improving evacuation speed cheaper. However, we focused

only on the benefit when faced with a hurricane, and other benefits from the infrastructure are not fully captured. Forecast improvement can conceivably provide benefit nationwide, whereas evacuation speed improvement provides benefit only locally. These facts could have affected the optimal investment decision but are left for future research.

This study also illustrated how to verify the assessed probabilities as a critical part of making good decisions. From this verification, one could decide which aspect of the forecast to improve.

Despite the difficulty of drawing general conclusions, we hope this framework will be of value in particular settings, helping policy makers choose between roads or radar.

Future research will include the improvement of landfall intensity forecasts, the tradeoff between track forecast improvement and intensity forecast improvement, scaling up the results to statewide or nationwide, partial improvement of the PER network, and insights or patterns from the Markov Decision Process (MDP) with simple cost structures.

REFERENCES

Bickel, J. E., & Kim, S. D. (2008). Verification of The Weather Channel Probability of Precipitation Forecasts. *Monthly Weather Review, 136*(12), 4867-4881.

Bickel, J. E., & Smith, J. E. (2006). Optimal Sequential Exploration: A Binary Learning Model. *Decision Analysis, 3*(1), 16-32.

Blake, E. S., Rappaport, E. N., & Landsea, C. W. (2007). The Deadliest, Costliest, and Most Intense United States Tropical Cyclones from 1851 to 2006 (And Other Frequently Requested Hurricane Facts). Miami, Florida: National Weather Service - National Hurricane Center, 45.

Broad, K., Leiserowitz, A., Weinkle, J., & Steketee, M. (2007). Misinterpretation of the "Cone of Uncertainty" in Florida during the 2004 Hurricane Season. *Bulletin of the American Meteorological Society, 88*(5), 651-667.

Considine, T. J., Jablonowski, C., Posner, B., & Bishop, C. H. (2004). The Value of Hurricane Forecasts to Oil and Gas Producers in the Gulf of Mexico. *Journal of Applied Meteorology, 43*(9), 1270-1281.

Cover, T. M., & Thomas, J. A. (1991). *Elements of Information Theory*. Hoboken, New Jersey: John Wiley & Sons, Inc.

Czajkowski, J. (2007). Is it Time to Go Yet? Dynamically Modeling Hurricane Evacuation Decisions. *Technical Report by International Hurricane Research Center, Florida International University*.

Gelman, A., Carlin, J. B., Stern, H. S., & Rubin, D. B. (2003). *Bayesian Data Analysis (2 ed.)*. Boca Raton, FL: Chapman & Hall/CRC.

Hoffer, S., Berardino, F., Smith, J., & Rubin, S. (1998). Economic Values for Evaluation of Federal Aviation Administration Investment and Regulatory Decisions. *Report FAA-APO-98-8*. Washington, D.C.: Federal Aviation Administration, U.S. Department of Transportation.

Hsu, W. R., & Murphy, A. H. (1986). The Attributes Diagram - A Geometrical Framework for Assessing the Quality of Probability Forecasts. *International Journal of Forecasting, 2*(3), 285-293.

Jaynes, E. T. (1957). Information Theory and Statistical Mechanics. *Physical Review, 106*(4), 620-630.

Jolliffe, I. T., & Stephenson, D. B. (2003). *Forecast Verification: A Practitioner's Guide in Atmospheric Science*. Chichester: John Wiley & Sons Ltd.

Katz, R. W., & Murphy, A. H. (1997). *Economic Value of Weather and Climate Forecasts*. Cambridge, UK: Cambridge University Press.

Lindell, M. K. (2008). EMBLEM2: An Empirically Based Large Scale Evacuation Time Estimate Model. *Transportation Research Part a-Policy and Practice*, *42*(1), 140-154.

Lindell, M. K., & Prater, C. S. (2007). A Hurricane Evacuation Management Decision Support System (EMDSS). *Natural Hazards*, *40*(3), 627-634.

Lindell, M. K., Prater, C. S., Lu, J. Y., Arlikatti, S., Zhang, Y., & Kang, J. E. (2004). Hurricane Lili Evacuation. College Station, TX: Hazard Reduction & Recovery Center, Texas A&M University.

Lindell, M. K., Prater, C. S., & Wu, J. Y. (2002). Hurricane Evacuation Time Estimates for the Texas Gulf Coast. College Station, TX: Hazard Reduction & Recovery Center, Texas A&M University.

Lodree Jr, E. J., & Taskin, S. (2009). Supply Chain Planning for Hurricane Response with Wind Speed Information Updates. *Computers & Operations Research*, *36*(1), 2-15.

McCardle, K. F. (1985). Information Acquisition and the Adoption of New Technology. *Management Science*, *31*(11), 1372-1389.

Murphy, A. H., & Winkler, R. L. (1977). Reliability of Subjective Probability Forecasts of Precipitation and Temperature. *Applied Statistics*, 26, 41-47.

Murphy, A. H., & Winkler, R. L. (1987). A General Framework for Forecast Verification. *Monthly Weather Review*, *115*(7), 1330-1338.

Murphy, A. H., & Winkler, R. L. (1992). Diagnostic Verification of Probability Forecasts. *International Journal of Forecasting*, *7*(4), 435-455.

NBO (2008). FY 2009 President's Request - Budget Estimates. Congressional Submission. NOAA Budget Office (NBO), 1052.

Raiffa, H., & Schlaifer, R. (1961). *Applied Statistical Decision Theory*. Boston: Division of Research, Harvard Business School.

Regnier, E. (2008). Public Evacuation Decisions and Hurricane Track Uncertainty. *Management Science*, *54*(1), 16-28.

Regnier, E., & Harr, P. A. (2006). A Dynamic Decision Model Applied to Hurricane Landfall. *Weather and Forecasting*, *21*(5), 764-780.

Viscusi, W. K. (2004). The value of life: Estimates with Risks by Occupation and Industry. *Economic Inquiry*, *42*(1), 29-48.

Washington State Department of Transportation (2002). Highway Construction Cost Comparison Survey. Author.

APPENDIX A

MODELING REVISION OF BELIEF USING CONJUGATE PAIR DISTRIBUTION

We assume that the information structure is represented by the conjugate pair Beta-Bernoulli.[31] According to this information structure, the DM's prior distribution on the probability of hurricane strike is a Beta with parameters (α, β) and the information comes from a Bernoulli distribution with parameter p^*. Here, stage 0 represents when a hazard is detected and it increases with time. Counting-up stage is used here to match the stage with the cumulative amount of information collected. We denote the information at stage k as binary random variable X_k, where $X_k = 1$ is a forecast that the hurricane will strike and $X_k = 0$ is a miss forecast. The probability of receiving information that the hurricane will strike is $P(X_k = 1) = p^* = 1 - P(X_k = 0)$. The prior probability of a strike p_0 is the mean of this distribution, which is equal to $\alpha/(\alpha+\beta)$.

Upon the arrival of information, the DM updates his/her prior distribution in the standard Bayesian fashion. Under the Beta(α, β) prior and Bernoulli information, the posterior distribution of P, given the k observed pieces of information X_1, X_2,⋯, X_k, is Beta ($\alpha + S_k$, $\beta + k - S_k$), where $S_k = X_1 + X_2 + \cdots + X_k$. This distribution has a mean of ($\alpha + S_k$) / ($\alpha + \beta + k$). As the X_i's are either 0 or 1, S_k is just the number of positive signals, which mean "Hurricane will hit the target" from the first k pieces of information, and $k - S_k$ is the number of negative signals, which mean "Hurricane will miss the target." Here,

[31] For background about conjugate pairs, see Raiffa and Schlaifer (1961).

the range of S_k is from 0 to k. This model structure is clearly limited because hurricane forecasts are richer than "hit" or "miss." We plan to relax this assumption in future work.

Given the assumption that the DM can collect only one piece of information at each stage, we consider the DM to be at stage k when he or she has collected exactly k pieces of information. If the DM is at stage k with prior probability p_k, then with probability $1 - p_k$ the next piece of information is a 0 (miss) and the point estimate decreases to $(\alpha + \beta + k)p_k / (\alpha + \beta + k + 1)$, whereas with probability p_k, the next piece of information is a 1 (hit) and the point estimate increases to $((\alpha + \beta + k)p_k + 1) / (\alpha + \beta + k + 1)$. At stage k, the posterior distribution is $Beta\left(\alpha + \sum_{i=1}^{k} x_i, \beta + k - \sum_{i=1}^{k} x_i\right)$ or $Beta(\alpha + S_k, \beta + k - S_k)$. The mean or point estimate of posterior distribution is $\frac{\alpha + S_k}{\alpha + \beta + k}$. In this Beta-Bernoulli conjugate pair information structure, the impact of a piece of information is large ($\frac{\alpha}{\alpha + \beta + 1}$ vs. $\frac{\alpha + 1}{\alpha + \beta + 1}$) at the first stage, but it decreases over stages ($\frac{\alpha + S_{k-1}}{\alpha + \beta + k}$ vs. $\frac{\alpha + S_{k-1} + 1}{\alpha + \beta + k}$).

We use dynamic programming to model this problem. Let $V_k(p_k)$ be the anticipated expense from following an optimal policy at stage k, when the current probability of hurricane strike is p_k. We assume either that the detected hurricane will hit the vulnerable area at stage N or that it will not. This assumption will be relaxed in future research so that the uncertainty of landfall timing is also considered. p_k is the stage k estimate of the probability that the hurricane will strike, which is estimated using the information

collected up to stage *k*. L_k is the loss if evacuation is begun at stage *k;* therefore, L_N represents the loss if evacuation is not completed before the hurricane strikes.

If the DM ignores the oncoming hurricane without further information gathering, the loss will be L_N with probability p_k. We refer to this as the "Ignore" alternative. If the DM takes action ("Act") at stage *k*, there will be an evacuation cost C_k and loss L_k with probability p_k. If the DM defers the decision ("Wait") and collects additional information at cost γ, the anticipated expense from the deferred decision depends on the additional information. This leads to the following dynamic programming functional equation:

$$V_k(p_k) = \min\left\{p_k L_N, C_k + p_k \cdot L_k, \gamma + \bar{V}_{k+1}(p_k)\right\}, \text{ for } p_k \in (0,1)^{32}$$

$$\bar{V}_{k+1}(p_k) \equiv (1-p_k)V_{k+1}\left(\frac{(\alpha+\beta+k)p_k}{\alpha+\beta+k+1}\right) + p_k V_{k+1}\left(\frac{(\alpha+\beta+k)p_k+1}{\alpha+\beta+k+1}\right)$$

$$\bar{V}_N(p_{N-1}) = p_{N-1}L_N .$$

$\bar{V}_{k+1}(p_k)$ is the expected value from following an optimal policy at stage *k*+1, given the current posterior probability p_k at stage *k*. $\bar{V}_N(p_{N-1})$ is the terminal value of $\bar{V}_{k+1}(p_k)$. This is equivalent to the value of decision "Ignore" at stage *N*-1 because the DM's only choice at the terminal stage is to face the risk if he or she didn't take action previously.

In order to make the impact of each piece of information constant over stages, we introduce a modified Beta-Bernoulli conjugate pair information structure with increasing weight W_k. W_k is the weight of a piece of information at stage *k* or the amount of infor-

[32] The range of p_k does not include 0 or 1, given that we assume that the prior probability is between 0 and 1 and posterior probability never reaches 0 or 1.

mation obtained at stage k. Therefore, the value of x_k is 0 or W_k. T_k is the cumulative sum of information up to stage k or $\sum_{i=1}^{k} W_i$. In this case, W_k / T_k is constant for all k.

If the impact of a piece of information or W_k/T_k were assumed to be constant at 1/2 (for $k > 1$), the value of W_k and T_k changes as in the following table:

k	1	2	3	4	5	6	7	…	N-1	N
W_k	1	1	2	4	8	16	32	…	2^{N-3}	2^{N-2}
T_k	1	2	4	8	16	32	64	…	2^{N-2}	2^{N-1}

If W_k/T_k were assumed to be constant at 2/3 (for $k > 1$), the value of W_k and T_k changes as in the following table:

k	1	2	3	4	5	6	7	…	N-1	N
W_k	1	2	6	18	54	162	486	…	$2\cdot3^{N-3}$	$2\cdot3^{N-2}$
T_k	1	3	9	27	81	243	729	…	3^{N-2}	3^{N-1}

If W_k/T_k were assumed to be constant at 3/4 (for $k > 1$), the value of W_k and T_k changes as in the following table:

k	1	2	3	4	5	6	7	…	N-1	N
W_k	1	3	12	48	192	768	3072	…	$3\cdot4^{N-3}$	$3\cdot4^{N-2}$
T_k	1	4	16	64	256	1024	4096	…	4^{N-2}	4^{N-1}

At stage k, the posterior distribution is

$$Beta\left(\alpha+\sum_{i=1}^{k}x_i,\beta+T_k-\sum_{i=1}^{k}x_i\right) \text{ or } Beta\left(\alpha+S_k,\beta+T_k-S_k\right).$$

The mean or point estimate of posterior distribution is

$$\frac{\alpha+S_k}{\alpha+\beta+T_k}.$$

At the first stage, the impact of a piece of information is

$$\frac{W_1}{\alpha+\beta+T_1}\ (\frac{\alpha}{\alpha+\beta+T_1}\ \text{vs.}\ \frac{\alpha+W_1}{\alpha+\beta+T_1})$$

and it converges to a constant rate

$$\frac{W_k}{\alpha+\beta+T_k}\to\frac{W_k}{T_k}\ (\frac{\alpha+S_{k-1}}{\alpha+\beta+T_k}\ \text{vs.}\ \frac{\alpha+S_{k-1}+W_k}{\alpha+\beta+T_k})$$

over stages.

Meanwhile, in order to increase the impact of each piece of information, we just need to make W_k increase faster.

APPENDIX B

DIFFERENT INFORMATION STRUCTURES (CONJUGATE PAIRS)

In Bayesian probability theory, a class of prior probability distributions $p(\theta)$ is said to be conjugate to a class of likelihood functions $p(x|\theta)$ if the resulting posterior distributions $p(\theta|x)$ are in the same family as $p(\theta)$. A conjugate prior is an algebraic convenience; otherwise, a difficult numerical integration may be necessary. All members of the exponential family have conjugate priors.

Beta-Bernoulli is a typical example of conjugate pairs. This section uses different conjugate pairs for possibly different types of information. There are many kinds of conjugate distributions, discrete as well as continuous.

In this section, stage k starts with 0 when a hazard is detected. It increases by 1 until it reaches the final stage, which is stage N. k also means the amount of information collected until stage k.

Discrete likelihood distributions applicable to our problem are as follows:[33](July 29)[**27, 28**]

Likelihood $p(x\|\theta)$	**Model parameters** θ	**Conjugate prior distribution** $p(\theta)$	**Prior hyperparameters** $p(\theta)$	**Posterior hyperparameters** $p(\theta\|\mathbf{x})$
Bernoulli	p (probability)	Beta	α, β	$\alpha + \sum_{i=1}^{k} x_i, \beta + k - \sum_{i=1}^{k} x_i$
Binomial	p (probability)	Beta	α, β	$\alpha + \sum_{i=1}^{k} x_i, \beta + \sum_{i=1}^{k} (n_i - x_i)$

[33] For more details about different conjugate pairs, see Raiffa and Schlaifer (1961) and Gelman, Carlin, et al. (2003).

Geometric	p_0 (probability)	Beta	α, β	$\alpha + k, \beta + \sum_{i=1}^{k} x_i$

Beta-Bernoulli

Prior is p (probability), whose distribution is Beta(α, β), and information is x (binary signal), whose distribution is Bernoulli(p). Posterior distribution is determined by the amount of information up to the current stage (k) and the sum of positive signals up to the current stage ($\sum_{i=1}^{k} x_i$ or S_k).

Likelihood function is

$$p(x \mid p_k) = p_k{}^{x}(1 - p_k)^{1-x} \qquad x \in \{0,1\}.$$

Pdf of prior is

$$\frac{x^{\alpha-1}(1-x)^{\beta-1}}{B(\alpha,\beta)}, \quad 0 \le x \le 1, \quad \alpha > 0, \quad \beta > 0,$$

where $B(\alpha,\beta) = \frac{\Gamma(\alpha)\Gamma(\beta)}{\Gamma(\alpha+\beta)}$. Mean of prior is $\frac{\alpha}{\alpha+\beta}$. Variance of prior is

$\frac{\alpha\beta}{(\alpha+\beta)^2(\alpha+\beta+1)}$. Posterior distribution is

$$p_k \mid \mathbf{x} \sim \text{Beta}\left(\alpha + \sum_{i=1}^{k} x_i, \beta + k - \sum_{i=1}^{k} x_i\right) \text{ or } \text{Beta}\left(\alpha + S_k, \beta + k - S_k\right).$$

Mean of posterior $p_k|\mathbf{x}$ (conditional mean) is

$$\frac{\alpha + \sum_{i=1}^{k} x_i}{\alpha + \beta + k} = \frac{\alpha + S_k}{\alpha + \beta + k}.$$

Variance of posterior (conditional variance) is

$$\frac{(\alpha + S_k)(\beta + k - S_k)}{(\alpha + \beta + k)^2(\alpha + \beta + k + 1)}.$$

Given that

$$p_k = \frac{\alpha + S_k}{\alpha + \beta + k}$$

$$S_{k+1} = S_k + x_{k+1},$$

p_{k+1} can be expressed as

$$p_{k+1} = \frac{\alpha + S_{k+1}}{\alpha + \beta + k + 1} = \frac{\alpha + S_k + x_{k+1}}{\alpha + \beta + k + 1} = \frac{(\alpha + \beta + k)p_k + x_{k+1}}{\alpha + \beta + k + 1}.$$

If $x_{k+1} = 0$, then $S_{k+1} = S_k$ and

$$p_{k+1} = \frac{\alpha + S_{k+1}}{\alpha + \beta + k + 1} = \frac{\alpha + S_k}{\alpha + \beta + k + 1} = \frac{(\alpha + \beta + k)p_k}{\alpha + \beta + k + 1}.$$

If $x_{k+1} = 1$, then $S_{k+1} = S_k + 1$ and

$$p_{k+1} = \frac{\alpha + S_{k+1}}{\alpha + \beta + k + 1} = \frac{\alpha + S_k + 1}{\alpha + \beta + k + 1} = \frac{(\alpha + \beta + k)p_k + 1}{\alpha + \beta + k + 1}.$$

Then the dynamic program is structured as

$$V_k(p_k) = \min\left\{L \cdot p_k, C + L_k \cdot p_k, \gamma + \delta \bar{V}_{k+1}(p_k)\right\}, \text{ for } p_k \in (0,1)$$

$$\bar{V}_{k+1}(p_k) \equiv (1 - p_k)V_{k+1}\left(\frac{(\alpha + \beta + k)p_k}{\alpha + \beta + k + 1}\right) + p_k V_{k+1}\left(\frac{(\alpha + \beta + k)p_k + 1}{\alpha + \beta + k + 1}\right)$$

$$\bar{V}_N(p_{N-1}) = L \cdot p_{N-1}.$$

Beta-Binomial

Prior is p (probability), whose distribution is Beta(α, β), and information is the number of positive signals x_i out of sample size n_i at stage i, whose distribution is Binomial(n_i, p). Posterior distribution is determined by cumulative amount of information or samples up to the current stage ($\sum_{i=1}^{k} n_i$) and cumulative number of positive signals up to the current stage ($\sum_{i=1}^{k} x_i$ or S_k).

This information structure is the same as Beta-Bernoulli except that the cumulative amount of information or samples is not identical to the current stage. But Beta-Bernoulli can be viewed as Beta-Binomial if it can jump more than one stage at a time. In other words, Beta-Bernoulli is a special case of Beta-Binomial where $n_i = 1$ for all i.

Likelihood function is

$$p(x \mid p_k) = \binom{n_k}{x} p_k{}^x (1-p_k)^{n_k - x} \qquad x \in \{0,1,2,...,n_k\}.$$

Pdf of prior is

$$\frac{x^{\alpha-1}(1-x)^{\beta-1}}{B(\alpha,\beta)}, \quad 0 \le x \le 1, \quad \alpha > 0, \quad \beta > 0,$$

where $B(\alpha,\beta) = \frac{\Gamma(\alpha)\Gamma(\beta)}{\Gamma(\alpha+\beta)}$. Mean of prior is $\frac{\alpha}{\alpha+\beta}$. Variance of prior is

$\frac{\alpha\beta}{(\alpha+\beta)^2(\alpha+\beta+1)}$. Posterior distribution is

$$p_k \mid \mathbf{x} \sim \text{Beta}\left(\alpha + \sum_{i=1}^{k} x_i, \beta + \sum_{i=1}^{k}(n_i - x_i)\right) \text{ or } \text{Beta}\left(\alpha + S_k, \beta + \sum_{i=1}^{k} n_i - S_k\right).$$

Mean of posterior $p_k|\mathbf{x}$ (conditional mean) is

$$\frac{\alpha + \sum_{i=1}^{k} x_i}{\alpha + \beta + \sum_{i=1}^{k} n_i} = \frac{\alpha + S_k}{\alpha + \beta + \sum_{i=1}^{k} n_i}.$$

Variance of posterior (conditional variance) is

$$\frac{(\alpha + S_k)(\beta + \sum_{i=1}^{k} n_i - S_k)}{(\alpha + \beta + \sum_{i=1}^{k} n_i)^2 (\alpha + \beta + \sum_{i=1}^{k} n_i + 1)}.$$

Given that

$$p_k = \frac{\alpha + S_k}{\alpha + \beta + \sum_{i=1}^{k} n_i}$$

and

$$S_{k+1} = S_k + x_{k+1},$$

p_{k+1} can be expressed as

$$p_{k+1} = \frac{\alpha + S_{k+1}}{\alpha + \beta + \sum_{i=1}^{k+1} n_i} = \frac{\alpha + S_k + x_{k+1}}{\alpha + \beta + \sum_{i=1}^{k+1} n_i} = \frac{(\alpha + \beta + \sum_{i=1}^{k} n_i) p_k + x_{k+1}}{\alpha + \beta + \sum_{i=1}^{k+1} n_i}.$$

Then the dynamic program is structured as

$$V_k(p_k) = \min\left\{L \cdot p_k, C + L_k \cdot p_k, \gamma + \delta \bar{V}_{k+1}(p_k)\right\}, \text{ for } p_k \in (0,1)$$

$$\bar{V}_{k+1}(p_k) \equiv \sum_{x=0}^{n_k} \binom{n_k}{x} p_k{}^x (1 - p_k)^{n_k - x} V_{k+1}\left(\frac{(\alpha + \beta + \sum_{i=1}^{k} n_i) p_k + x}{\alpha + \beta + \sum_{i=1}^{k+1} n_i}\right)$$

$$\bar{V}_N(p_{N-1}) = L \cdot p_{N-1}.$$

Beta-Geometric

Prior is p_0 (probability), whose distribution is Beta(α, β), and information is the number of Bernoulli trials needed to get one success (X supported on the set $\{1,2,3,...\}$) or the number of failures before the first success (Y=X-1 supported on the set $\{0,1,2,3,...\}$), whose distribution is Geometric(p_0). Posterior distribution is determined by current stage or amount of information up to current stage (k) and the sum of information up to the current stage ($\sum_{i=1}^{k} x_i$ or S_k).

Likelihood function is

$$p(x \mid p_k) = p_k(1-p_k)^{x-1} \qquad x \in \{1,2,...\}$$

or

$$p(y \mid p_k) = p_k(1-p_k)^{y} \qquad y \in \{0,1,2,...\}.$$

Pdf of prior is

$$\frac{x^{\alpha-1}(1-x)^{\beta-1}}{B(\alpha,\beta)}, \quad 0 \le x \le 1, \quad \alpha > 0, \quad \beta > 0,$$

where $B(\alpha,\beta) = \frac{\Gamma(\alpha)\Gamma(\beta)}{\Gamma(\alpha+\beta)}$. Mean of prior is $\frac{\alpha}{\alpha+\beta}$. Variance of prior is

$\frac{\alpha\beta}{(\alpha+\beta)^2(\alpha+\beta+1)}$. Posterior distribution is

$$p_k \mid \mathbf{x} \sim \text{Beta}\left(\alpha + k, \beta + \sum_{i=1}^{k}(x_i - 1)\right) \text{ or } \text{Beta}\left(\alpha + k, \beta - k + S_k\right)$$

$$p_k \mid \mathbf{y} \sim \text{Beta}\left(\alpha + k, \beta + \sum_{i=1}^{k} y_i\right) \text{ or } \text{Beta}\left(\alpha + k, \beta + R_k\right).$$

Mean of posterior $p_k|\mathbf{x}$ (conditional mean) is

$$\frac{\alpha+k}{\alpha+\beta+\sum_{i=1}^{k}x_i}=\frac{\alpha+k}{\alpha+\beta+S_k} \text{ or } \frac{\alpha+k}{\alpha+\beta+k+\sum_{i=1}^{k}y_i}=\frac{\alpha+k}{\alpha+\beta+k+R_k}.$$

Variance of posterior (conditional variance) is

$$\frac{(\alpha+k)(\beta-k+S_k)}{(\alpha+\beta+S_k)^2(\alpha+\beta+S_k+1)} \text{ or } \frac{(\alpha+k)(\beta+R_k)}{(\alpha+k+\beta+R_k)^2(\alpha+k+\beta+R_k+1)}.$$

Given that

$$p_k=\frac{\alpha+k}{\alpha+\beta+S_k} \text{ or } \frac{\alpha+k}{\alpha+\beta+k+R_k}$$

and

$$S_{k+1}=S_k+x_{k+1},$$

p_{k+1} can be expressed as

$$p_{k+1}=\frac{\alpha+k+1}{\alpha+\beta+S_{k+1}}=\frac{\alpha+k+1}{\alpha+\beta+S_k+x_{k+1}}=\frac{\alpha+k+1}{\frac{\alpha+k}{p_k}+x_{k+1}}$$

or

$$p_{k+1}=\frac{\alpha+k+1}{\alpha+\beta+k+1+R_{k+1}}=\frac{\alpha+k+1}{\alpha+\beta+k+1+R_k+y_{k+1}}=\frac{\alpha+k+1}{\frac{\alpha+k}{p_k}+1+y_{k+1}}.$$

Then the dynamic program is structured as

$$V_k(p_k)=\min\left\{L\cdot p_k, C+L_k\cdot p_k, \gamma+\delta\bar{V}_{k+1}(p_k)\right\}, \text{ for } p_k\in(0,1)$$

$$\bar{V}_{k+1}(p_k)\equiv\sum_{x=1}^{\infty}p_k(1-p_k)^{x-1}V_{k+1}\left((\alpha+k+1)/\left(\frac{\alpha+k}{p_k}+x\right)\right)$$

or

$$\bar{V}_{k+1}(p_k)\equiv\sum_{y=0}^{\infty}p_k(1-p_k)^{y}V_{k+1}\left((\alpha+k+1)/\left(\frac{\alpha+k}{p_k}+1+y\right)\right)$$

$$\bar{V}_N(p_{N-1}) = L \cdot p_{N-1}.$$

There are also continuous conjugate distributions, but they are not applicable to our model due to the range of its parameters.

VITA

Seong Dae Kim received his Bachelor of Science degree in industrial engineering from Sungkyunkwan University, South Korea in 1999. He entered the Industrial Engineering program at Sungkyunkwan University in March 1999 and received his Master of Science degree in February 2002. He received his Ph.D. degree in industrial engineering from Texas A&M University in May 2009. His research interests include decision and risk analysis, emergency response and preparedness, and value of information.

Mr. Kim may be reached at Texas A&M University, Department of Industrial and Systems Engineering, 241 Zachry, 3131 TAMU, College Station, TX 778431-3131. His email is sdkim@tamu.edu.